Institut Langevin
ONDES ET IMAGES

Reflection Matrix Imaging: From Quantitative Ultrasound to Deep Optical Microscopy and Passive Seismology

Alexandre AUBRY

Elsa Giraudat, Flavien Bureau, William Lambert, Paul Balondrade, Victor Barolle, Ulysse Najar, Antton Goicoechea, Claire Prada, Arnaud Derode, Claude Boccara, Mathias Fink

Institut Langevin, ESPCI Paris, PSL University, CNRS, Paris, France

erc ESPCI PARIS cnrs PSL UNIVERSITÉ PARIS

Waves and Imaging in Complex Media Workshop – Paris, France – June 12th, 2025

Multidisciplinary subject:
solid-state physics, **optics**, **microwaves**, **acoustics**, **seismology**, *etc.*


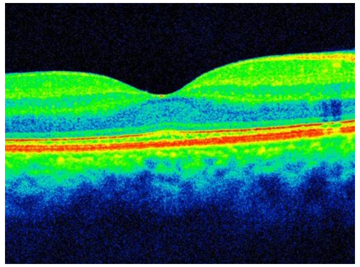


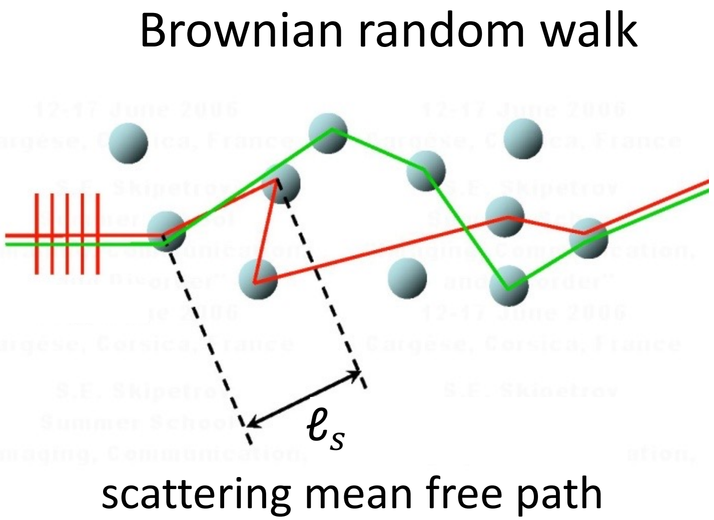

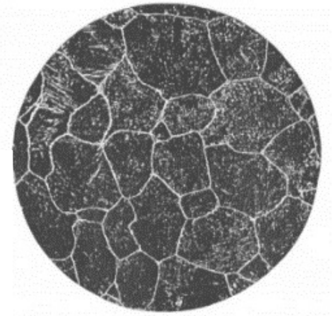

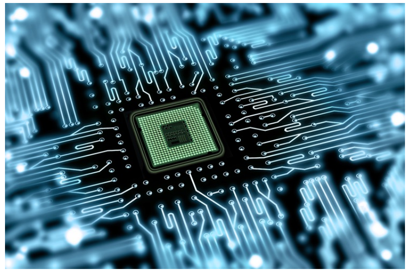


The propagation of waves in complex media is of fundamental interest for many applications:

Imaging/sensing/communications/therapy/energy harvesting

What About Imaging?

Optical microscopy

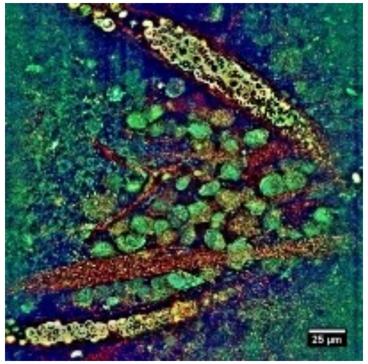

Ultrasound imaging

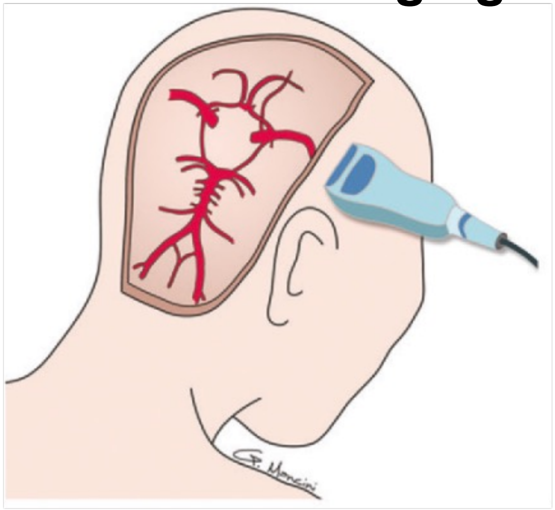

Seismology

Same limitations due to inhomogeneities
(aberrations/multiple scattering)

European Research Council
Established by the European Commission

ERC Consolidator, Reminiscence Project, 2019-2024

What About Imaging?

Optical microscopy

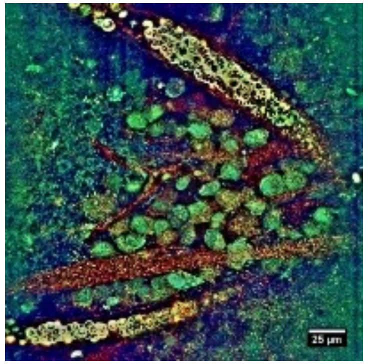

Ultrasound imaging

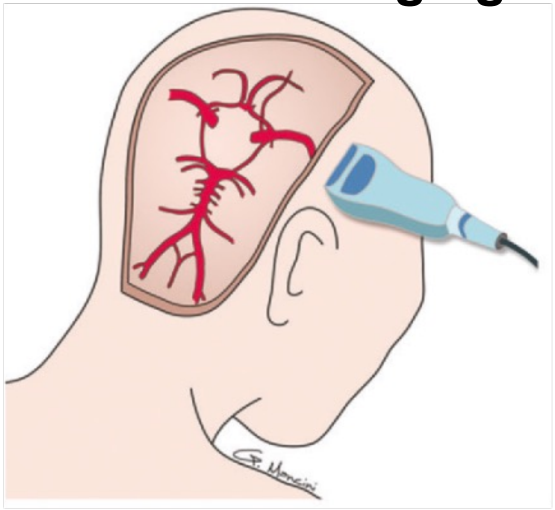

Seismology

Same limitations due to inhomogeneities
(aberrations/multiple scattering)

Our holy grail:
Universal and *non-invasive* approach of wave imaging in complex media

ERC Consolidator, Reminiscence Project, 2019-2024

Reflection Matrix

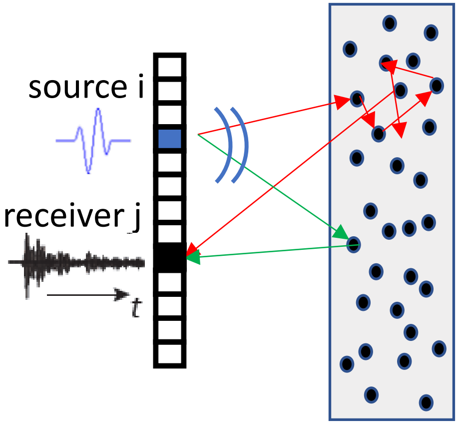

$$\boldsymbol{\Psi}_{\mathrm{out}} = \mathbf{R}\times\boldsymbol{\Psi}_{\mathrm{in}}$$

Single scattering

Multiple scattering

W. Lambert, L. A. Cobus, M. Fink, A. Aubry, Phys. Rev. X (2020)

Outline

I. Introduction

II. Ultrasound Matrix Imaging: Self-Portrait of the Focusing Process

III. Overcoming Wave Distortions: Adaptive Focusing in Post-Processing

IV. Beating Diffraction: Passive Seismic Imaging of a Volcano

V. Harnessing Forward Multiple Scattering for Deep Optical maging

VI. Towards Quantitative Imaging: Wave Velocity and Scattering Tomography in Reflection

VII. Conclusion

Ultrasound Imaging

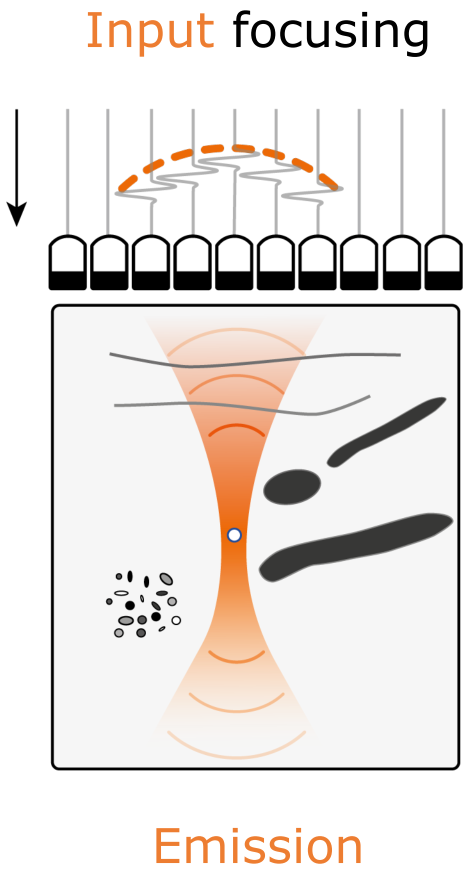

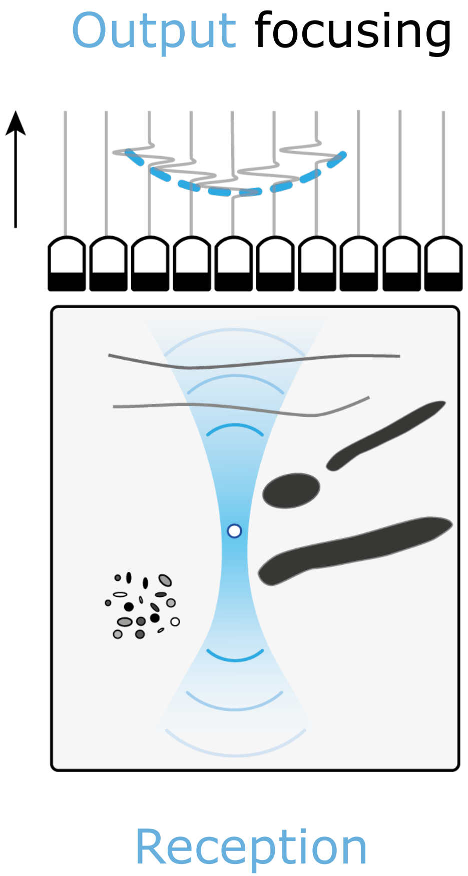

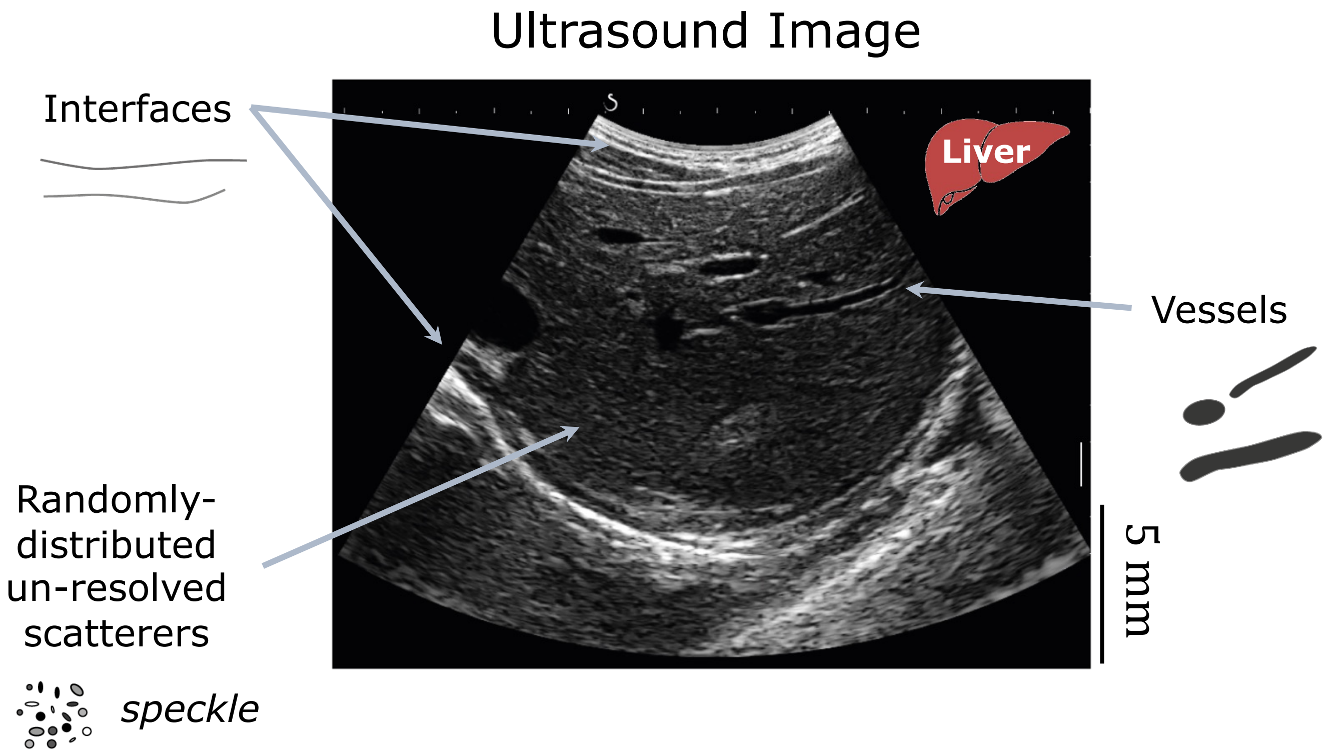

The ultrasound image relies on a confocal beamforming scheme

It is an estimator of the medium local reflectivity

Limits of confocal imaging

Hypotheses
- Homogeneous velocity c_0
- **Single** scattering

→ Depth ∝ Echo Time
$$z = c_0 t/2$$

in vivo
- **Heterogeneous** speed-of-sound
- **Multiple** scattering

→ ~~Depth ∝ Echo Time~~
$$\cancel{z = c_0 t/2}$$

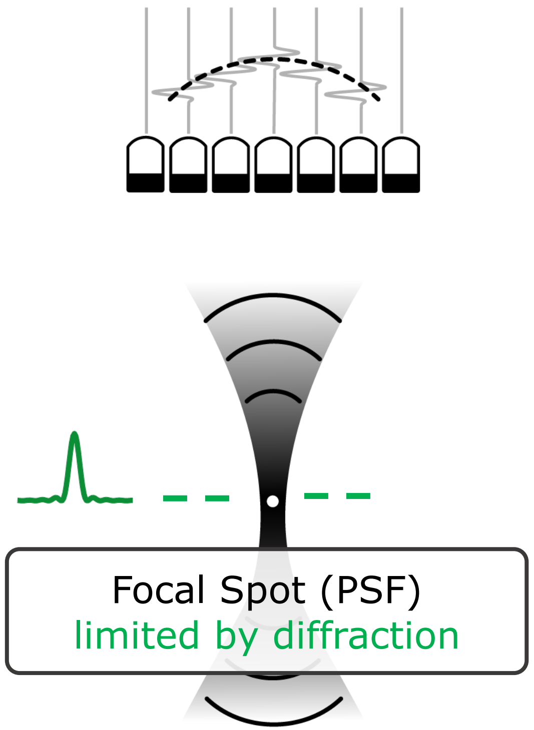

Focal Spot (PSF)
limited by diffraction

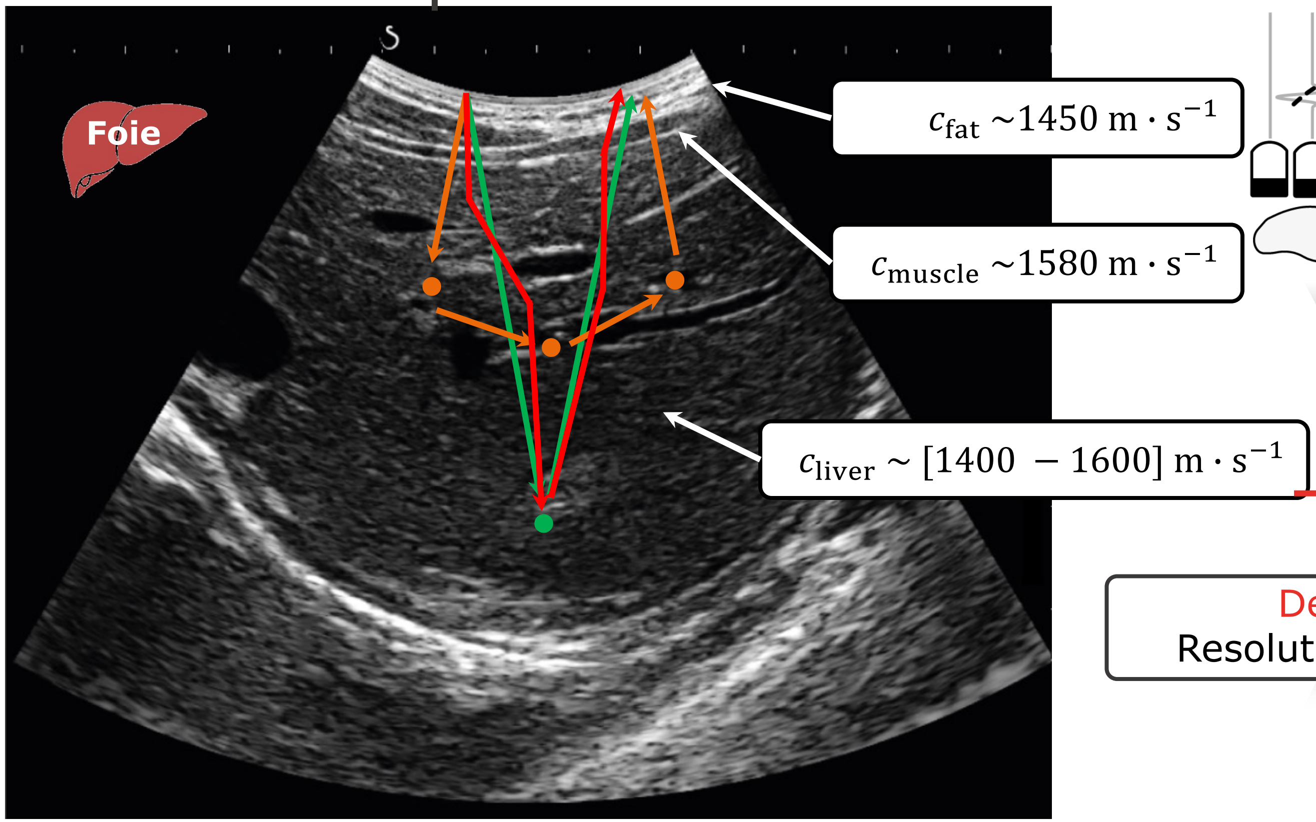

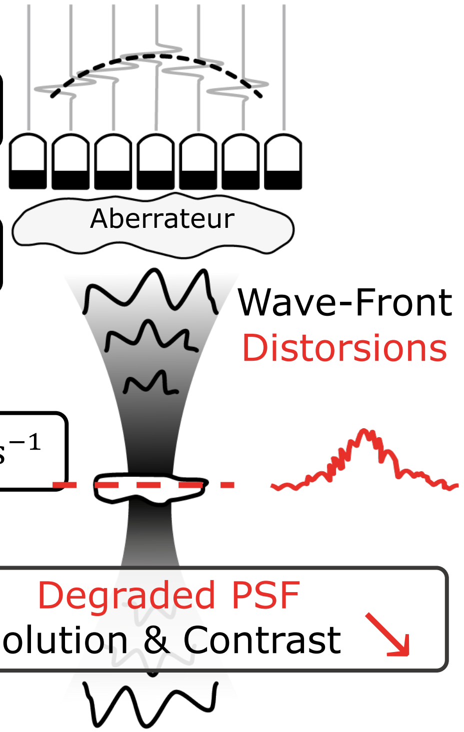

Degraded PSF
Resolution & Contrast ↘

The image quality is often degraded by the mismatch between the propagation model and the real speed-of-sound distribution inside the medium

[Duck, 1990] "Acoustics Properties of Tissue at Ultrasonic Frequencies". *Physical Properties of Tissues*

Challenges for Transcranial Imaging

Head Phantom

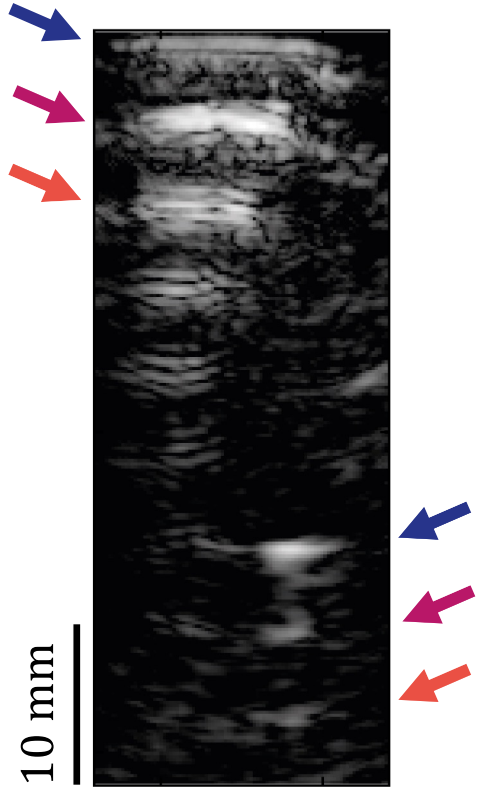

Artefacts

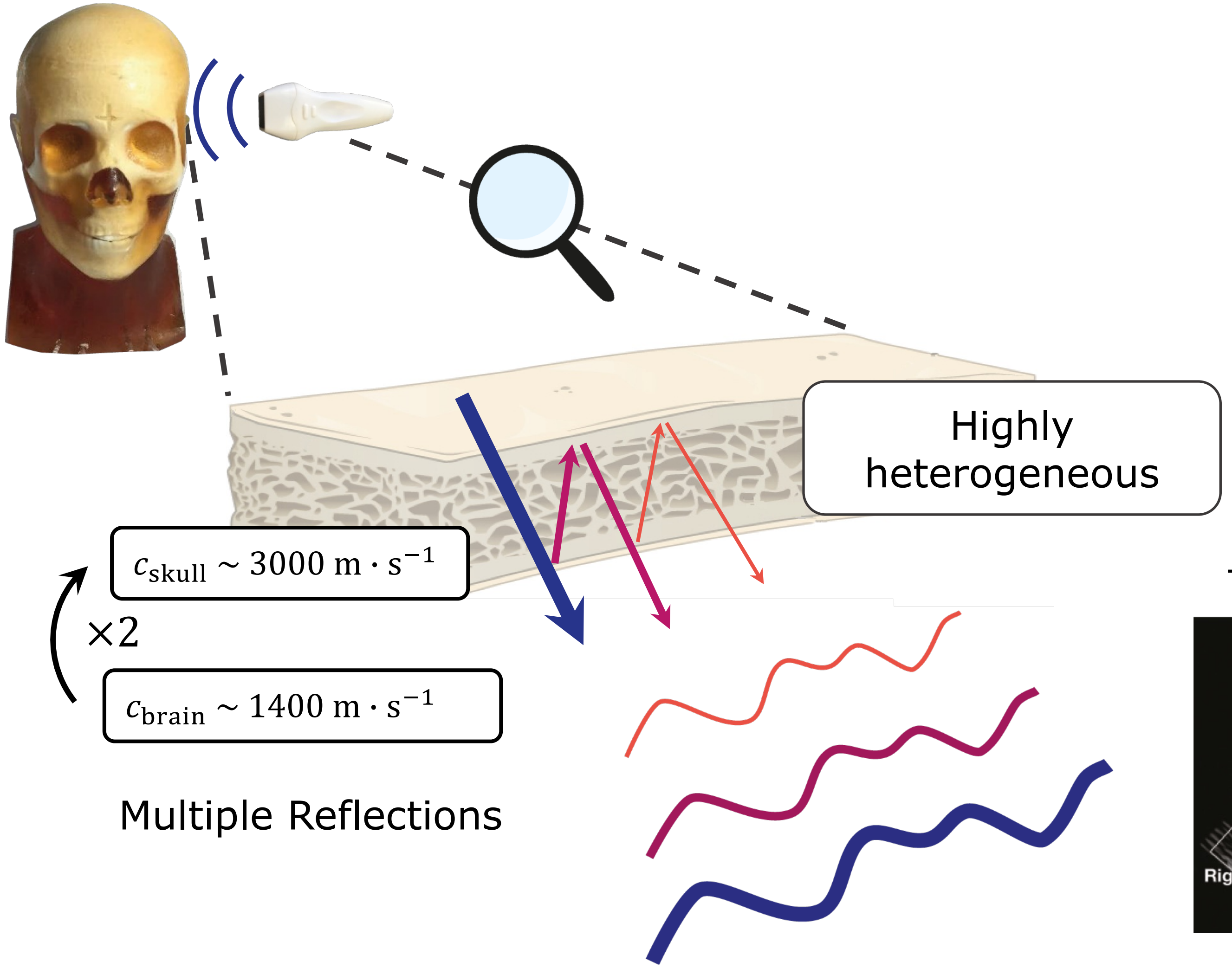

Limits

- Attenuation
- Strong Aberrations
- Multiple Scattering
- Reverberations

⇒ Drastic degradation of focusing

Transcranial Doppler

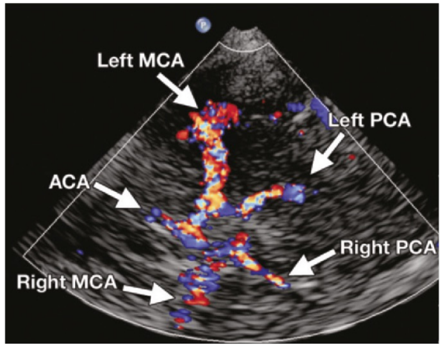

Acoustic window

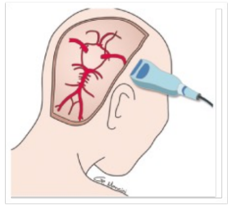

Kirsch et al., 2013

In complex media, confocal imaging fails.

How to overcome the current limits of ultrasound imaging?

[Kirsch et al., 2013] " Advances in Transcranial Doppler US: Imaging Ahead." *RadioGraphics*

Ultrasound Matrix Imaging

Quantifying the focusing process

Flavien Bureau

William Lambert

Ultrasound Matrix Imaging

① Acquisition : Canonical **Reflection** matrix $\mathbf{R} = [R(\mathbf{u}_{out}, \mathbf{u}_{in}, t)]$

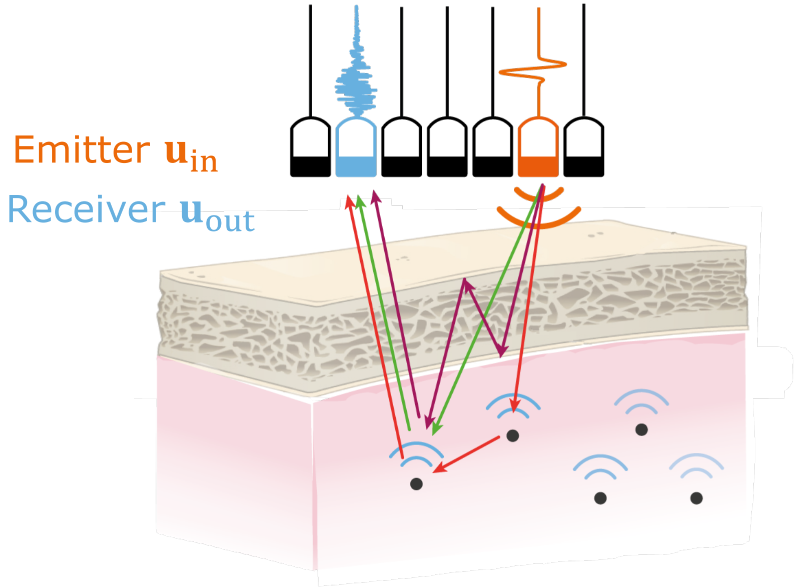

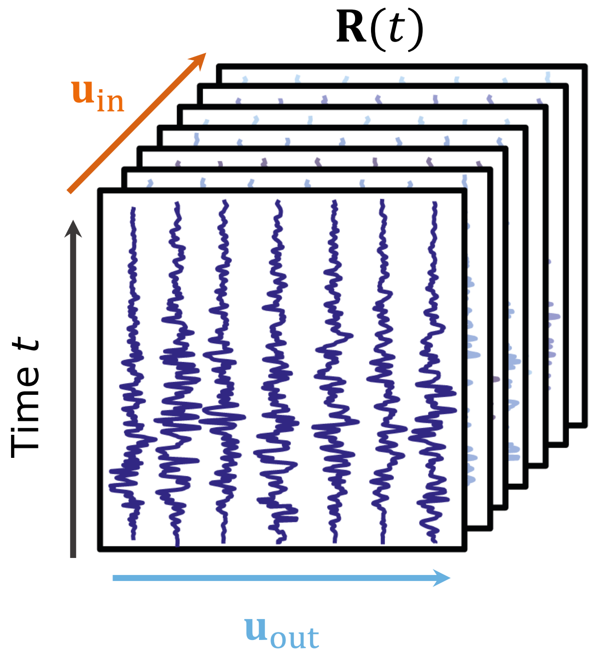

set of impulse reponses for each couple of transducers

Fourier Transform

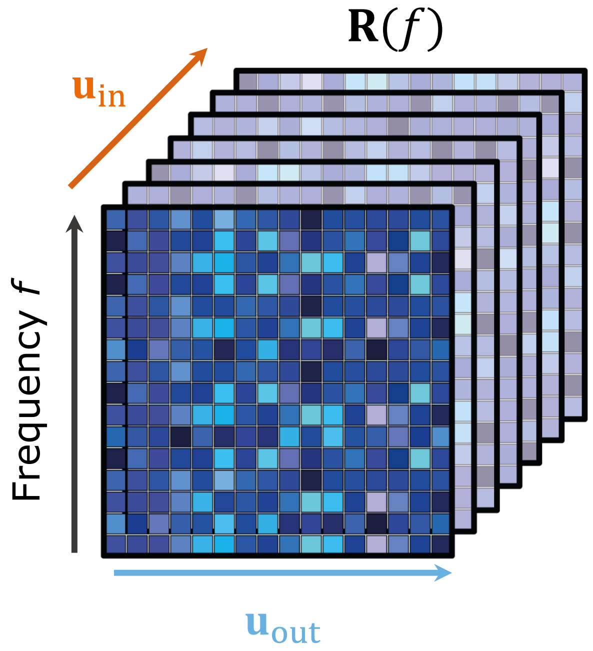

$$\mathbf{\Psi}_{\mathbf{out}}(f) = \mathbf{R}(f) \times \mathbf{\Psi}_{\mathbf{in}}(f)$$

The reflection matrix contains the whole information available on the medium (static & linear)

It gives access to the medium response for each insonification.

[Prada & Fink, 1994] "Eigenmodes of the Time Reversal Operator: A Solution to Selective Focusing in Multiple-Target Media". *Wave Motion*

[Aubry & Derode, 2009] "Random matrix theory applied to acoustic backscattering and imaging in complex media". *Phys. Rev. Lett.*

10

Numerical Focusing

1. Acquisition : Canonical **Reflection** Matrix $\mathbf{R} = [R(\mathbf{u}_{\text{out}}, \mathbf{u}_{\text{in}}, t)]$

2. Focusing in Post-processing

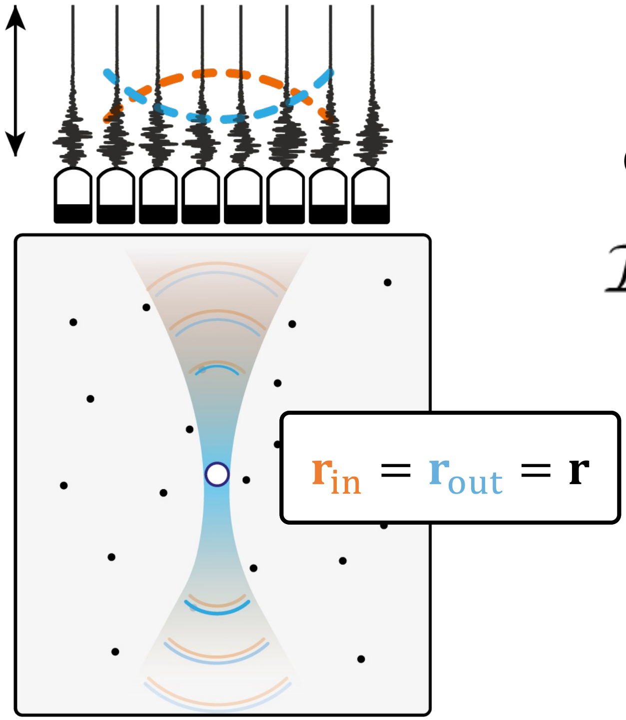

Emission & Reception

Confocal image

$$\mathcal{I}(\mathbf{r}) = \sum_{\mathbf{u}_{\text{in}}} \sum_{\mathbf{u}_{\text{out}}} R\Big(\mathbf{u}_{\text{out}}, \mathbf{u}_{\text{in}}, \underbrace{\Delta t(\mathbf{u}_{\text{in}} \to \mathbf{r})}_{\text{Input Focusing}} + \underbrace{\Delta t\,(\mathbf{r} \to \mathbf{u}_{\text{out}})}_{\text{Output Focusing}}\Big)$$

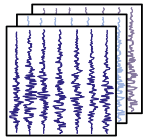

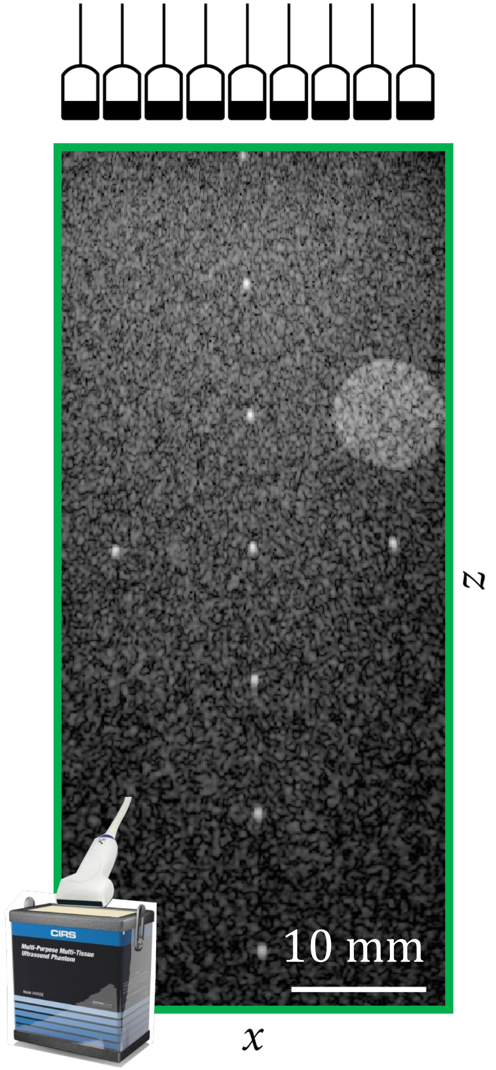

Ultrasound Phantom

Numerical Focusing

1. Acquisition : Canonical **Reflection** Matrix $\mathbf{R} = [R(\mathbf{u}_{out}, \mathbf{u}_{in}, t)]$

2. Focusing in Post-processing

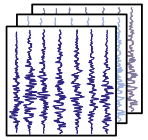

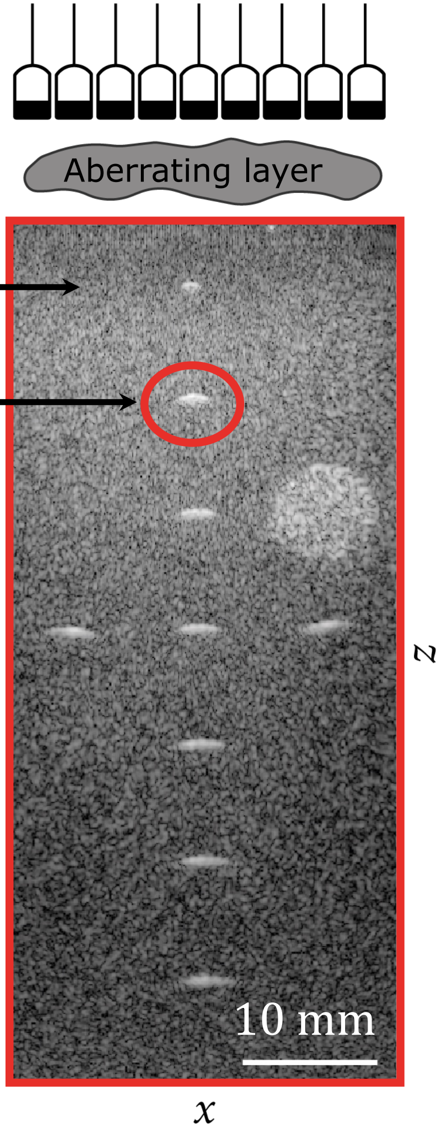

Ultrasound Phantom

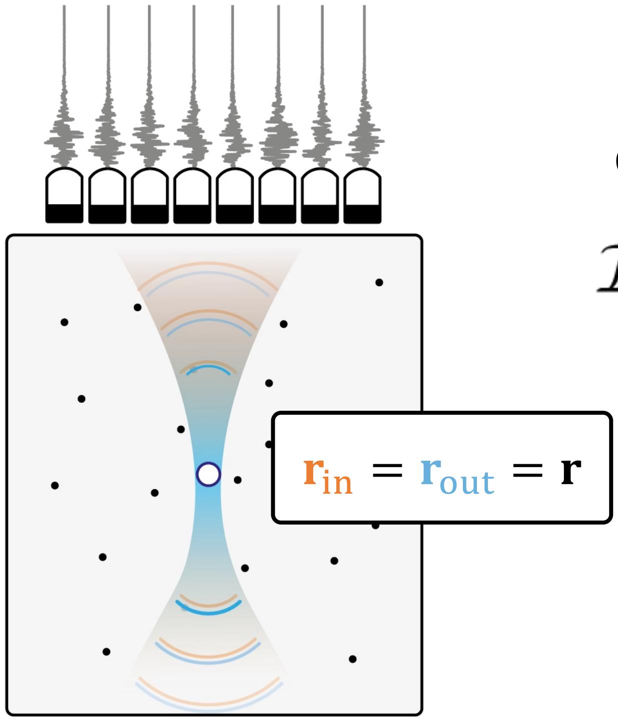

Emission & Reception

Confocal image

$$\mathcal{I}(\mathbf{r}) = \sum_{\mathbf{u}_{in}} \sum_{\mathbf{u}_{out}} R\big(\mathbf{u}_{out}, \mathbf{u}_{in}, \underbrace{\Delta t(\mathbf{u}_{in} \to \mathbf{r})}_{\text{Input Focusing}} + \underbrace{\Delta t\,(\mathbf{r} \to \mathbf{u}_{out})}_{\text{Output Focusing}}\big)$$

How to probe aberrations in speckle?

Matrix Imaging

1 Acquisition : Canonical **Reflection** Matrix $\mathbf{R} = [R(\mathbf{u}_{\text{out}}, \mathbf{u}_{\text{in}}, t)]$

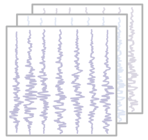

2 Focusing in Post-processing

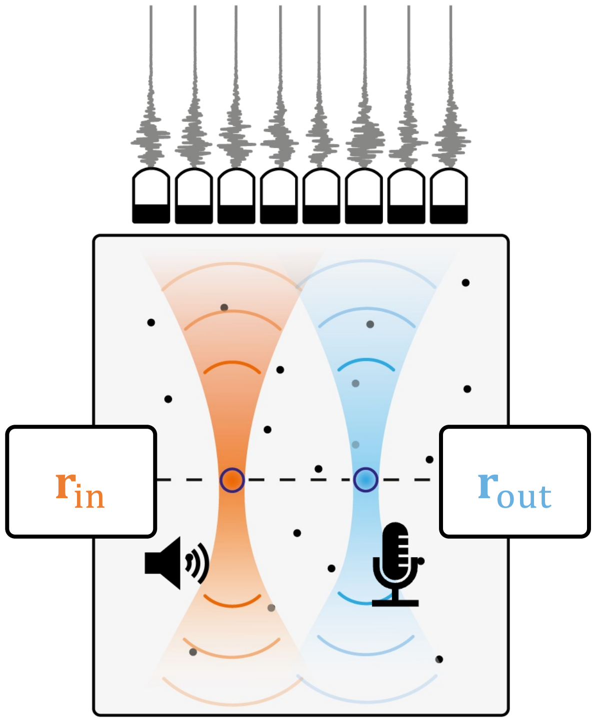

Decoupling of input and output focal spots

Focused Reflection Matrix $\overline{\mathbf{R}}_{\mathbf{rr}} = [\mathrm{R}(\mathbf{r}_{\text{out}}, \mathbf{r}_{\text{in}})]$

Impulse responses between **virtual** sources and receivers located inside the medium

$$\bar{R}(\mathbf{r}_{\text{out}}, \mathbf{r}_{\text{in}}) = \sum_{\mathbf{u}_{\text{in}}} \sum_{\mathbf{u}_{\text{out}}} R\big(\mathbf{u}_{\text{out}}, \mathbf{u}_{\text{in}}, \underbrace{\Delta t(\mathbf{u}_{\text{in}} \to \mathbf{r}_{\text{in}}) + \Delta t\,(\mathbf{r}_{\text{out}} \to \mathbf{u}_{\text{out}})}_{\text{Ballistic time}}\big)$$

Ballistic time

Way-and-return echo time

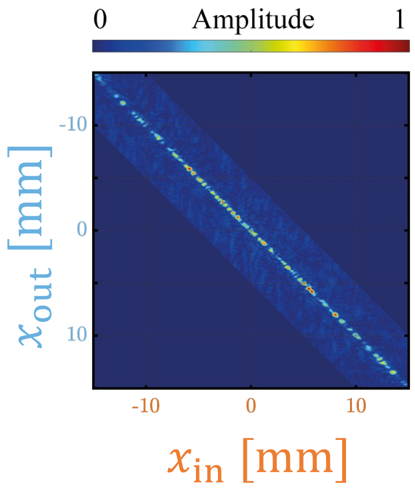

Projection of ultrasound data in a focused basis at a given depth

[Lambert et al, 2020] "Reflection Matrix Approach for Quantitative Imaging of Scattering Media". *Phys. Rev. X*

Matrix Imaging

Focused Reflection Matrix $\overline{\mathbf{R}}_{\mathbf{rr}} = [\mathrm{R}(\mathbf{r}_{\mathrm{out}}, \mathbf{r}_{\mathrm{in}})]$

Impulse responses between **virtual** sources and receivers located inside the medium

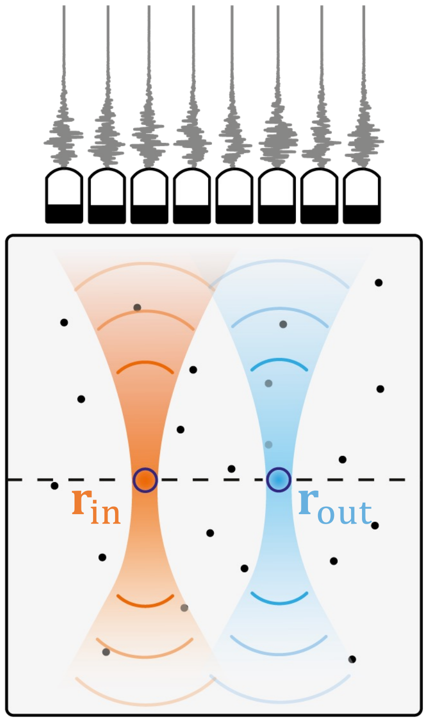

Diagonal elements
Confocal signal → image

Off-diagonal elements
Focusing quality

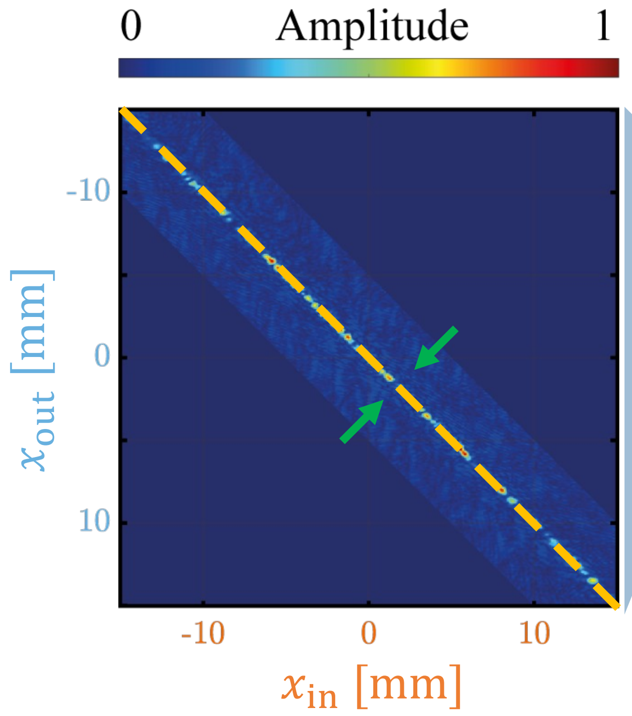

At a given depth z

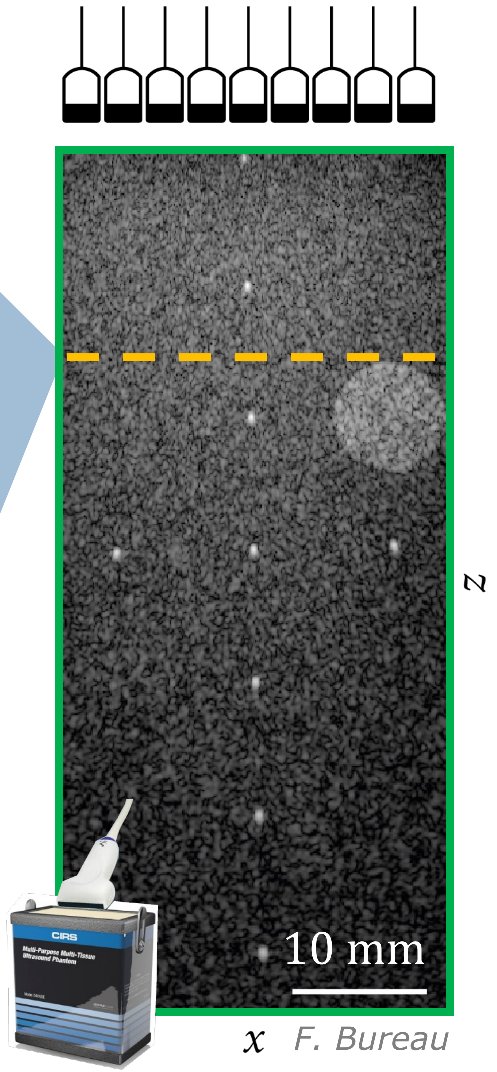

Ultrasound phantom

The focused reflection matrix contains much more information than a mere confocal image

Matrix Imaging

Focused Reflection Matrix $\overline{\mathbf{R}}_{\mathbf{rr}} = [\mathrm{R}(\mathbf{r}_{\mathrm{out}}, \mathbf{r}_{\mathrm{in}})]$

Impulse responses between **virtual** sources and receivers located inside the medium

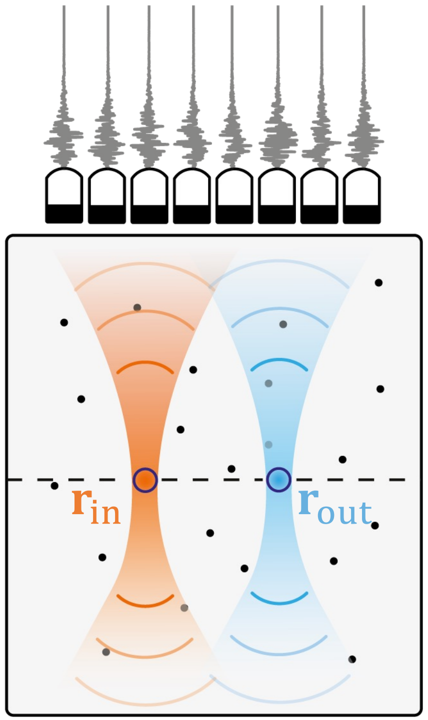

Diagonal elements
Confocal signal → image

Off-diagonal elements
Focusing quality

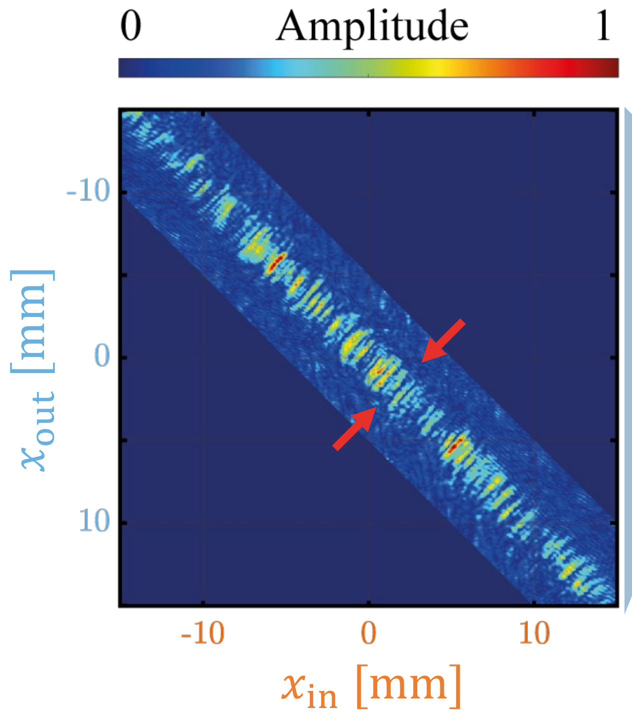

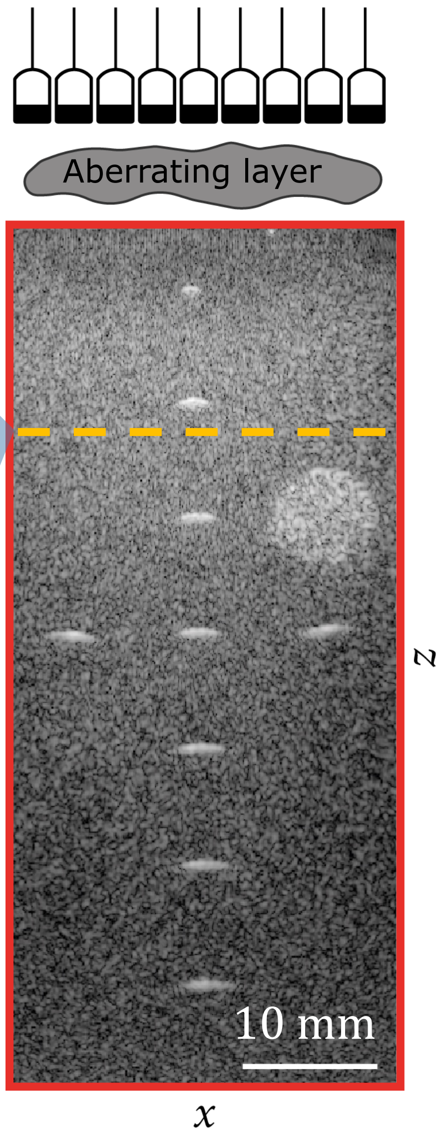

Fantôme ultrasonore

The focused reflection matrix enables us to probe the focusing quality and aberrations

But aberrations are 3D distributed…

From 2D to 3D Matrix Imaging

2D Probe

32x32 channels
1-5 MHz
Pitch: λ

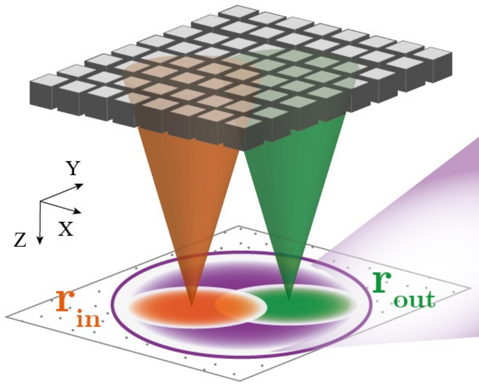

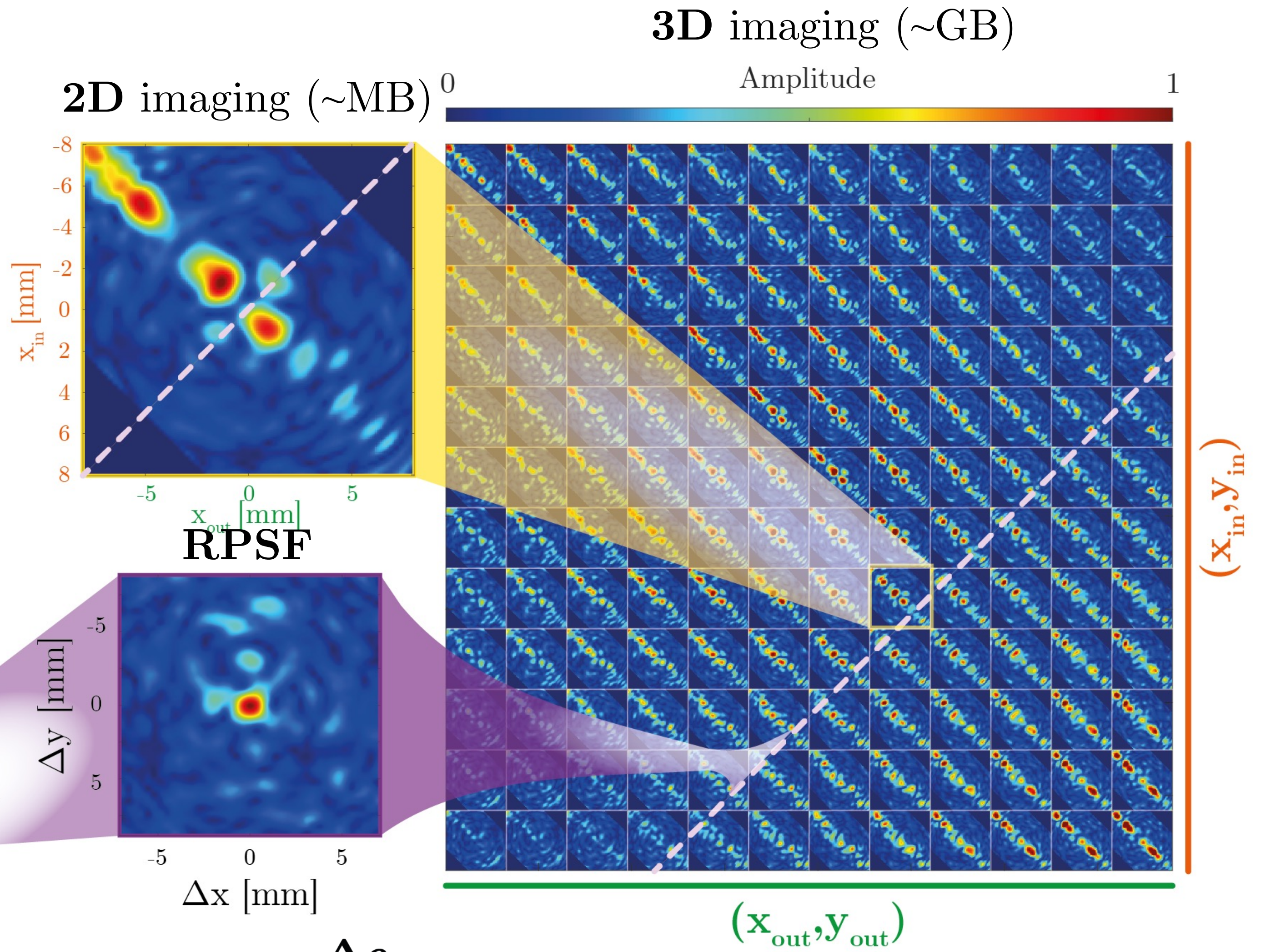

3D Confocal Image

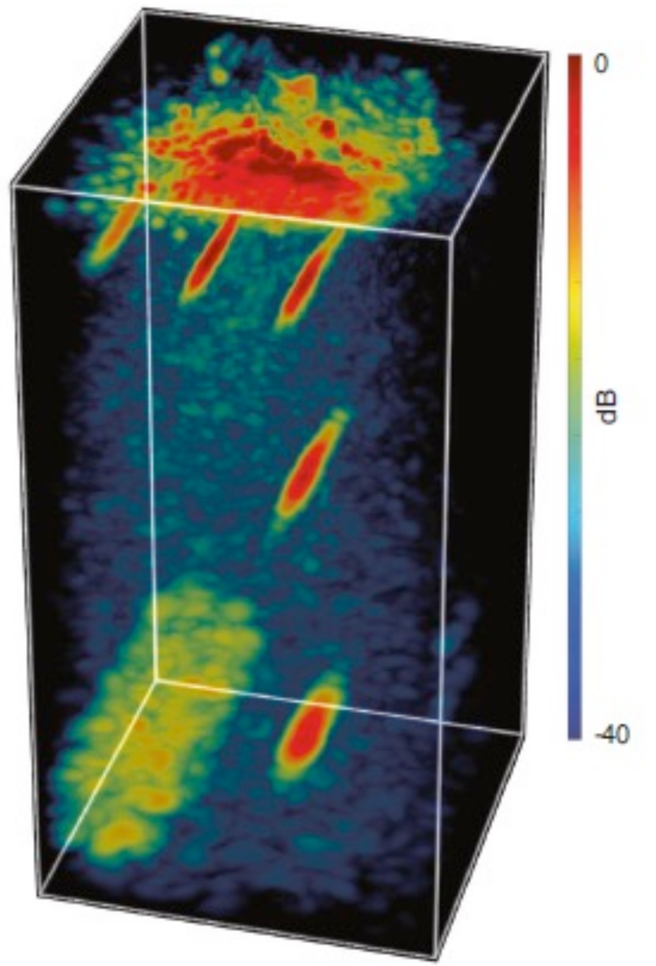

$$\langle \mathbf{RPSF} \rangle \propto |\mathbf{PSF}_{in}|^2 \overset{\Delta\rho}{\circledast} |\mathbf{PSF}_{out}|^2$$

Input PSF Output PSF

[Bureau et al, 2023] "Three-Dimensional Ultrasound Matrix Imaging", *Nature Commun.*

Transcranial Imaging Experiment

O. Couture

A. Coudert

L. Denis

32x32 channels
1-2 MHz
Pitch: λ

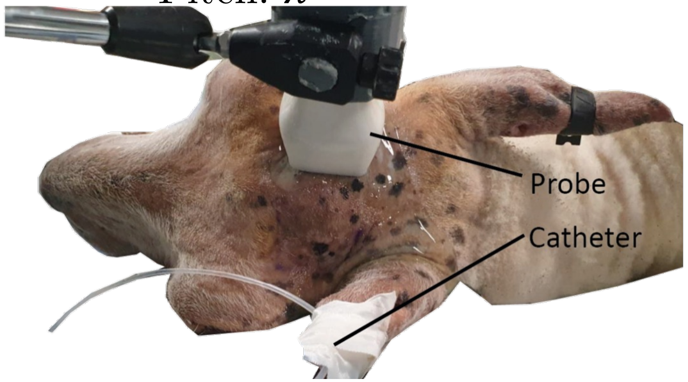

324 incident diverging waves
$-30 \rightarrow 30^o$

Laboratoire d'Imagerie Biomédicale

Reflection matrix **acquisition**

Canonical basis

$\mathbf{R}$=[R($\mathbf{u}_{in}$,$\mathbf{u}_{out}$,t)]

Fourier transform

$\Longleftrightarrow$

Plane wave basis

$\mathbf{R}$=[R($\mathbf{k}_{in}$,$\mathbf{u}_{out}$,t)]

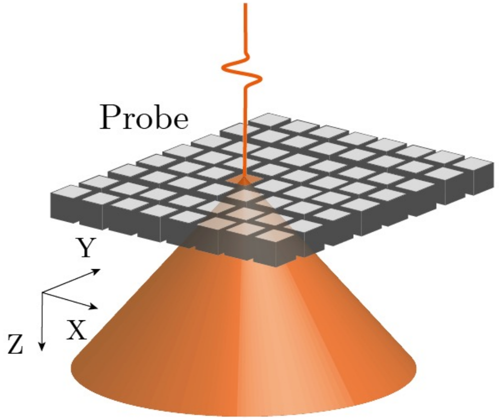

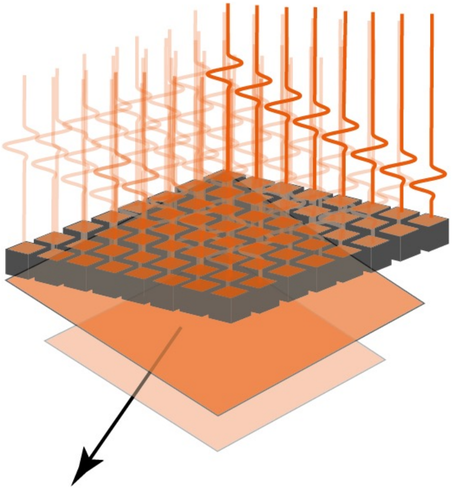

Low signal-to-noise ratio

Higher signal-to-noise ratio

[Coudert et al, 2024] "3D Transcranial ultrasound localization microscopy reveals major arteries in the sheep brain", *IEEE UFFC*

[Bureau et al, 2025] "Ultrasound matrix imaging for 3D transcranial in-vivo localization microscopy", Science Advances (to be published) - *arXiv:2410.14499*

Quantification of Aberrations and Multiple Scat.

32x32 channels
1-2 MHz
Pitch: λ

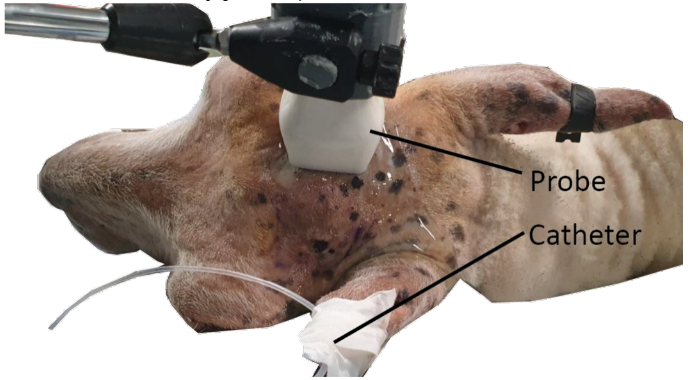

thickness	$L \sim 4.2 \pm 1.1$ mm	$L \sim 5.3 \pm 1$ mm	$L \sim 5.7 \pm 1.7$ mm
diploë volume ratio	$\upsilon \sim 14$ %	$\upsilon \sim 29$ %	$\upsilon \sim 56$ %

µ-CT

A

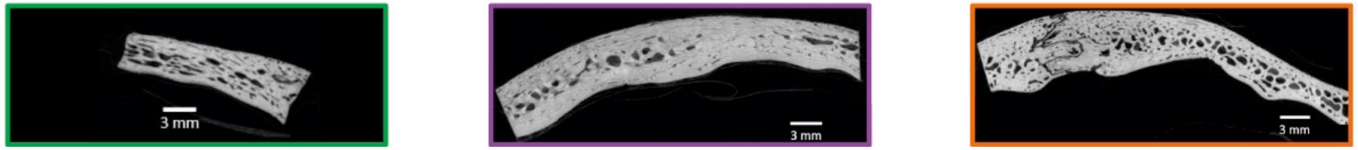

[Coudert et al, 2024] "3D Transcranial ultrasound localization microscopy reveals major arteries in the sheep brain", *IEEE UFFC*

[Bureau et al, 2025] "Ultrasound matrix imaging for 3D transcranial in-vivo localization microscopy", Science Advances (to be published) - *arXiv:2410.14499*

Quantification of Aberrations and Multiple Scat.

Flavien Bureau

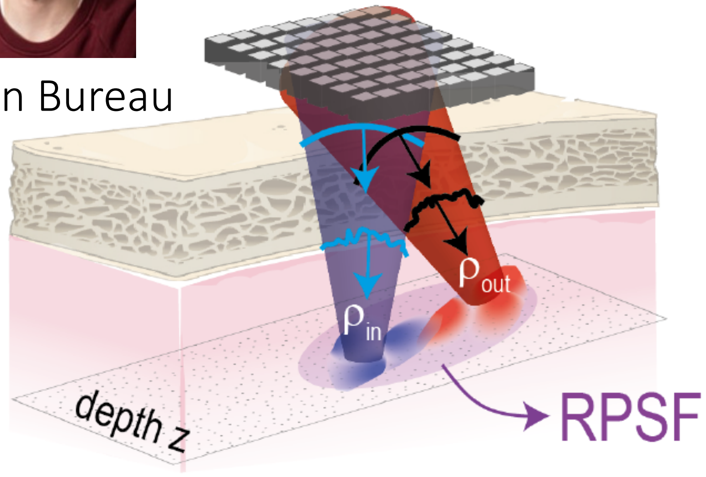

Transcranial ultrasound is drastically hampered by:

Aberrations (irregular thickness)

Multiple scattering (diploë volume ratio)

thickness	$L \sim 4.2 \pm 1.1$ mm	$L \sim 5.3 \pm 1$ mm	$L \sim 5.7 \pm 1.7$ mm
diploë volume ratio	$\upsilon \sim 14$ %	$\upsilon \sim 29$ %	$\upsilon \sim 56$ %

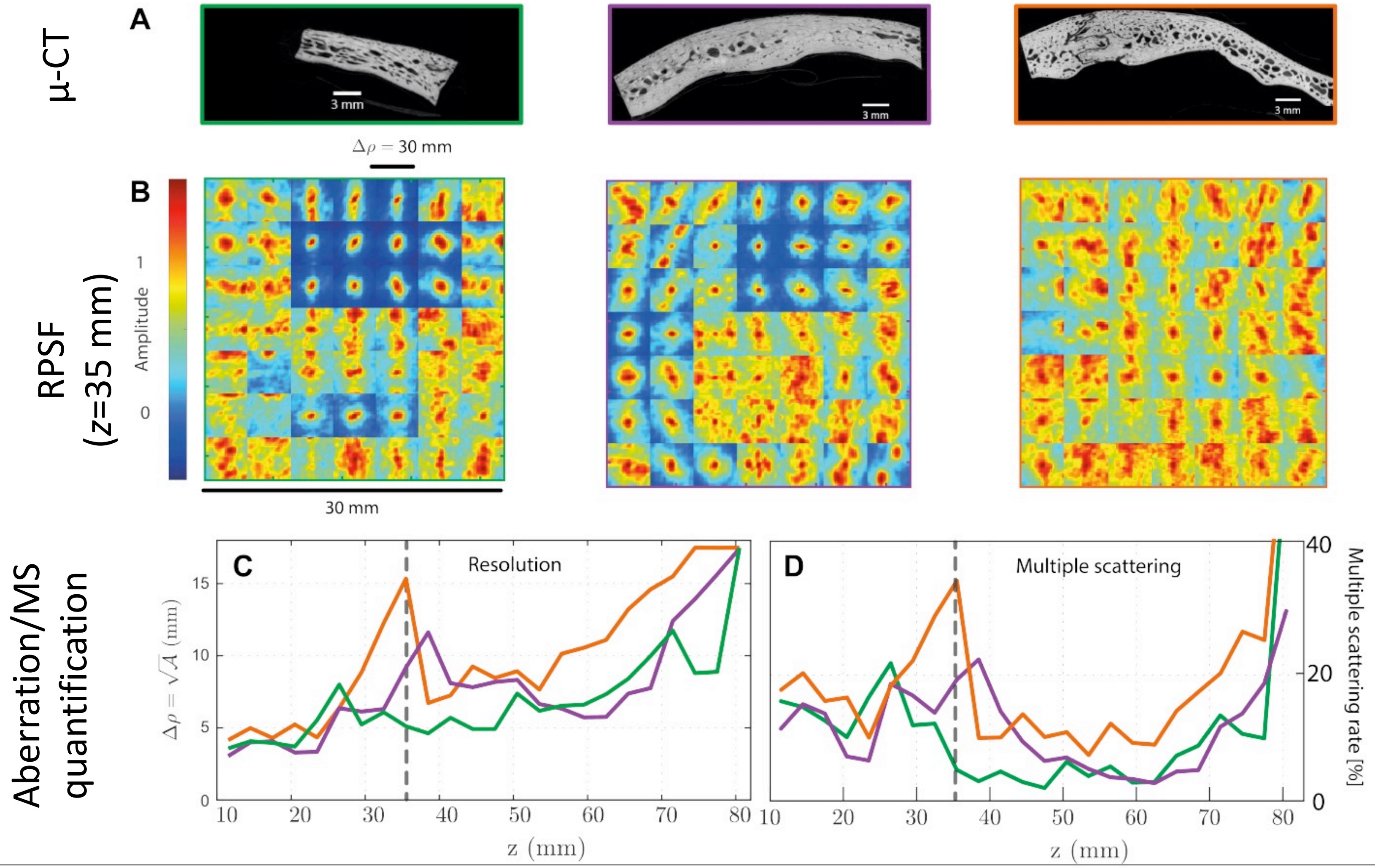

[Bureau et al, 2025] "Ultrasound matrix imaging for 3D transcranial in-vivo localization microscopy", Science Advances (to be published) - *arXiv:2410.14499*

Overcoming Aberrations

Adaptive focusing in post-processing

Flavien Bureau

William Lambert

Adaptive Focusing

Time delay laws dictated by the speed-of-sound model

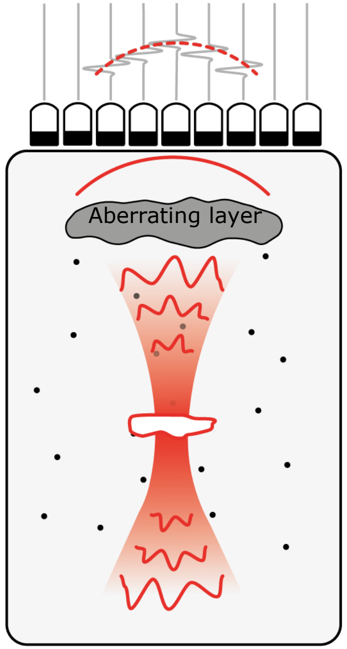

Degraded focal spot
(emission & reception)

Adaptive Focusing

How to find the adapted focusing law?

Time detay laws **adapted** to the medium heterogeneities

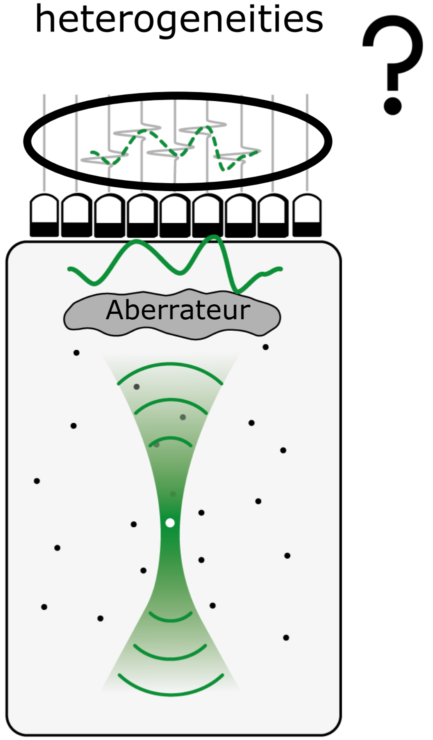

Diffraction-limited focal spot (*ideal* PSF)

Bright scatterer

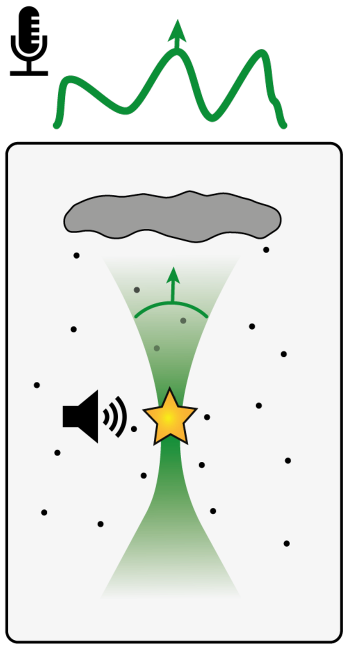

Ultrasound Guide Star

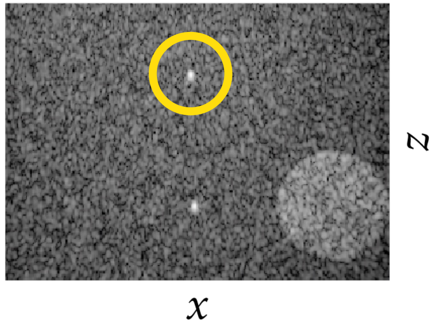

[Babock et al, 1953] "The Possibility of Compensating Astronomical Seeing." *Astronomical Society of the Pacific*

Adaptive Focusing

How to find the adapted focusing law?

Time detay laws **adapted** to the medium heterogeneities

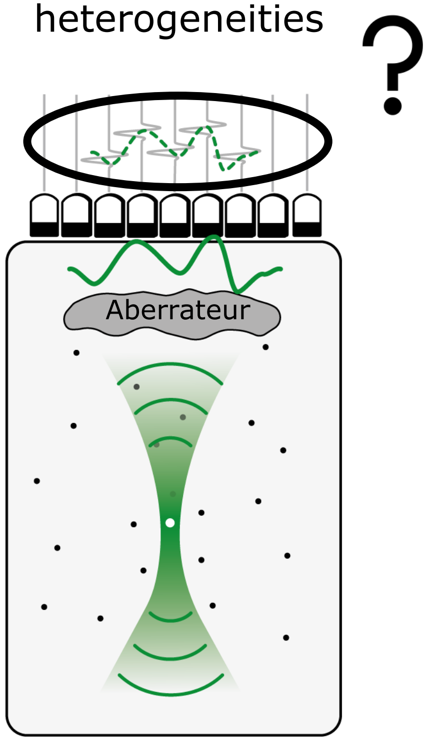

Diffraction-limited focal spot (*ideal* PSF)

Bright scatterer ⭐

Time reversal
⇒ Focusing law

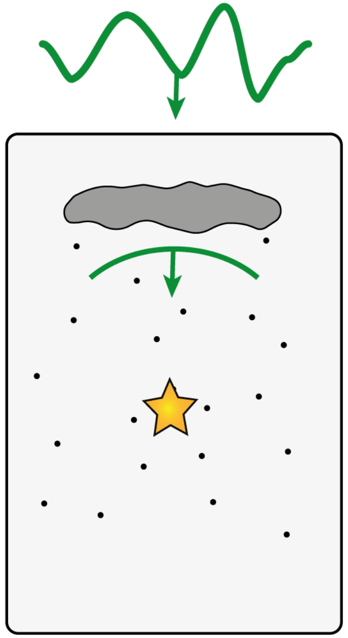

Ultrasound Guide Star

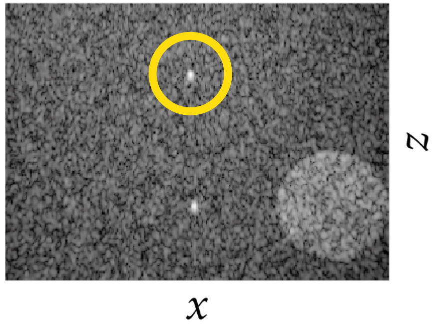

Adaptive Focusing

How to find the adapted focusing law?

Time detay laws **adapted** to the medium heterogeneities

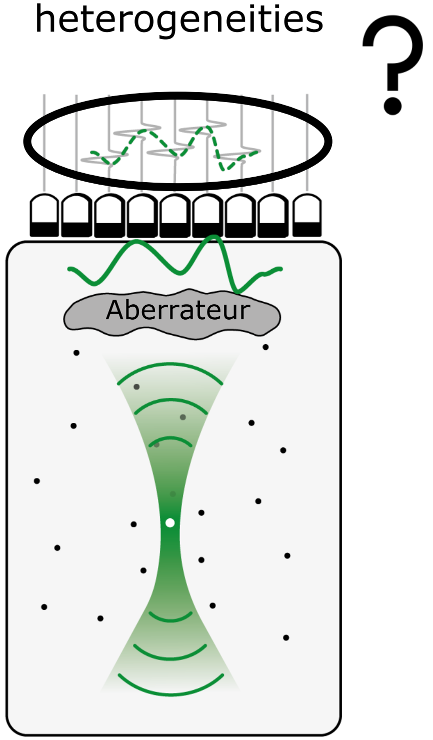

Diffraction-limited focal spot (*ideal* PSF)

Bright scatterer

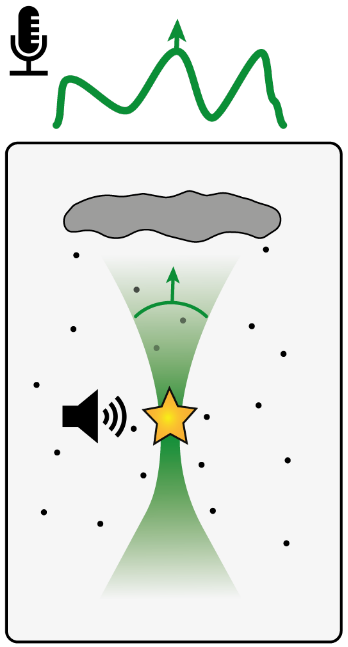

Ultrasound Guide Star

Ultrasound speckle

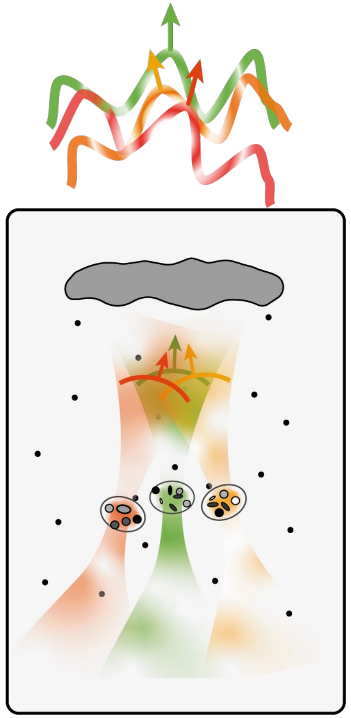

Memory Effect

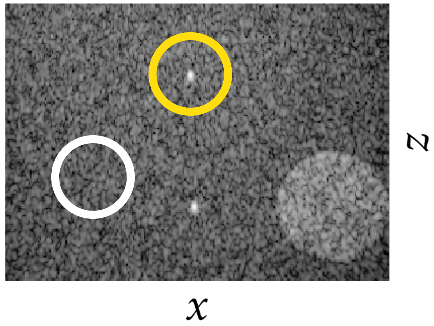

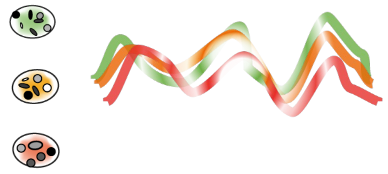

Cross-correlation between back-scattered echoes

⇓

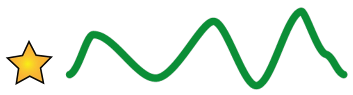

Focusing law

Coherent virtual reflector

[O'Donnel & Flax, 1988] "Phase-Aberration Correction Using Signals from Point Reflectors and Diffuse Scatterers : Measurements." *IEEE TUFFC*
[Robert & Fink,2008] "Green's Function Estimation in Speckle Using the Decomposition of the Time Reversal Operator : Application to Aberration Correction in Medical Imaging." *JASA*
[Montaldo et al, 2011] "Time Reversal of Speckle Noise." *PRL*

Compensating for Aberrations

Time reversal of aberration law + Geometric component = Model = Focusing law

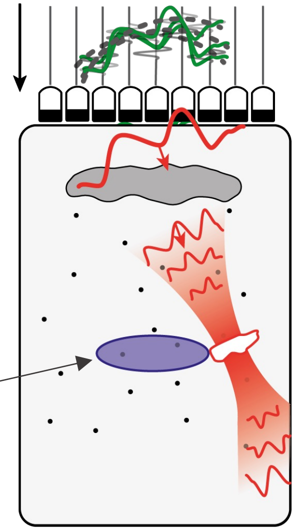

Isoplanatic area
= Spatial invariance of aberrations

- ✓ Isoplanatic area
- ✗ Beyond the isoplanatic area

  ⇒ need to learn the aberration law for each isoplanatic area
  = estimate the inner **T**-matrix

The focusing law is only valid over a restricted isoplanatic area

[O'Donnel & Flax, 1988] "Phase-Aberration Correction Using Signals from Point Reflectors and Diffuse Scatterers : Measurements." *IEEE TUFFC*
[Robert & Fink,2008] "Green's Function Estimation in Speckle Using the Decomposition of the Time Reversal Operator : Application to Aberration Correction in Medical Imaging." *JASA*
[Montaldo et al, 2011] "Time Reversal of Speckle Noise." *PRL*

Compensating for Aberrations

Time reversal of aberration law + Geometric component = Model = Focusing law

Isoplanatic area
= Spatial invariance of aberrations

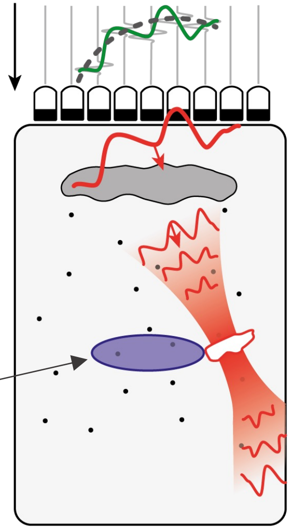

Isoplanatic area

Beyond the isoplanatic area

⇒ need to learn the aberration law for each isoplanatic area
= estimate the inner **T**-matrix

Today

Estimation of Aberration Laws in **post-processing**: high flexibility

Iteration of the aberration correction process for each isoplanatic area

[Chau et al, 2019] "A Locally Adaptive Phase Aberration Correction (LAPAC) Method for Synthetic Aperture Sequences". *Ultrasonic Imaging*

[Lambert et al, 2020] "Distortion matrix approach for ultrasound imaging of random scattering media". *PNAS*

[Bendjador et al, 2020] "The SVD Beamformer: Physical Principles and Application to Ultrafast Adaptive Ultrasound". *IEEE TMI*

Image Enhancement

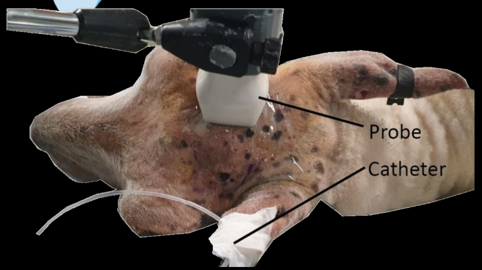


Flavien Bureau


Antoine Coudert

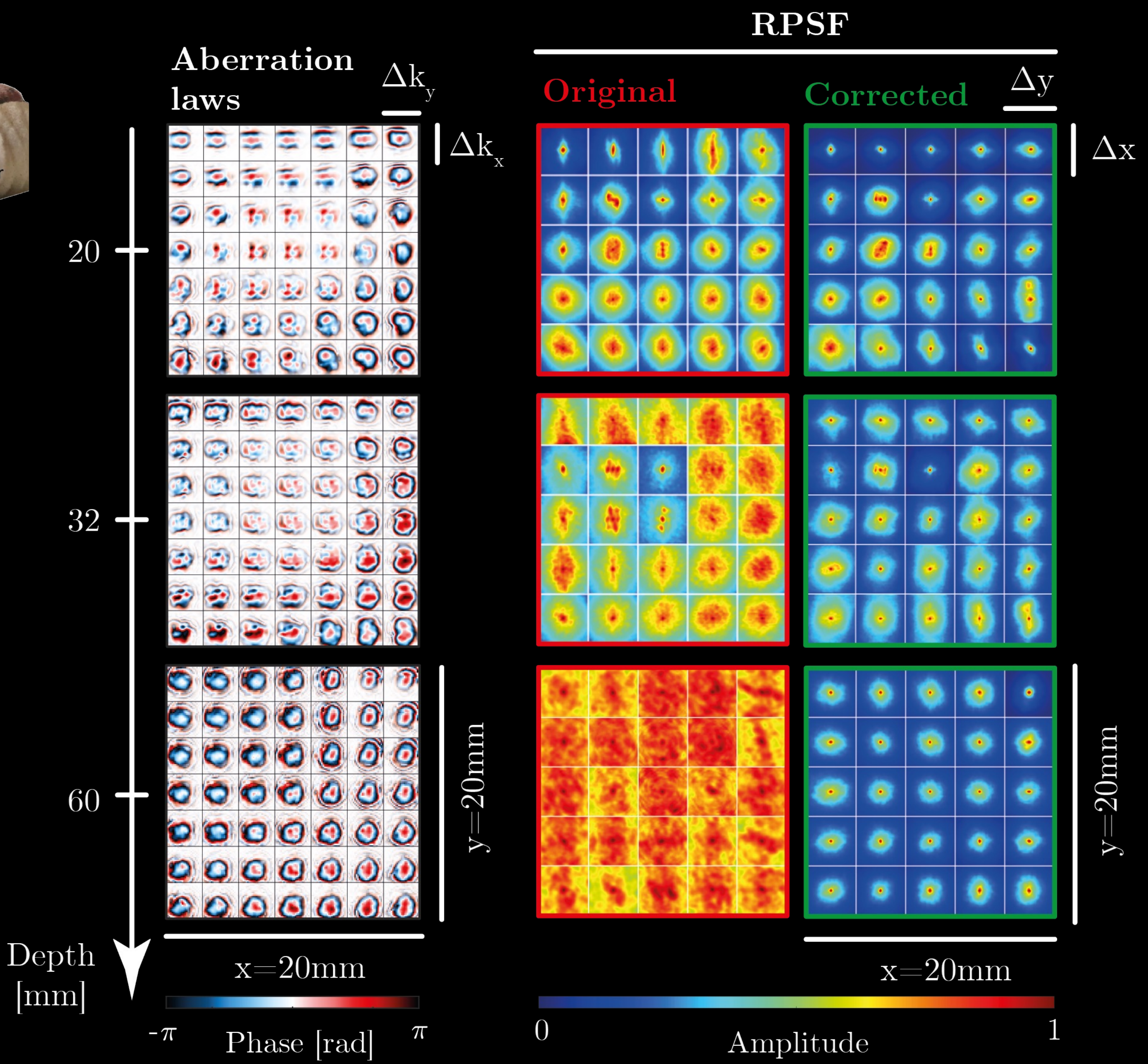

Resolution x3
Contrast +10 dB

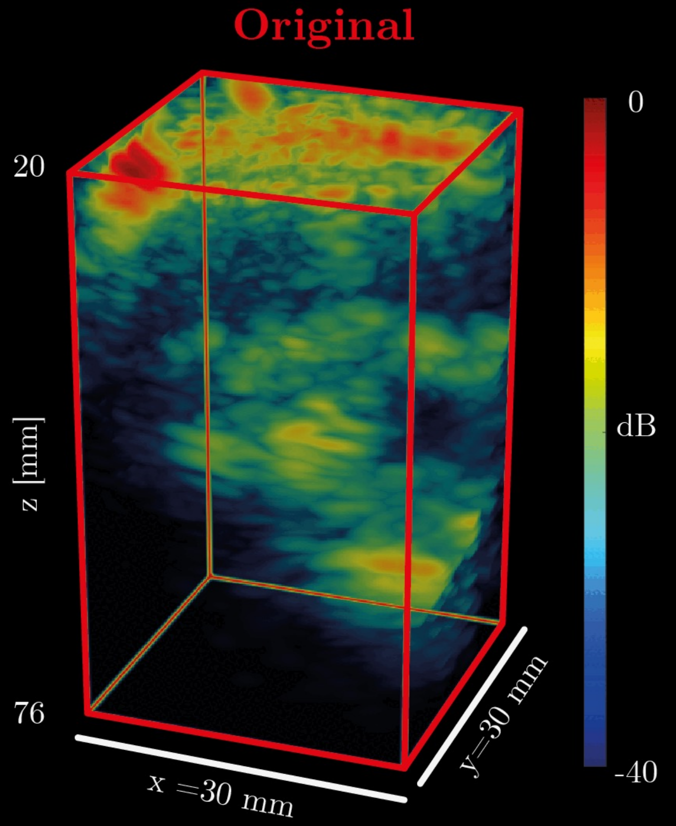

[Bureau et al, 2025] "Ultrasound matrix imaging for 3D transcranial in-vivo localization microscopy", Science Advances (in press) - *arXiv:2410.14499*

Ultrasound Localization Microscopy

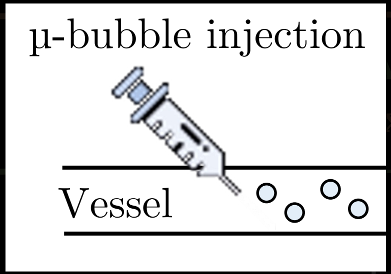

Aberrated PSF

Corrected PSF

Laboratoire d'Imagerie Biomédicale

O. Couture

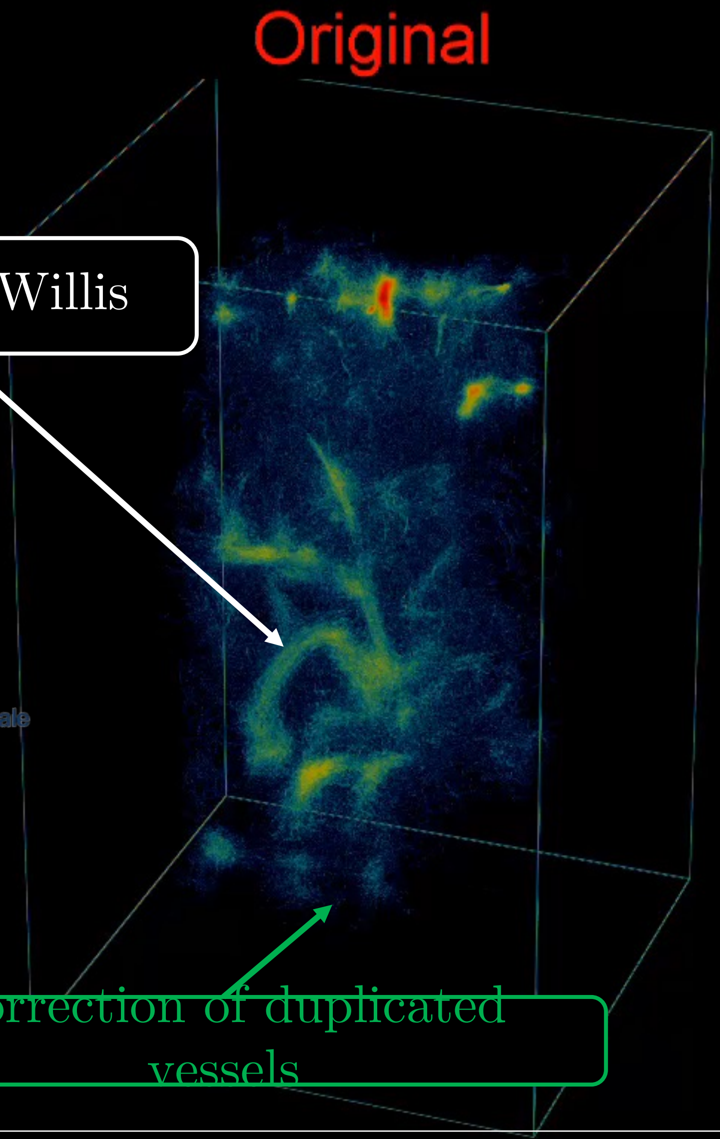

Circle of Willis

Correction of duplicated vessels

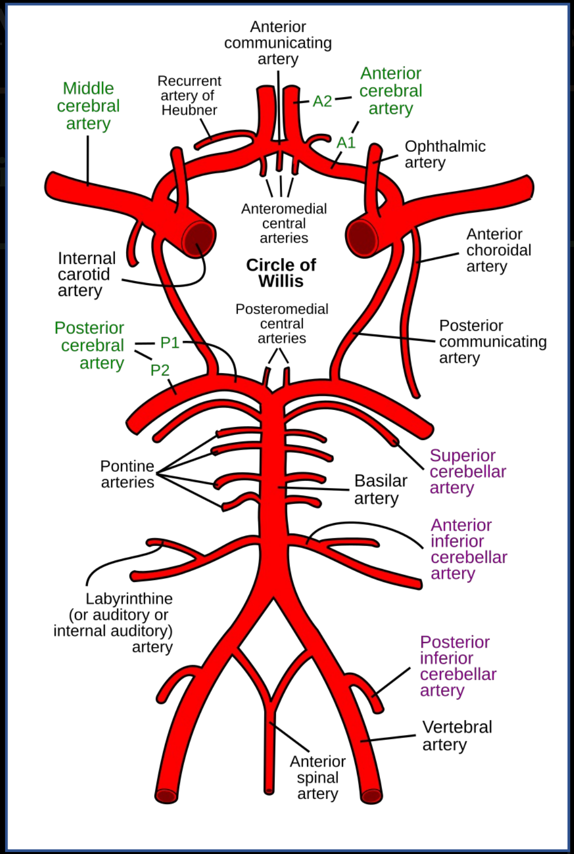

Super-Resolved Image of the Brain Vasculature

[**Errico et al, 2015**] "Ultrafast ultrasound localization microscopy for deep super-resolution vascular imaging", Nature.
[**Bureau et al, 2025**] "Ultrasound matrix imaging for 3D transcranial in-vivo localization microscopy ", Science Advances (in press) - *arXiv:2410.14499.*

Towards Super-Resolution

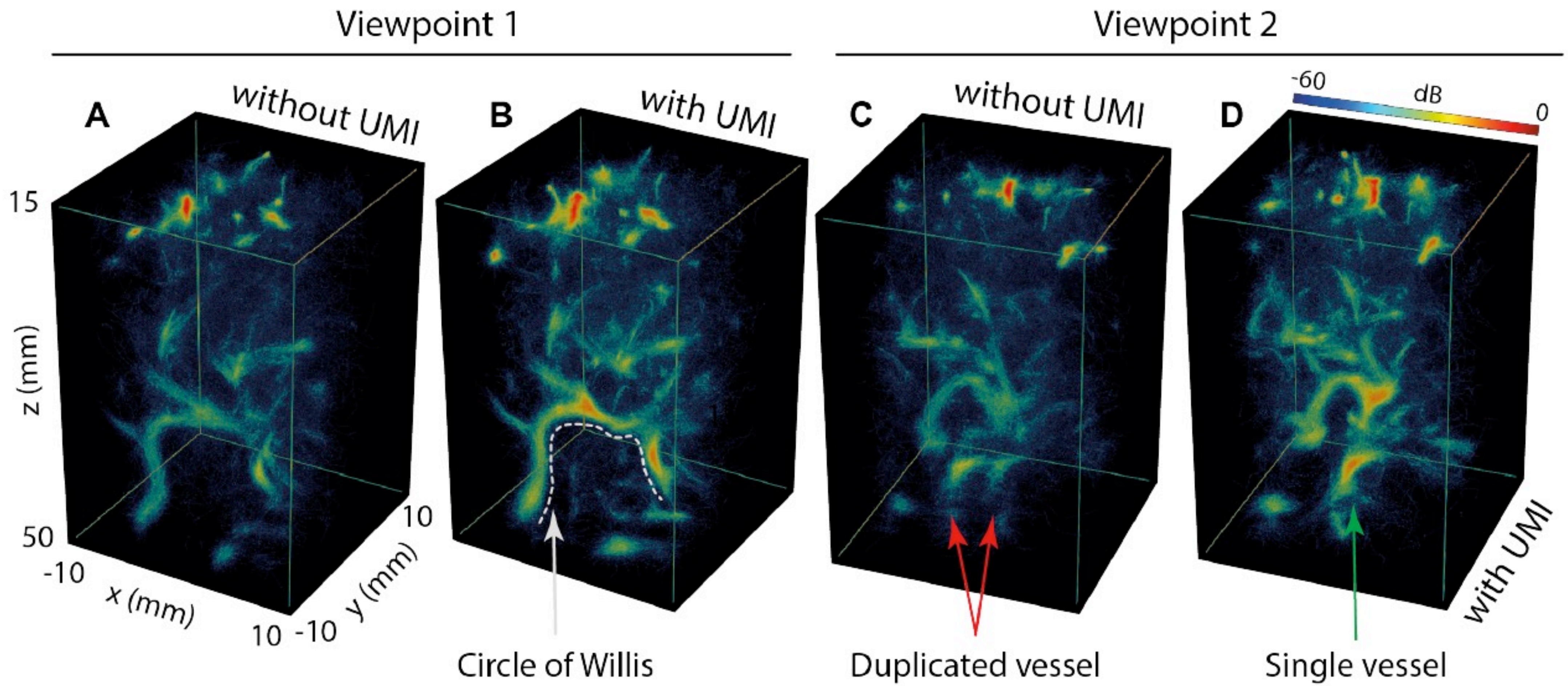

Besides repositioning large vessels, UMI reveals a complex network of small vessels on top of the Willis polygon.

[Bureau et al, 2025] “Ultrasound matrix imaging for 3D transcranial in-vivo localization microscopy”, *Science Advances* (in press) - *arXiv:2410.14499.*

Beating Diffraction

Passive Seismic Matrix Imaging

Elsa Giraudat

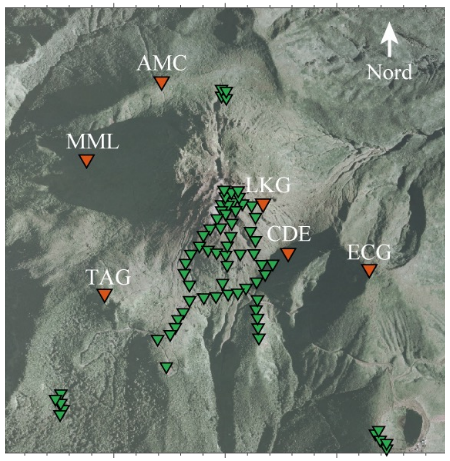

Arnaud Burtin & Jean-Christophe Komorowski

IPGP
INSTITUT DE PHYSIQUE DU GLOBE DE PARIS

OVSG

Passive Seismology

Passive Seismic Imaging – Analysis of ambient seismic noise

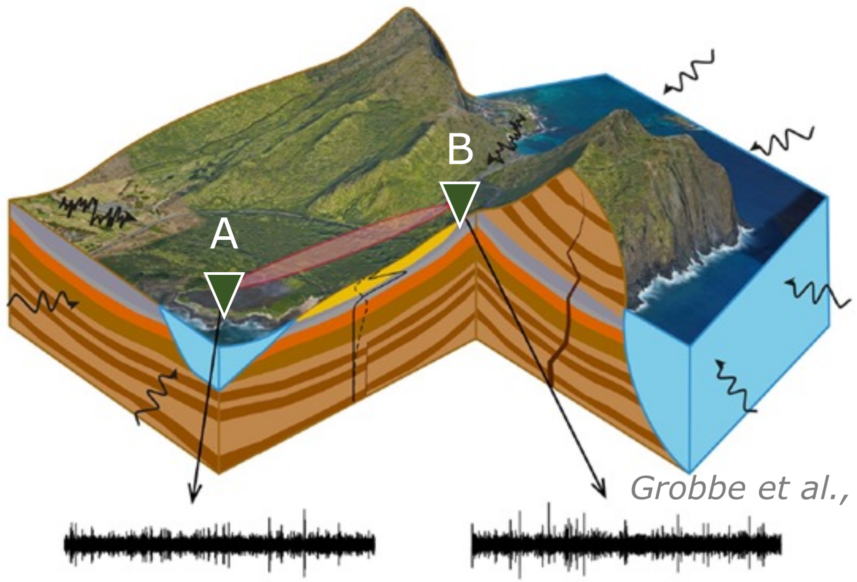

Grobbe et al., 2021

Seismic noise sources:

- Natural: wind, precipitation, ocean, volcanic activities,…
- Anthropic: transport, industrial activities,…

[Lobkis and Weaver, 2001] « On the Emergence of the Green's Function in the Correlations of a Diffuse Field. » *JASA*
[Campillo and Paul, 2003] « Long-Range Correlations in the Diffuse Seismic Coda. » *Science*
[Wapenaar 2004] « Retrieving the Elastodynamic Green's Function of an Arbitrary Inhomogeneous Medium by Cross-Correlation. » *PRL*
[Shapiro et al., 2004] « Emergence of Broadband Rayleigh Waves from Correlations of the Ambient Seismic Noise. » *GRL*

Passive Seismology in Reflection

Passive Seismic Imaging – Analysis of ambient seismic noise

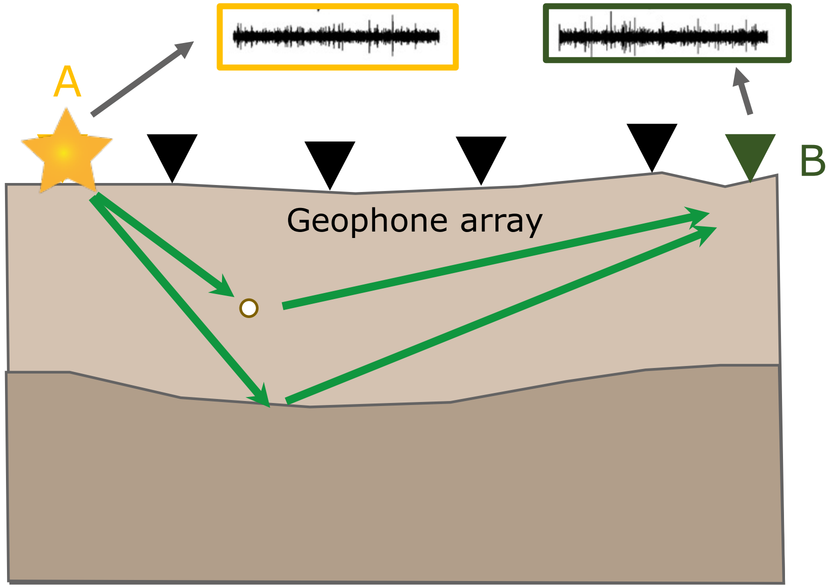

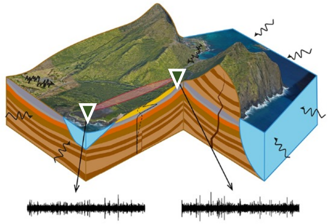

1. Recording of seismic noise
2. Cross-correlation

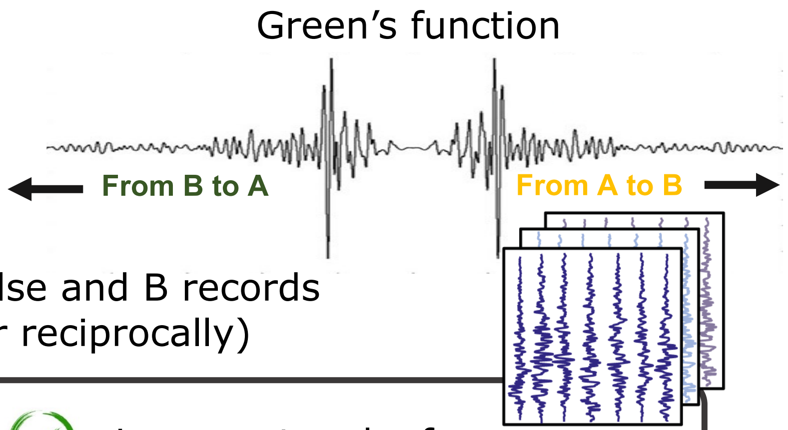

~ equivalent to: A emits a pulse and B records the induced wave-field (or reciprocally)

- ✓ No active source
- ✓ Large network of sensors
- ✓ Lower environmental impact
- ✓ More flexibility ⇒ volcano

Seismic noise correlation can provide the Earth response associated with the geophone network

[Lobkis and Weaver, 2001] « On the Emergence of the Green's Function in the Correlations of a Diffuse Field. » *JASA*

[Campillo and Paul, 2003] « Long-Range Correlations in the Diffuse Seismic Coda. » *Science*

[Wapenaar 2004] « Retrieving the Elastodynamic Green's Function of an Arbitrary Inhomogeneous Medium by Cross-Correlation. » *PRL*

[Shapiro et al., 2004] « Emergence of Broadband Rayleigh Waves from Correlations of the Ambient Seismic Noise. » *GRL*

Reflection Seismology

Specular Reflection

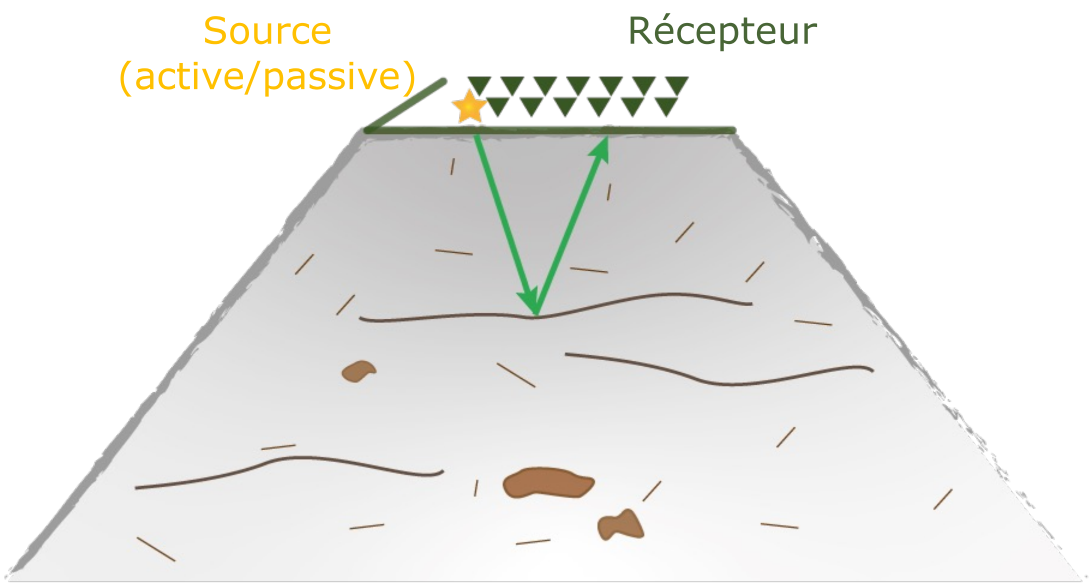

Interface between geological units, rocks *etc.*

Scattering

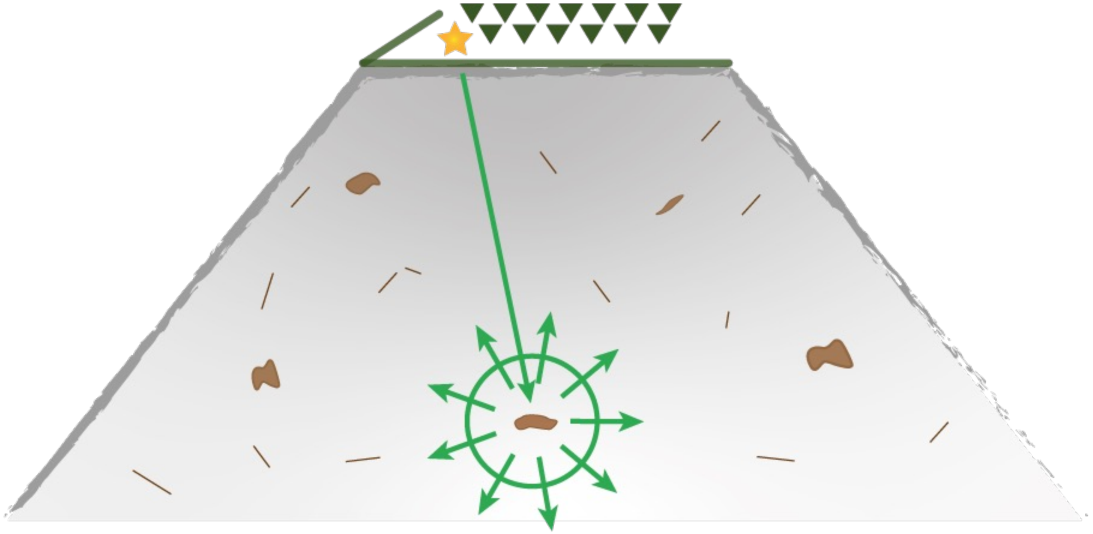

Local variations of density and/or elasticity

Heterogeneous rocks, damaged areas, fractures, fluids *etc.*

The presence of scatterers can allow the imaging of complex structures such as volcanoes or fault areas

Limits of conventional migration techniques

Propagation Model

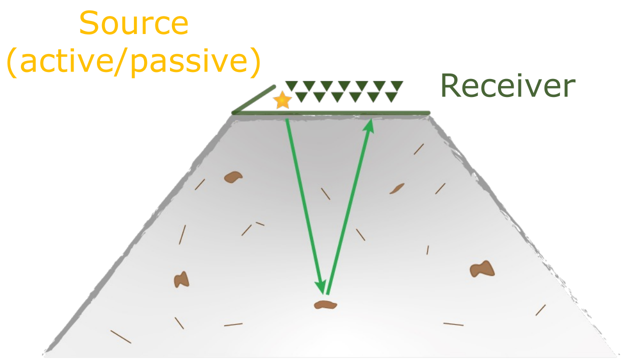

Homogeneous wave velocity model
Single scattering regime

Depth ∝ Echo Time
$z = c_0 t/2$

Reality

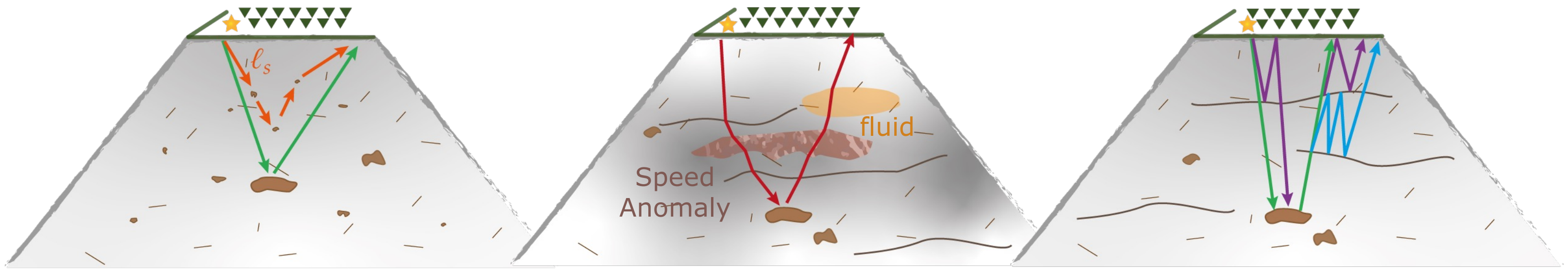

Multiple scattering

Heterogeneous velocity
Phase distorsions

Multiple reflections

~~Depth ∝ Echo Time~~
$\cancel{z = c_0 t/2}$

Loss of Resolution and Contrast

Same issues in ultrasound and seismic imaging.

⇒ Exploit Matrix Imaging to overcome those limits

Passive Imaging of *La Soufrière*

La Soufrière of Guadeloupe

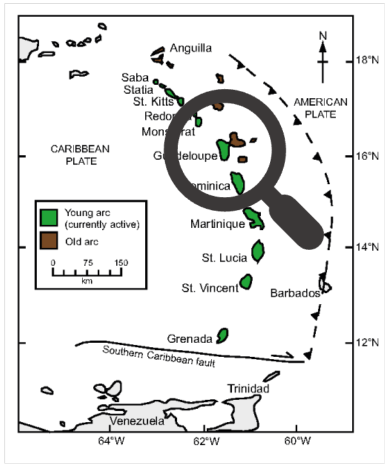

Array of 76 geophones

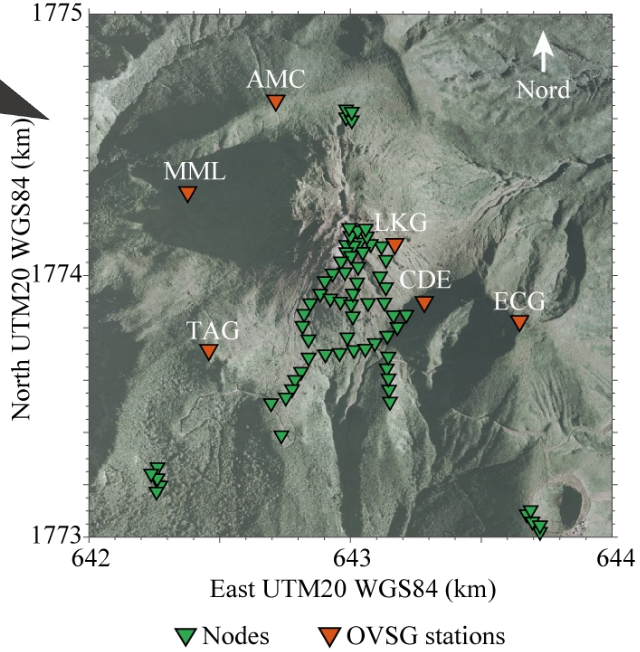

- Inter-station distance $\lambda/2 \sim 50$ m
- Correlations of seismic noise over 2 months (ZZ)
- Frequency bandwidth $[10 - 20]$ Hz

Reflection Matrix $\mathbf{R_{gg}} = [R(\mathbf{g}_{\mathrm{out}}, \mathbf{g}_{\mathrm{in}}, t)]$
in the geophone basis

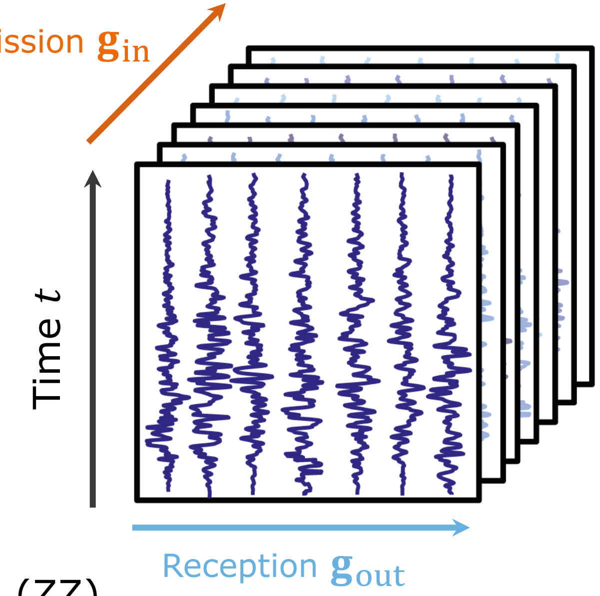

Passive Measurement of the Reflection Matrix

Seismic data collected and cross-correlations processed by Arnaud Burtin

[Burtin et al., 2018] Dense Seismic Monitoring of La Soufrière de Guadeloupe Hydrothermal System. *https://www.fdsn.org/networks/detail/ZK_2017/*
[IPGP 2021] Data collection of the seismological and volcanological observatory of Guadeloupe *https://doi.org/10.18715/GUADELOUPE.OVSG*

Redatuming Process

Geophone Array

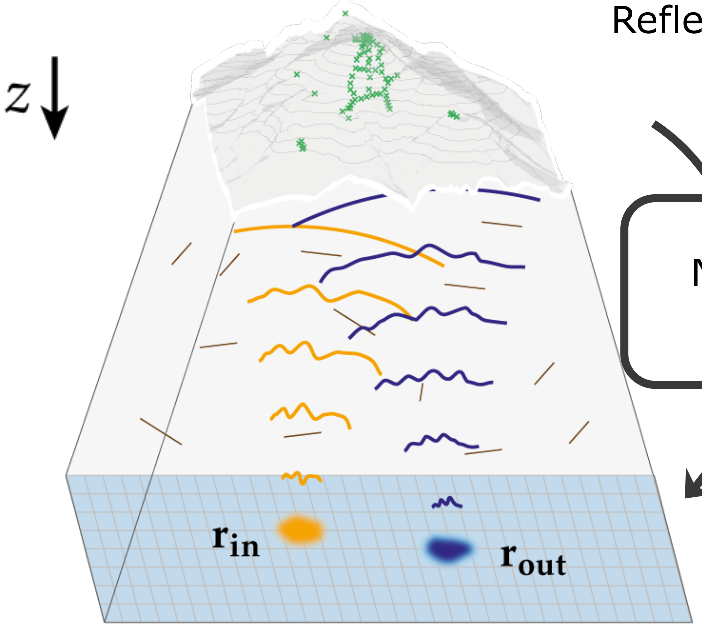

Focal plane at depth z

Reflection Matrix
$\mathbf{R_{gg}}$

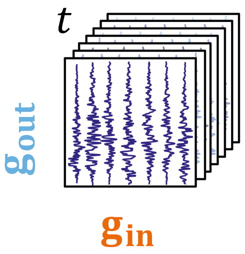

Numerical Focusing | wave velocity model $c_0(z)$
= *Redatuming*

Focused Reflection Matrix
(Ballistic time)

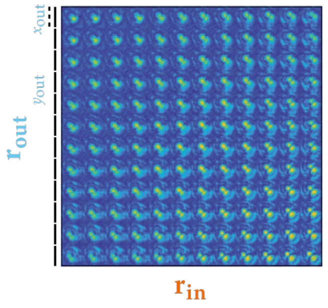

velocity model c_0

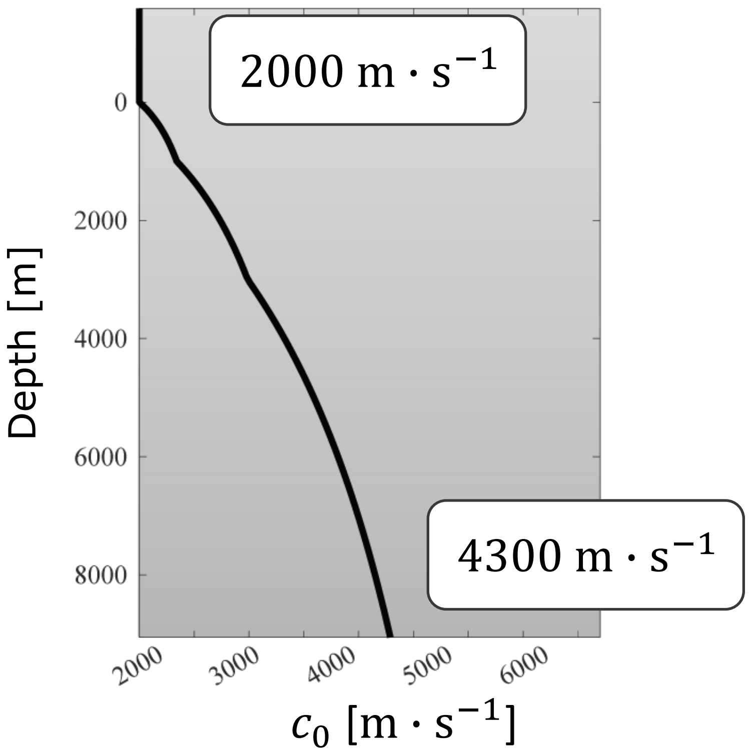

[Dorrel et al., 1979] « Coupes sismiques des structures superficielles dans les petites antilles - I: Guadeloupe ». *Pure and Applied Geophysics*

[Berryhill, 1984] " Wave-Equation Datuming Before Stack." *Geophysics*

[Berkout and Wapenaar, 1993] "A Unified Approach to Acoustical Reflection Imaging. II: The Inverse Problem." *JASA*

[Blondel et al., 2018] " Matrix Approach of Seismic Imaging: Application to the Erebus Volcano, Antarctica." *JGR Solid Earth*

Focused Reflection Matrix

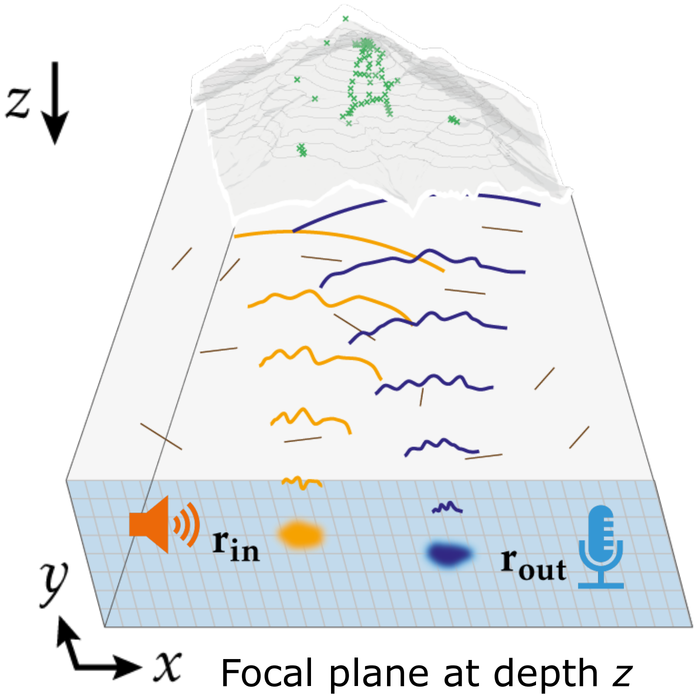

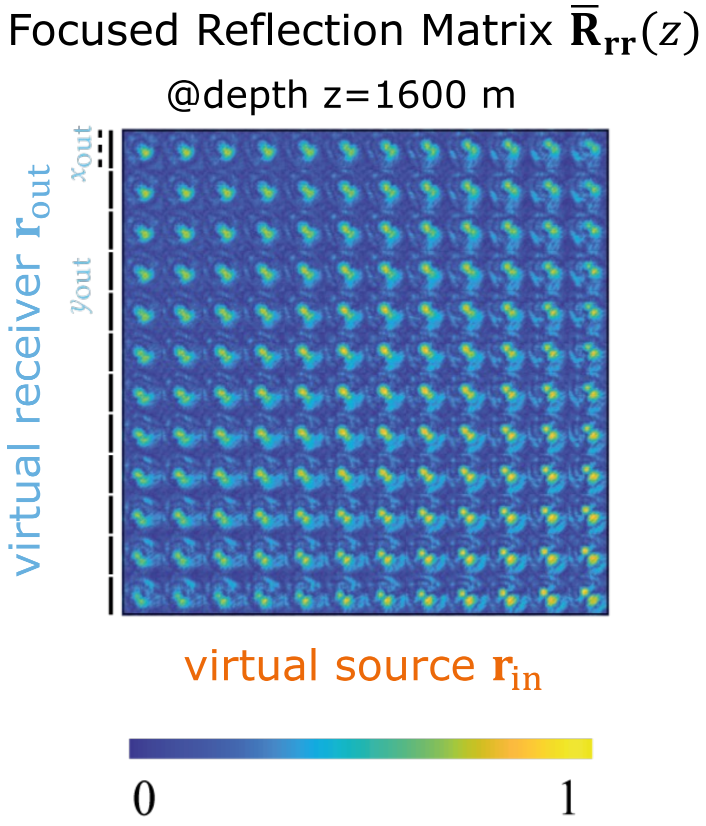

The focused reflection matrix contains the impulse responses between **virtual** geophones in the underground

[Blondel et al., 2018] " Matrix Approach of Seismic Imaging: Application to the Erebus Volcano, Antarctica." *JGR Solide Earth*

[Touma et al., 2021] "A distortion matrix framework for high-resolution passive seismic 3-D imaging: application to the SJFZ, California." *GJI*

Focused Reflection Matrix

Geophone Array

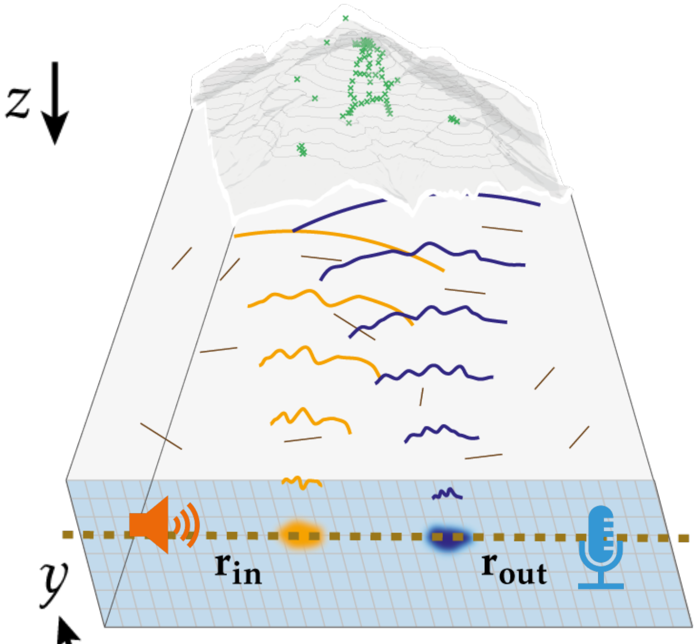

Focal plane at depth z

Focused Reflection Matrix $\overline{\mathbf{R}}_{\mathbf{rr}}(z)$

@depth z=1600 m

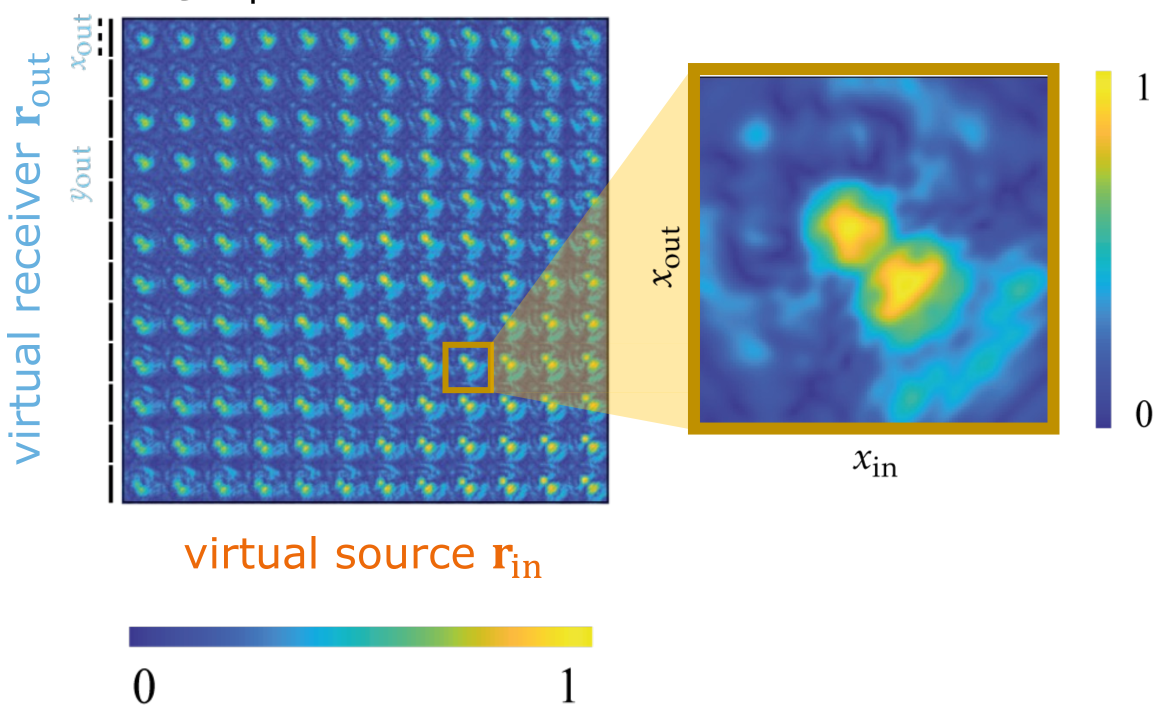

The focused reflection matrix contains the impulse responses between **virtual** geophones in the underground

[Blondel et al., 2018] " Matrix Approach of Seismic Imaging: Application to the Erebus Volcano, Antarctica." *JGR Solid Earth*
[Touma et al., 2021] "A distortion matrix framework for high-resolution passive seismic 3-D imaging: application to the SJFZ, California." *GJI*

Confocal Image (reflectivity)

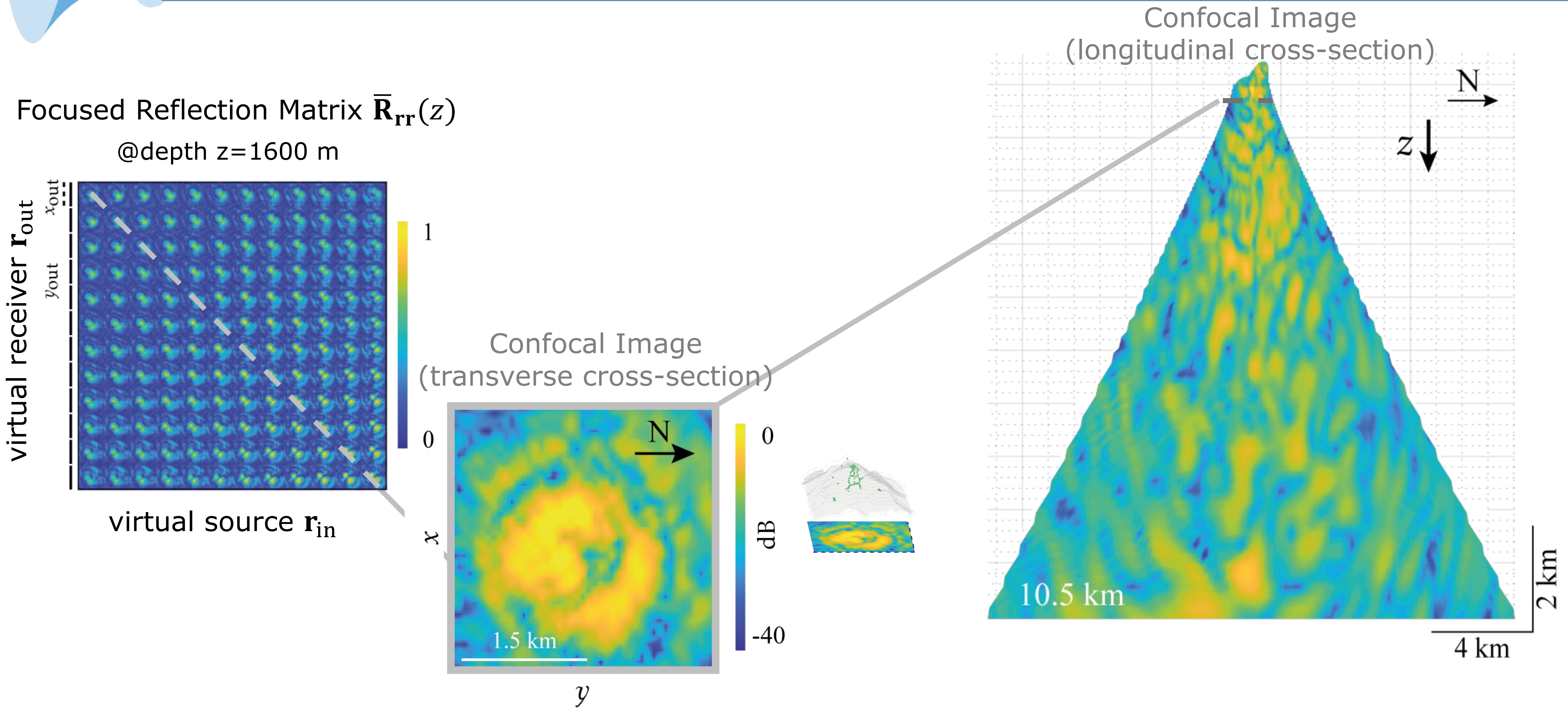

[Blondel et al., 2018] " Matrix Approach of Seismic Imaging: Application to the Erebus Volcano, Antarctica." *JGR Solide Earth*

[Touma et al., 2021] "A distortion matrix framework for high-resolution passive seismic 3-D imaging: application to the SJFZ, California." *GJI*

Focusing Quality

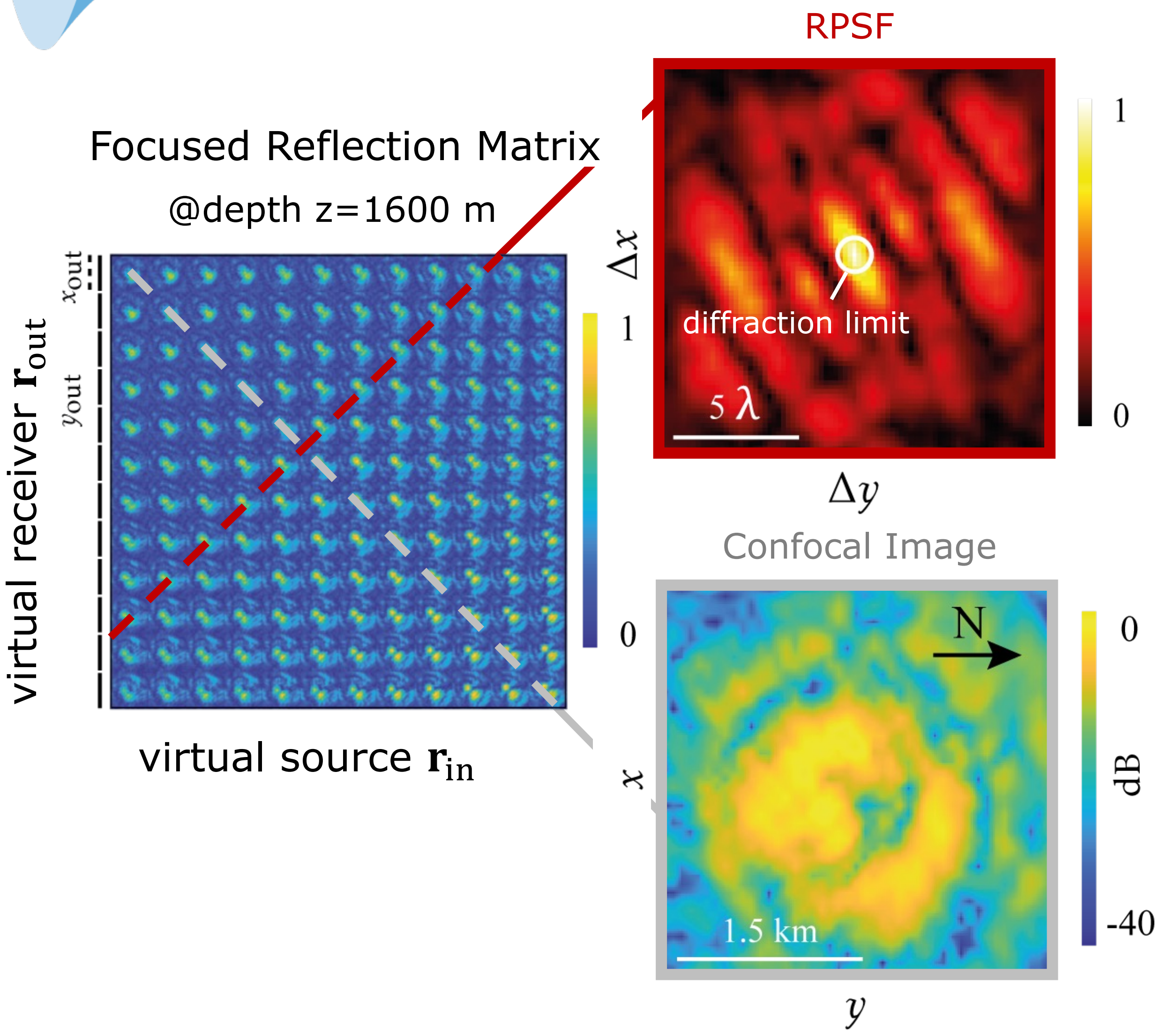

Focusing quality
(sparse medium)

$$\boxed{\mathrm{RPSF} \propto \mathrm{PSF_{in}}(-\Delta\mathbf{r})\times\mathrm{PSF_{out}}(\Delta\mathbf{r})}$$

input focusing

output focusing

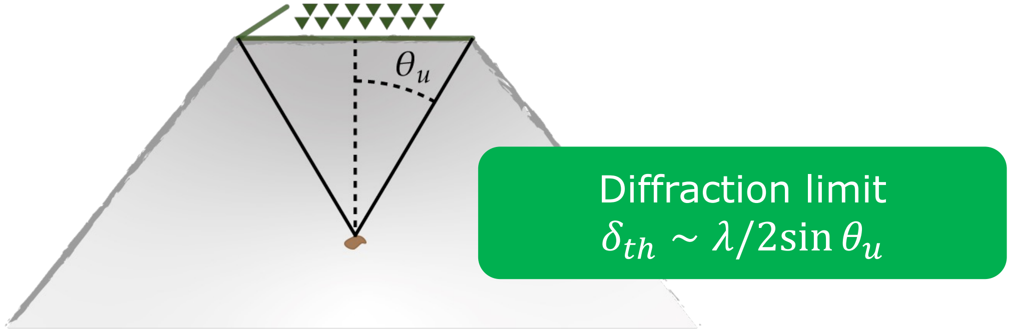

The inaccuracy of the wave velocity model hampers wave focusing and prevents the visualization of the volcano internal structure

[Blondel et al., 2018] " Matrix Approach of Seismic Imaging: Application to the Erebus Volcano, Antarctica." *JGR Solid Earth*

[Touma et al., 2021] "A distortion matrix framework for high-resolution passive seismic 3-D imaging: application to the SJFZ, California." *GJI*

Focusing quality

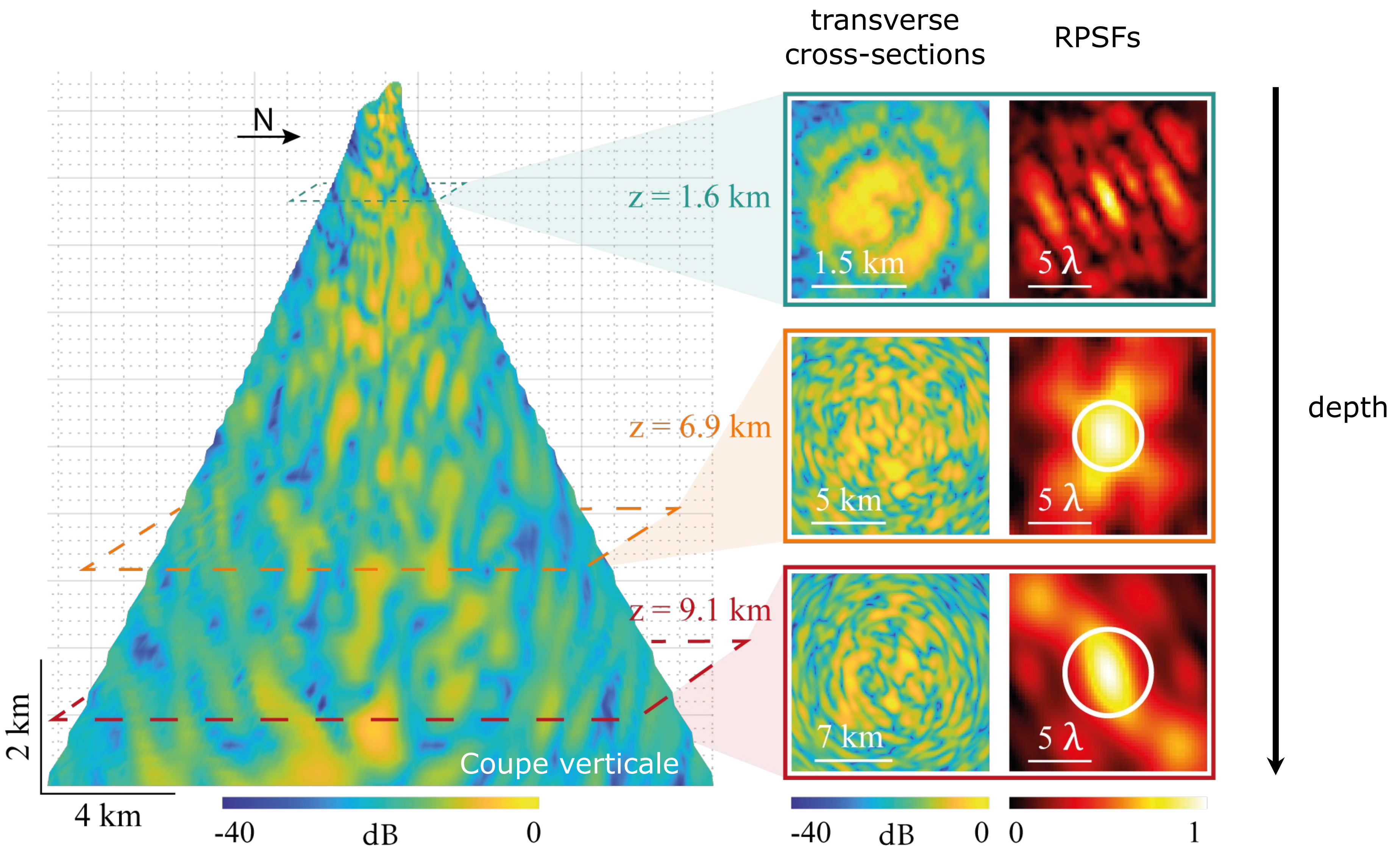

Aberration laws from the Earth surface

Dual reflection matrix
$\bar{R}\,(\mathbf{u}_{out}, \mathbf{r}_{in})$

Projection

Focused reflection matrix $\bar{R}\,(\mathbf{r}_{out}, \mathbf{r}_{in})$

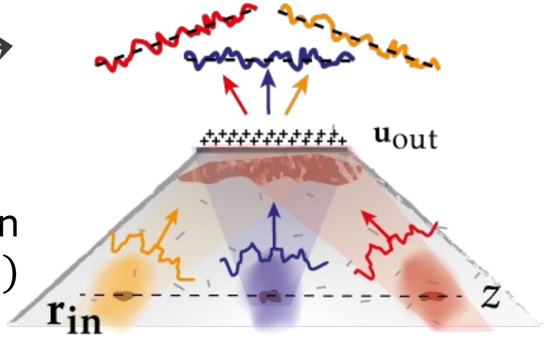

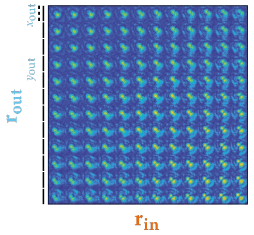

Earth surface basis $(\mathbf{u})$

Dense and regular virtual geophone network

reflected wave-front geometric component

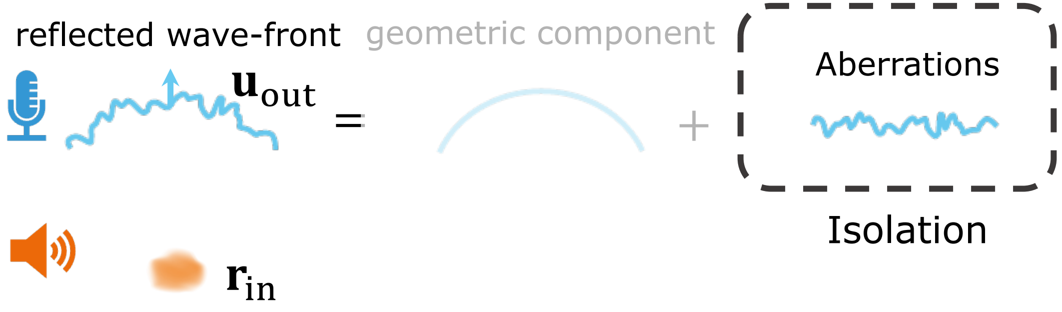

Isolation

virtual source

Aberration laws from the Earth surface

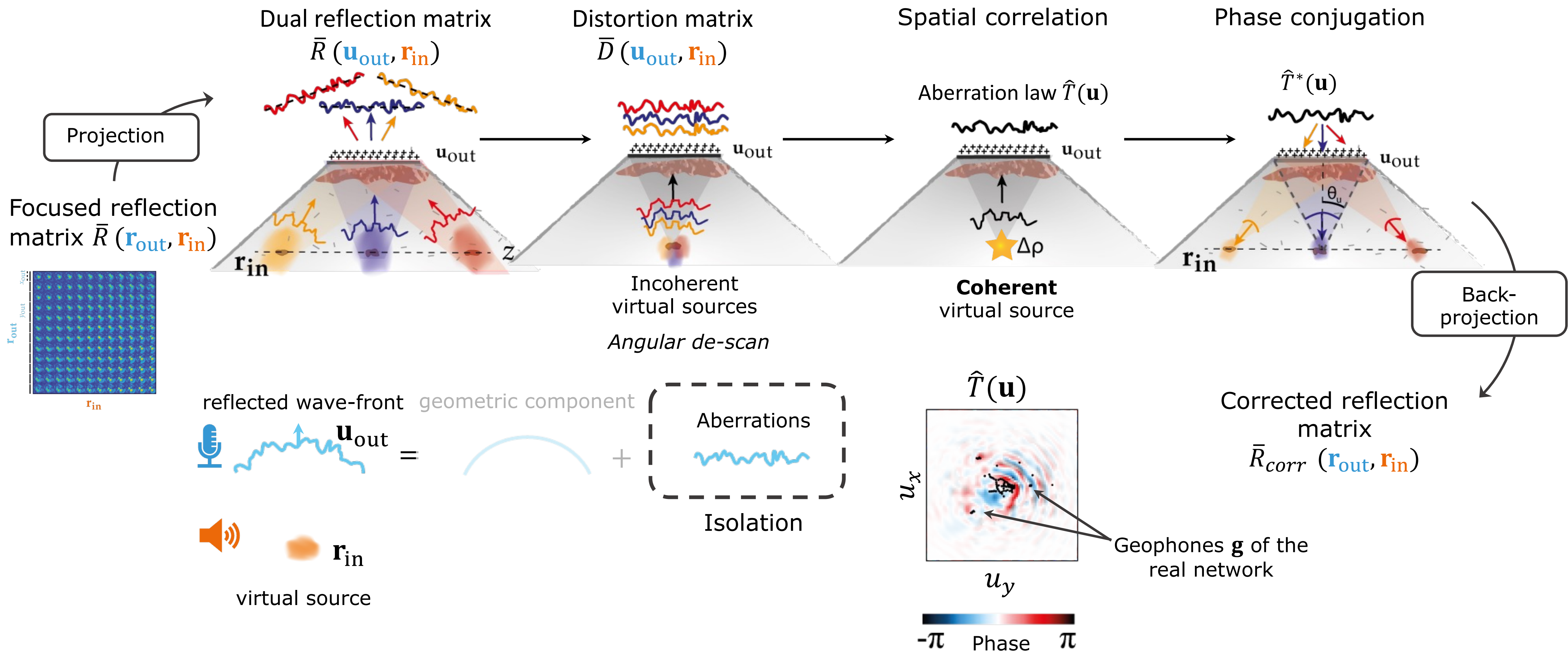

Aberration compensation from the Earth surface

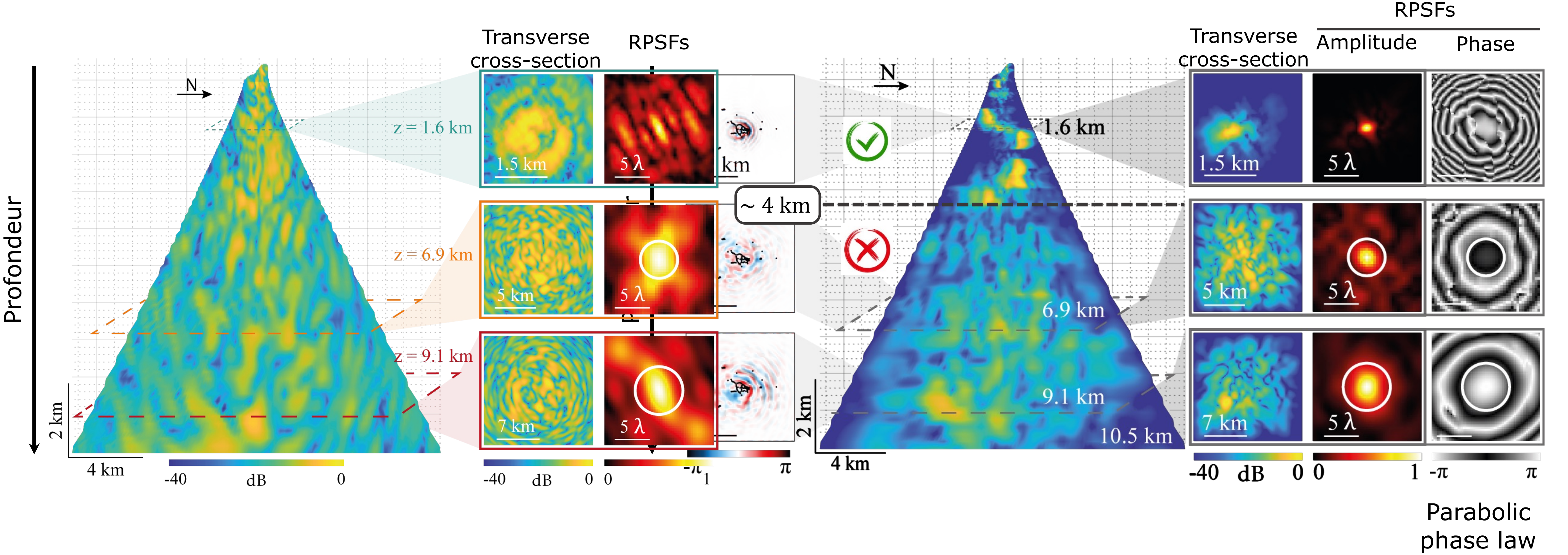

The resolution dictated by the network aperture is not sufficient to visualize the internal structure of the volcano beyond 4 km-depth

[Giraudat et al., 2024] "Matrix imaging as a tool for high-resolution monitoring of deep volcanic plumbing systems with seismic noise." *Communications, Earth & Environment*

Analysis of wave distortions from Fourier basis

Analysis of the wave-field in the plane wave basis ($\mathbf{k}$)

$\bar{R}\,(\mathbf{k}_{\text{out}}, \mathbf{r}_{\text{in}})$

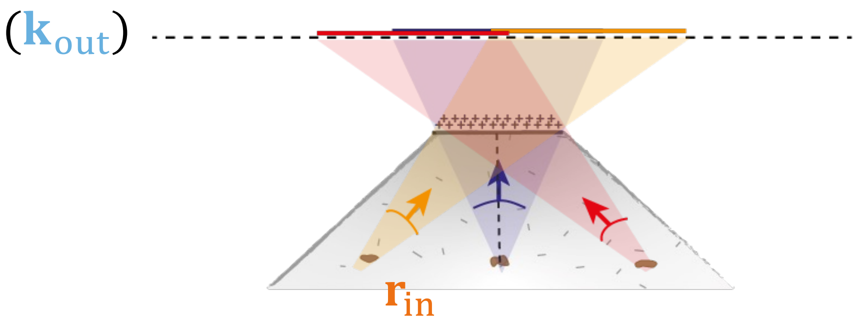

sparse medium:
Few isolated scatterers
at each depth

Analysis of wave distortions from Fourier basis

Analysis of the wave-field in the plane wave basis ($\mathbf{k}$)

$\bar{R}\,(\mathbf{k}_{\mathrm{out}}, \mathbf{r}_{\mathrm{in}})$

$(\mathbf{k}_{\mathrm{out}})$

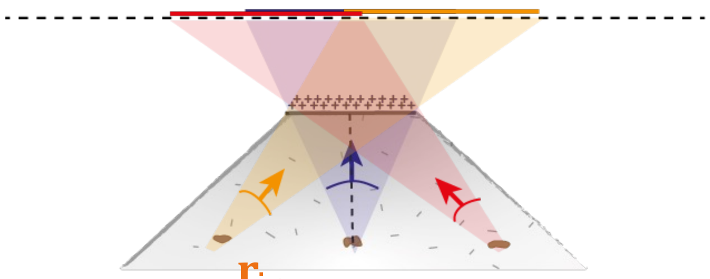

$\mathbf{r}_{\mathrm{in}}$

Distortions

$\bar{D}\,(\mathbf{k}_{\mathrm{out}}, \mathbf{r}_{\mathrm{in}})$

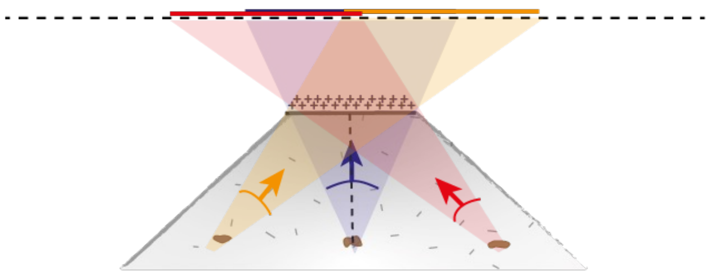

Lateral *de-scan*

sparse medium:
Few isolated scatterers
at each depth

Projection of each scatterer contribution on different parts of the spatial frequency spectrum

$\Downarrow$

Anisoplanicity

Analysis of wave distortions from Fourier basis

Analysis of the wave-field in the plane wave basis ($\mathbf{k}$)

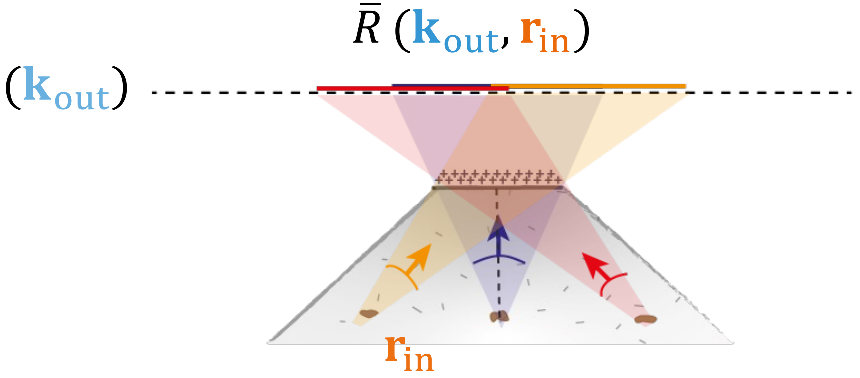

Distortions

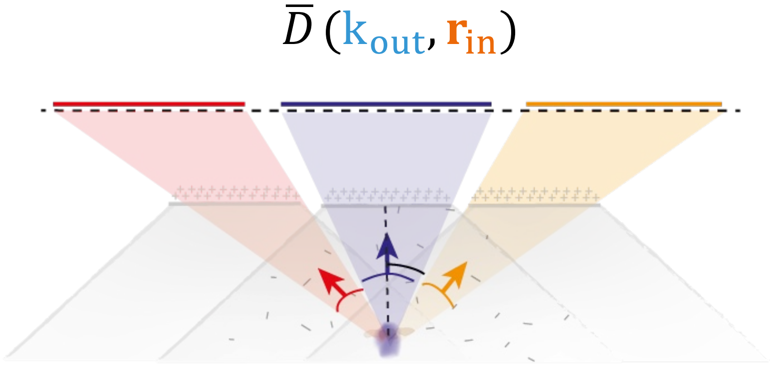

Lateral de-scan

Milieu **sparse**
Quelques diffuseurs isolés à chaque profondeur

Projection of each scatterer contribution on different parts of the spatial frequency spectrum

Fresnel Rings

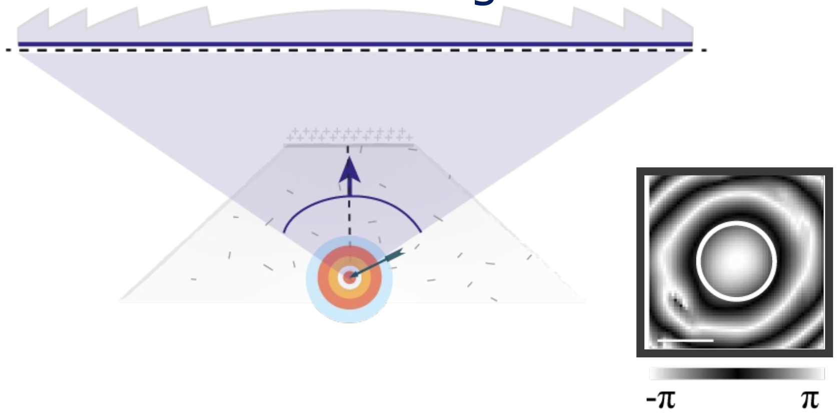

Parabolic phase law

PSF modulation by high spatial frequencies

⇒ Virtual increase of the geophone network aperture

Focusing law ($\mathbf{k}$)

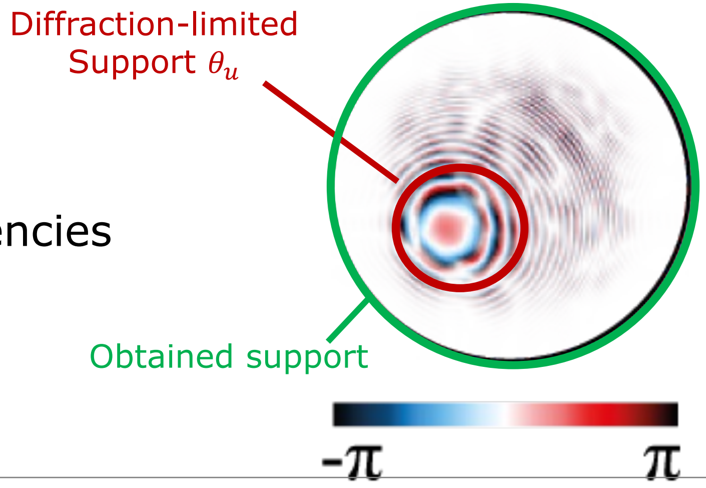

Diffraction Compensation from the Fourier basis

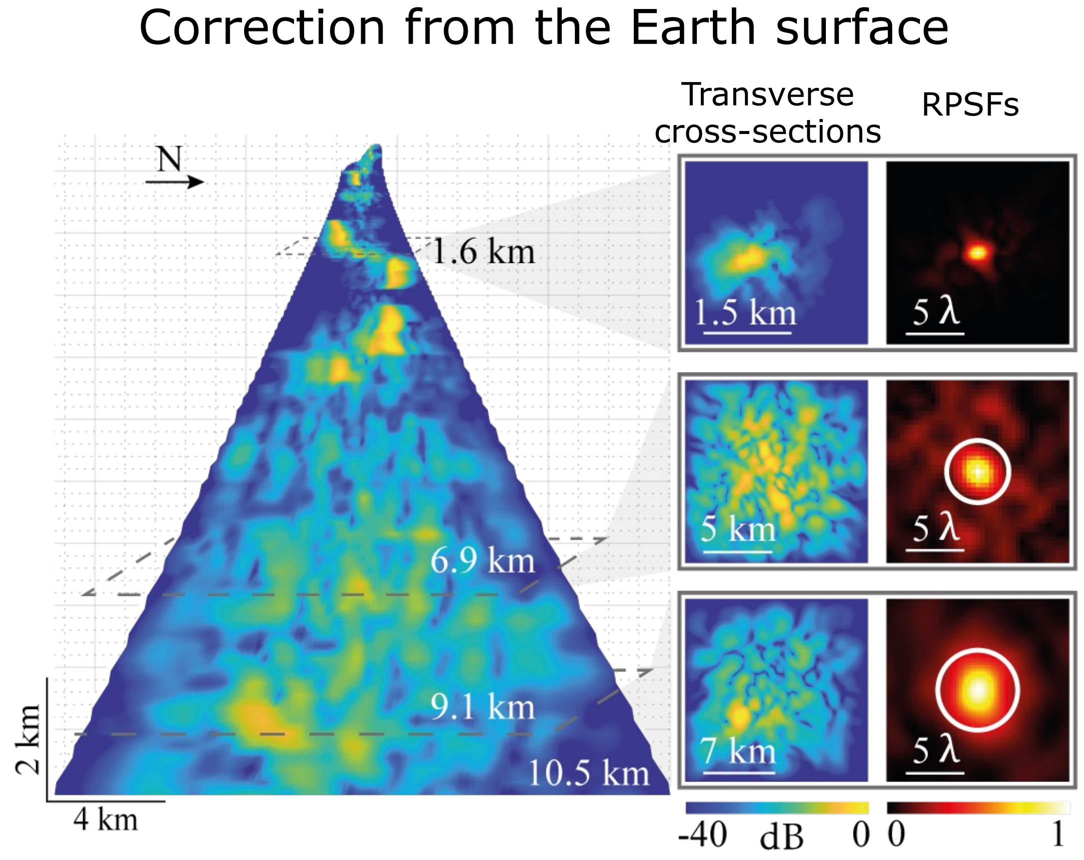

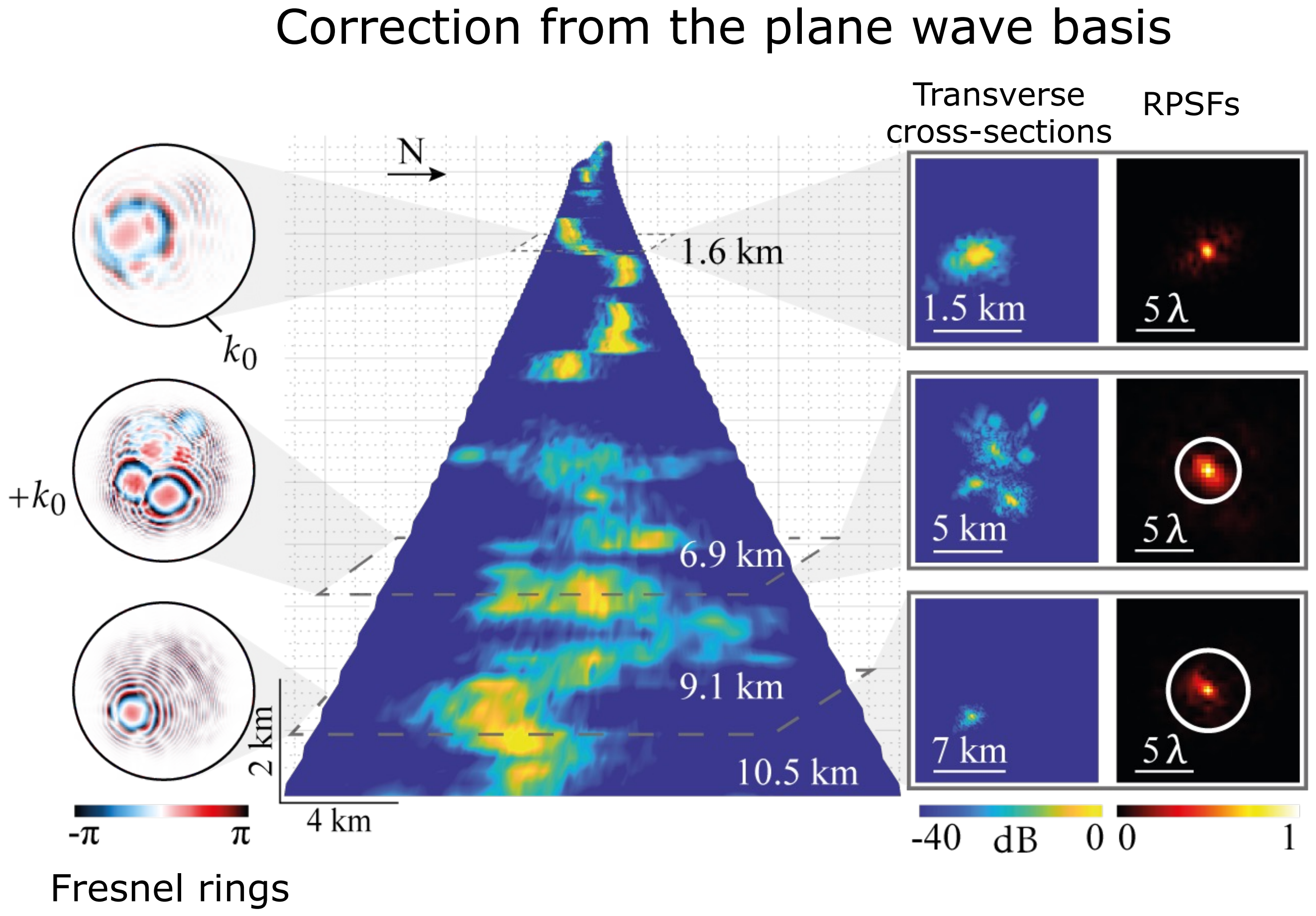

Correction from the plane wave basis provides a resolution of the order of $\lambda/2$ over the whole field-of-view

Three-dimensional image

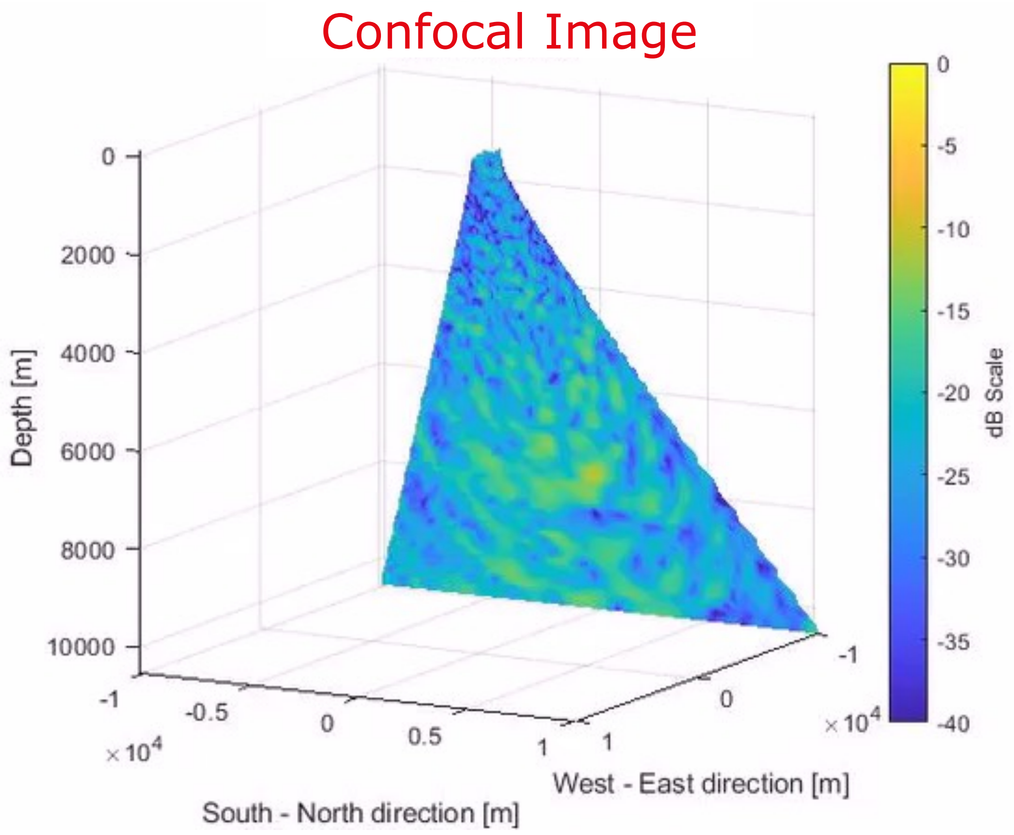

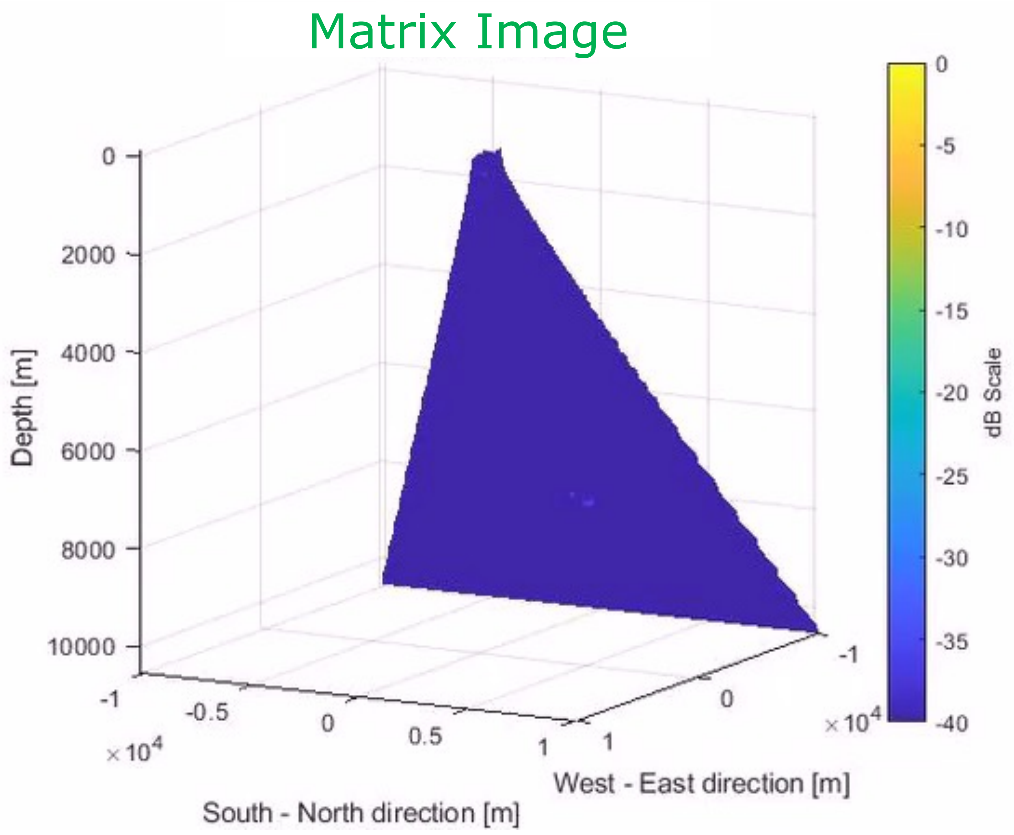

[Giraudat et al., 2024] "Matrix imaging as a tool for high-resolution monitoring of deep volcanic plumbing systems with seismic noise." *Communications, Earth & Environment*

Three-dimensional isosurface

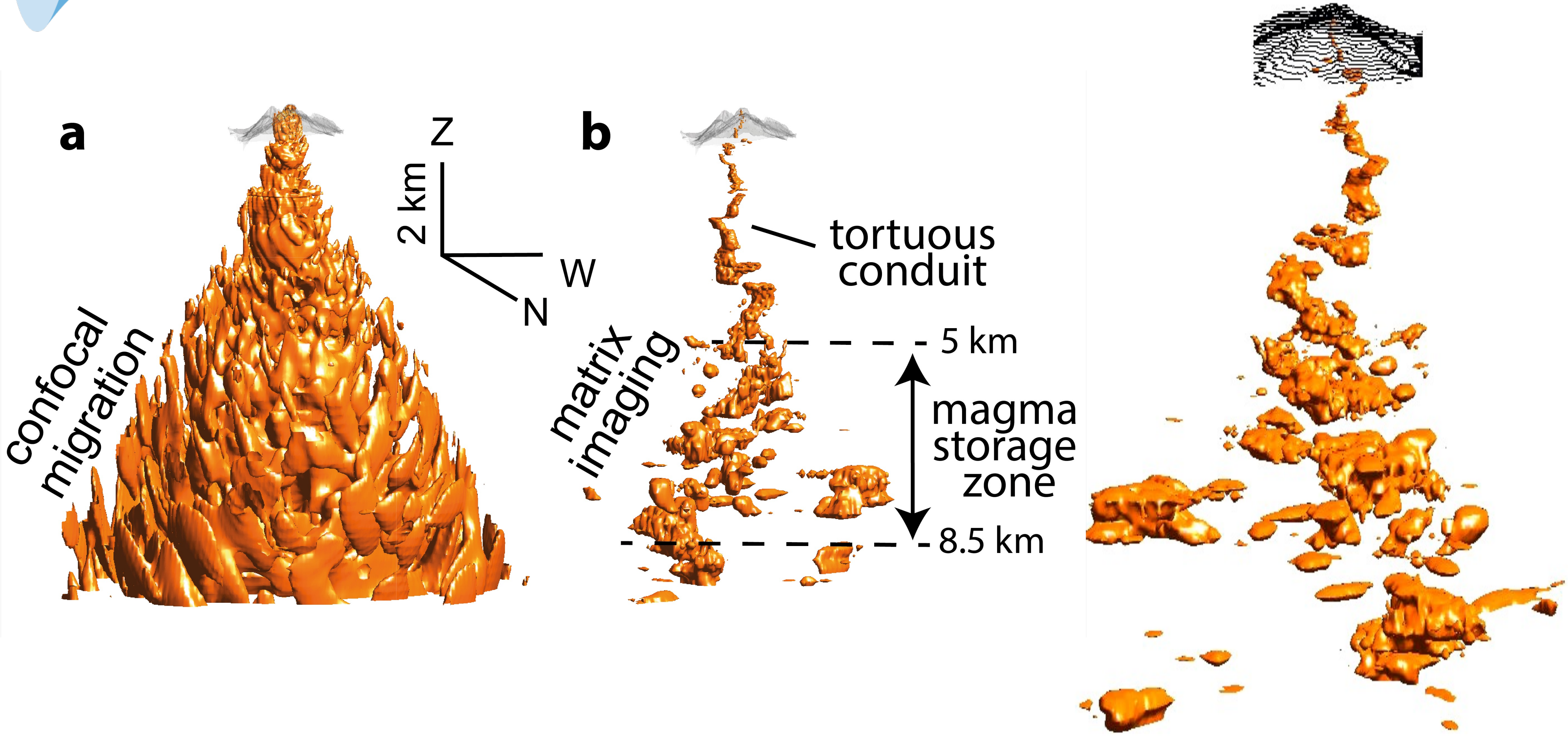

Internal structure of the volcano

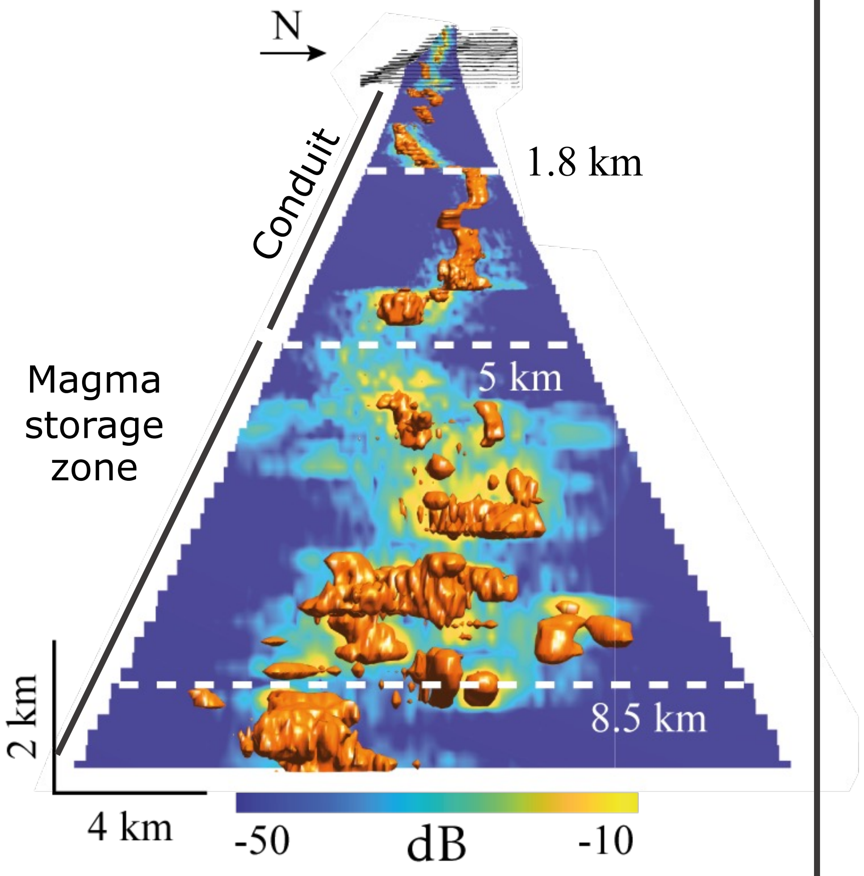

Unique magmatic chamber

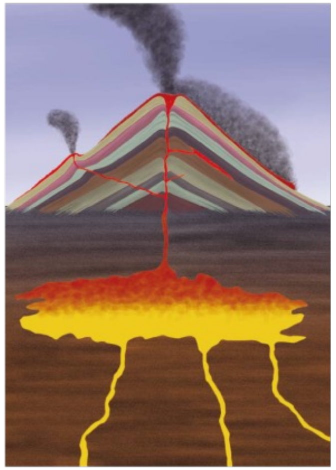

Caricchi et al., 2015

Transcrustal magmatic system vertically-arranged piles of lenses of magmatic mushes

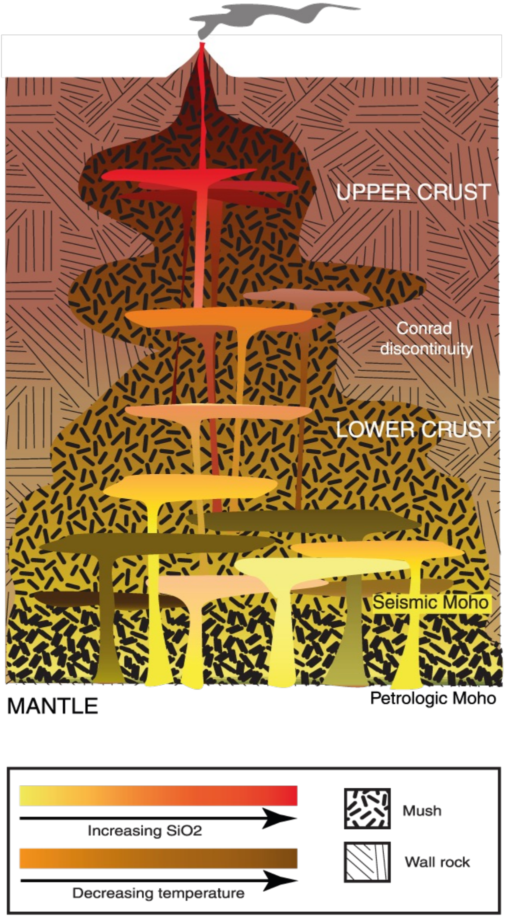

Cashman et al., 2017

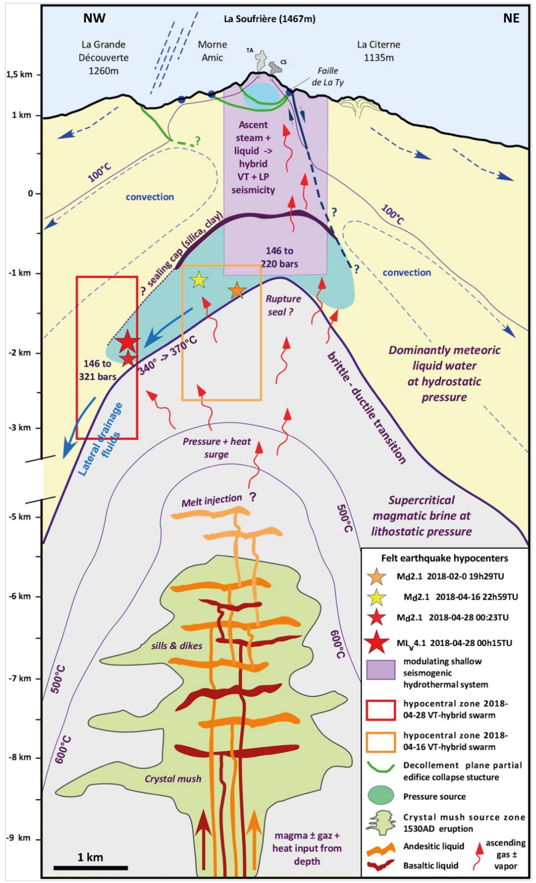

Moretti et al., 2020

Conceptual views

[Caricchi & Blundy, 2015] " The Temporal Evolution of Chemical and Physical Properties of Magmatic Systems." *GS*

[Cashman et al., 2017] "Vertically Extensive and Unstable Magmatic Systems: A Unified View of Igneous Processes." *Science*

[Moretti et al., 2020] "The 2018 Unrest Phase at La Soufrière of Guadeloupe Andesitic Volcano: Scrutiny of a Failed but Prodromal Phreatic Eruption." *JVGR*

High-Resolution Imaging of Fault Areas

San Jacinto (California)

M. Campillo
(ISTERRE)

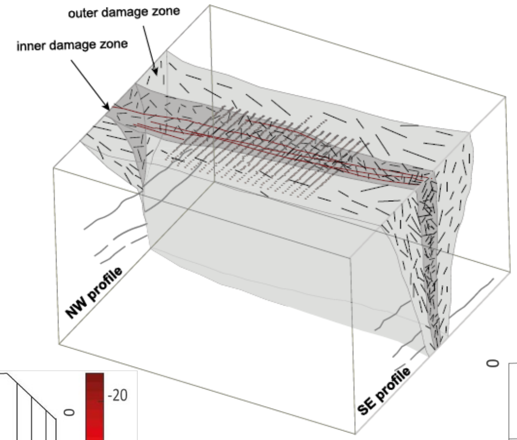

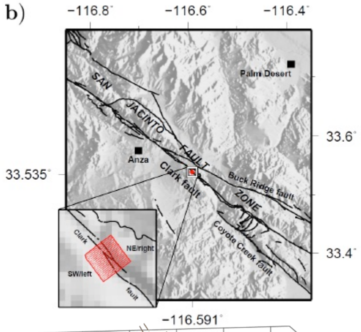

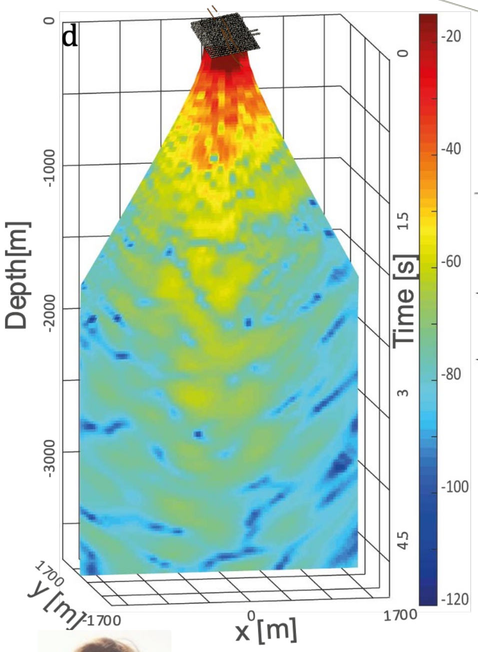

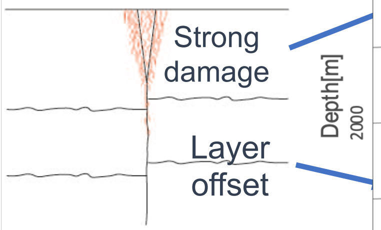

10-20 Hz

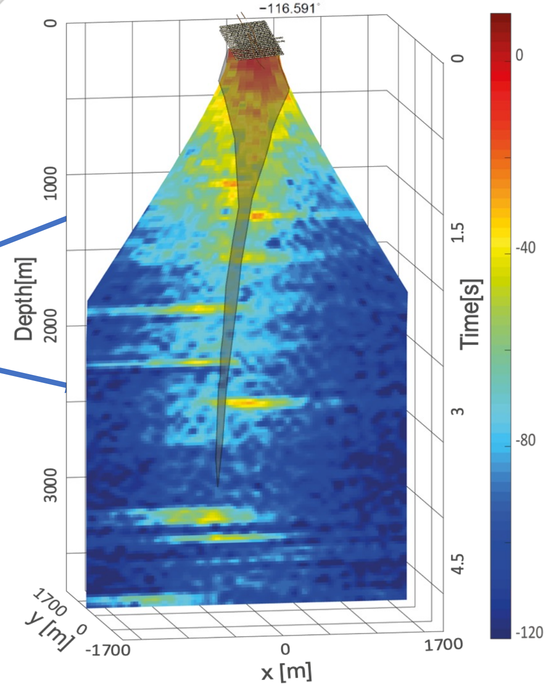

R. Touma

Revealing the fault position in depth

R. Touma, T. Blondel, A. Derode, M. Campillo, A. Aubry, Geophys J. Int. (2021)
R. Touma, A. Aubry, Y. Ben-Zion, M. Campillo, EPSL (2022)

North Anatolian Fault (Turkey)

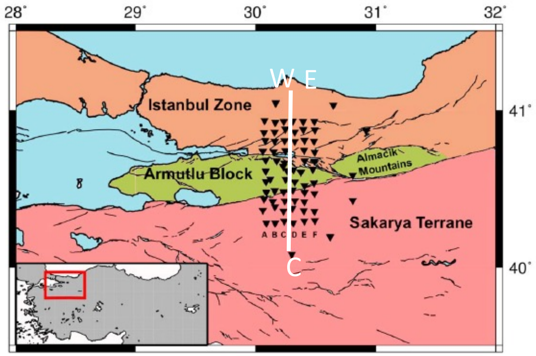

Taylor et al. 2016

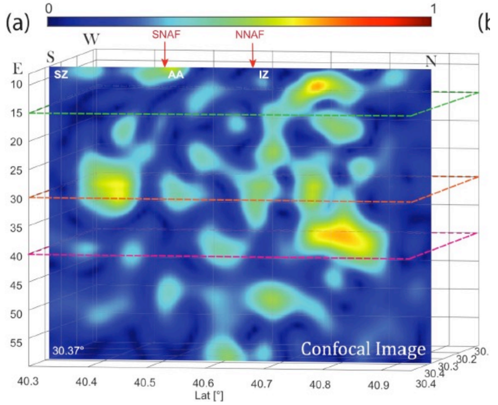

0.1-0.5 Hz

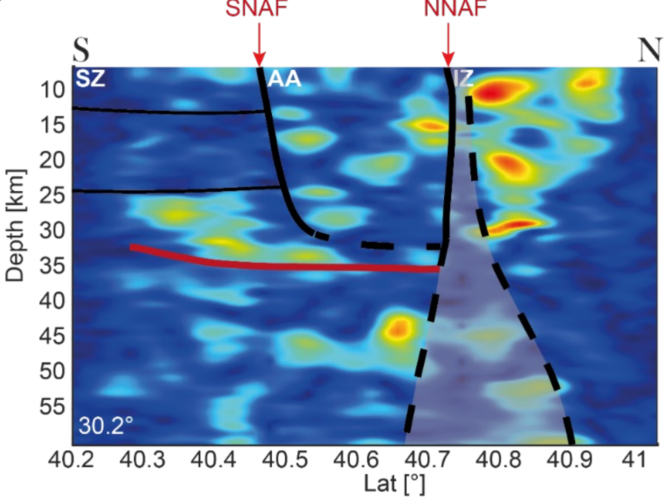

Revealing the Moho
and the geological blocks in depth

R. Touma, A. Le Ber, M. Campillo, A. Aubry, JGR: Solid Earth (2023)

Advantages and Limits of Matrix Imaging

- **Robust** to **data quality** and **rough velocity model** in contrast with full wave-form inversion
- Scalar model (P- or S-wave) – Mode conversion not taken into account
- No compensation of wave velocity dispersion and reverberations, so far…

Seismic imaging

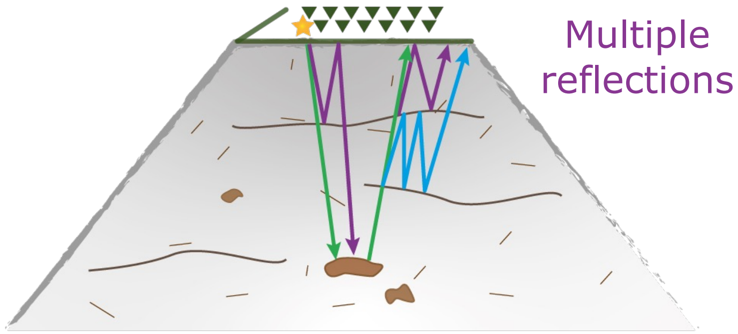

Multi-layered geological structure

Ultrasound imaging

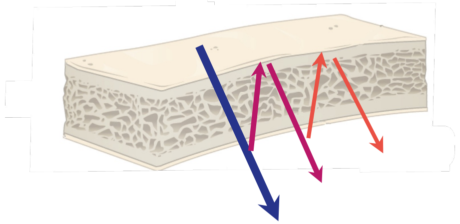

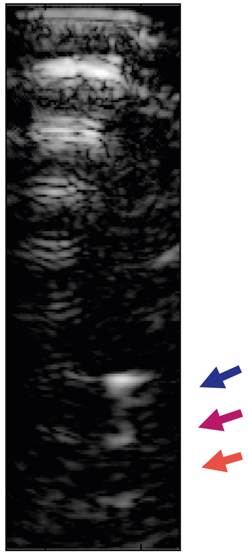

Transcranial imaging

Deep Optical Imaging

Harnessing Forward Multiple Scattering

Ulysse Najar

Paul Balondrade

Victor Barolle

N. Guigui

Deep Optical Imaging ($10\ell_s$)

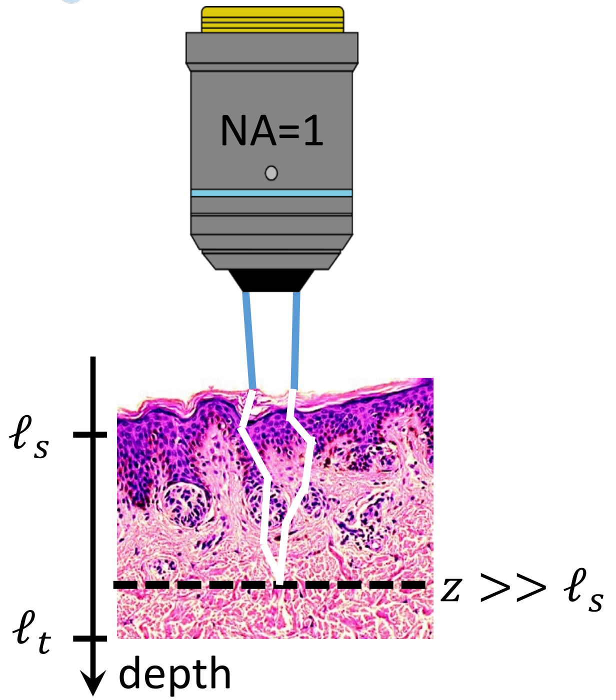

ℓ_s: scattering mean free path
ℓ_t: transport mean free path

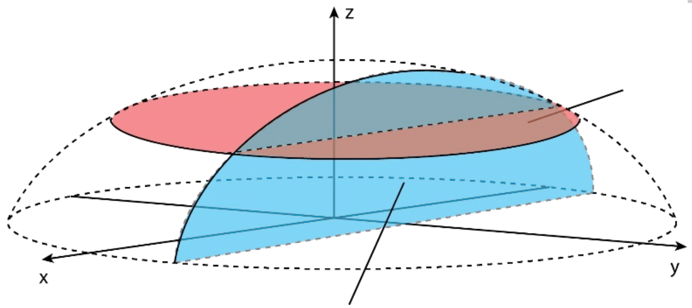

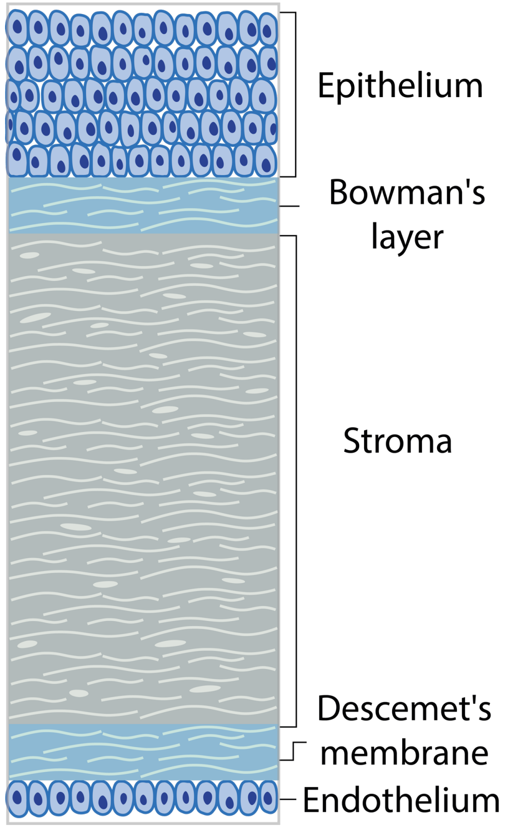

350-µm-thick extremely opaque human cornea ℓ_s~35 µm

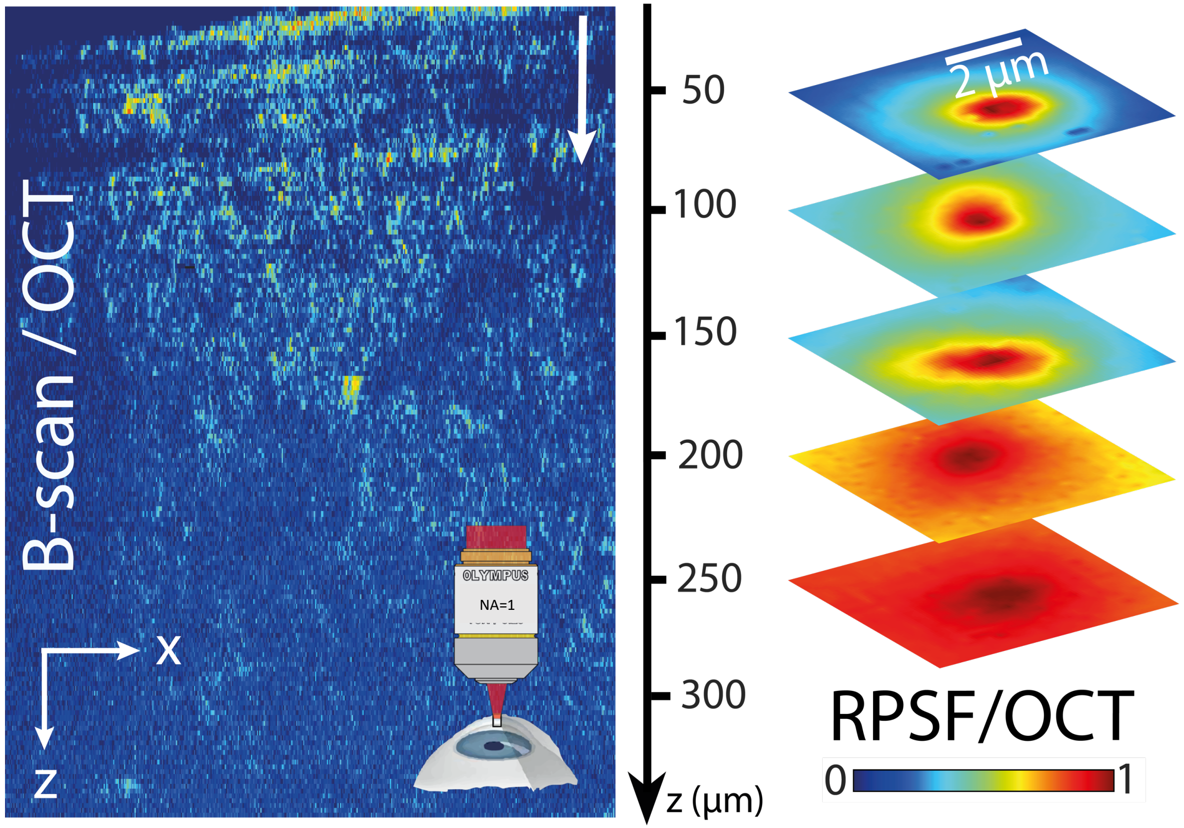

OCT image is strongly impacted by aberrations and multiple scattering

U. Najar *et al.*, Nat. Commun., 2024

Full-field Compensation of Aberrations

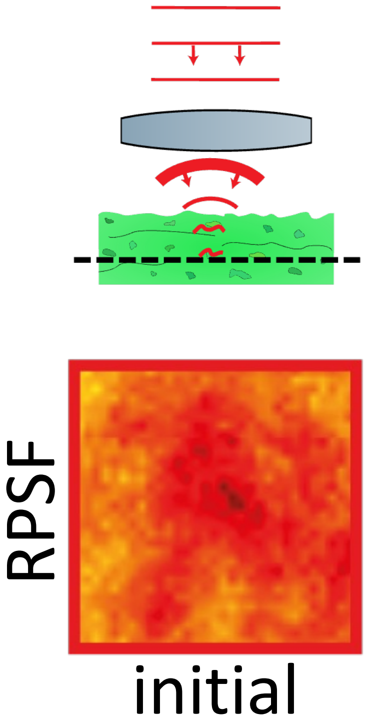

U. Najar *et al.*, Nat. Commun., 2024

Full-field Compensation of Aberrations

Aberration transmittance

$\mathcal{T}(\boldsymbol{u})$

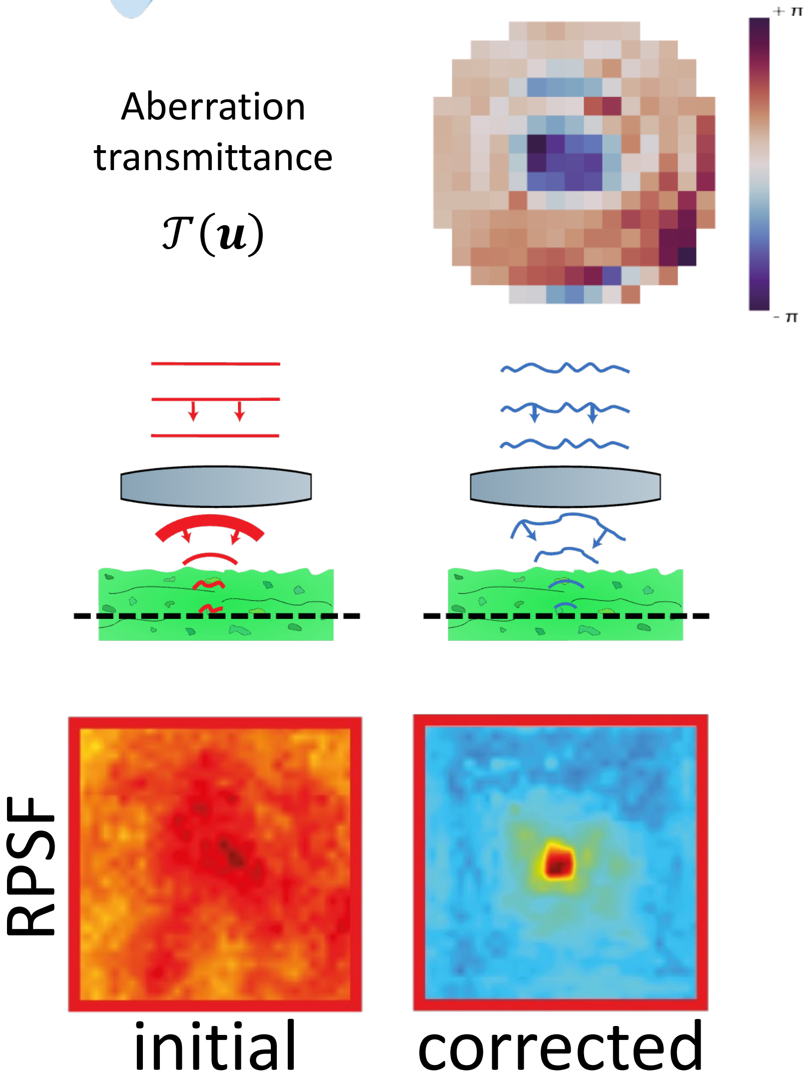

U. Najar *et al.*, Nat. Commun., 2024

Full-field Compensation of Aberrations

Aberration transmittance

$\mathcal{T}(\boldsymbol{u})$

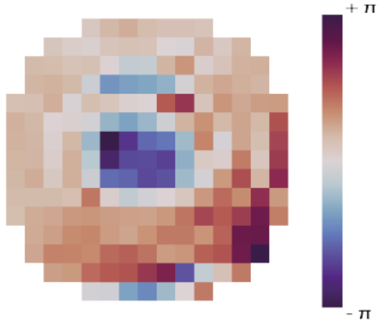

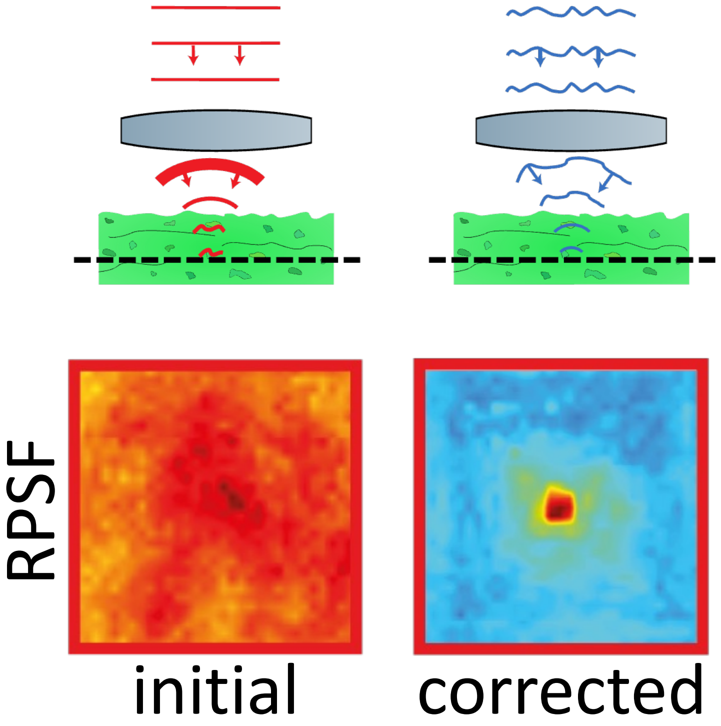

Phase conjugation of the aberration transmittance enables a compensation of isoplanatic (low-order) aberrations

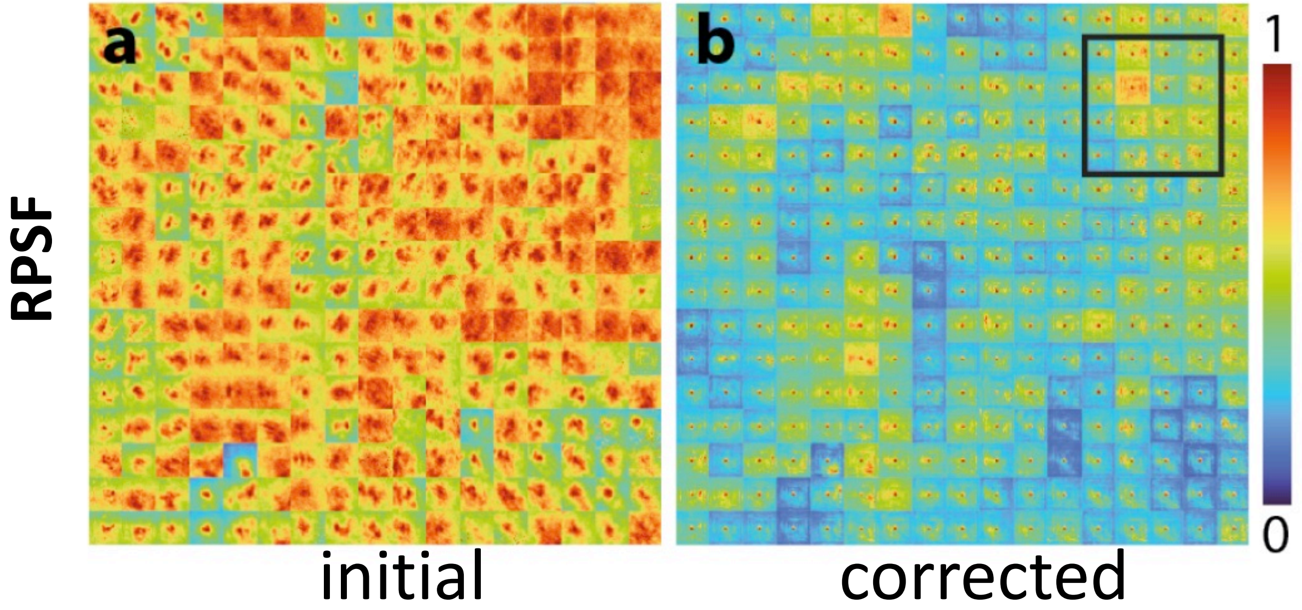

Subsistence of high-order aberrations

Multiple scattering ?

U. Najar *et al.*, Nat. Commun., 2024

Manifestation of Multiple Scattering

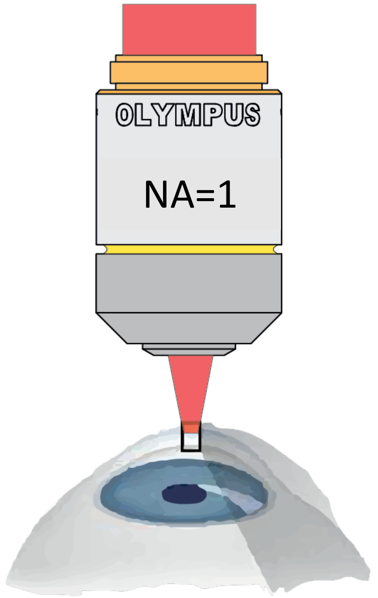

350-µm-thick
extremely opaque
human cornea
$\ell_s \sim 35$ µm

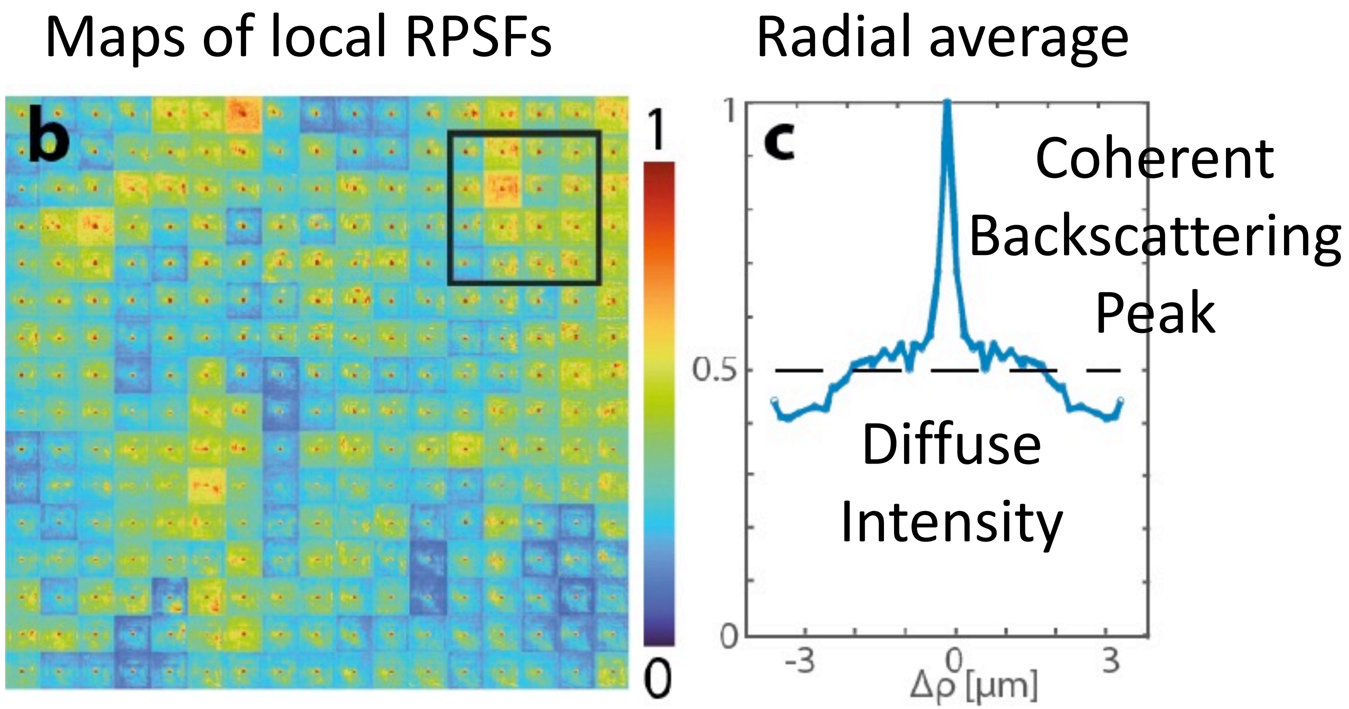

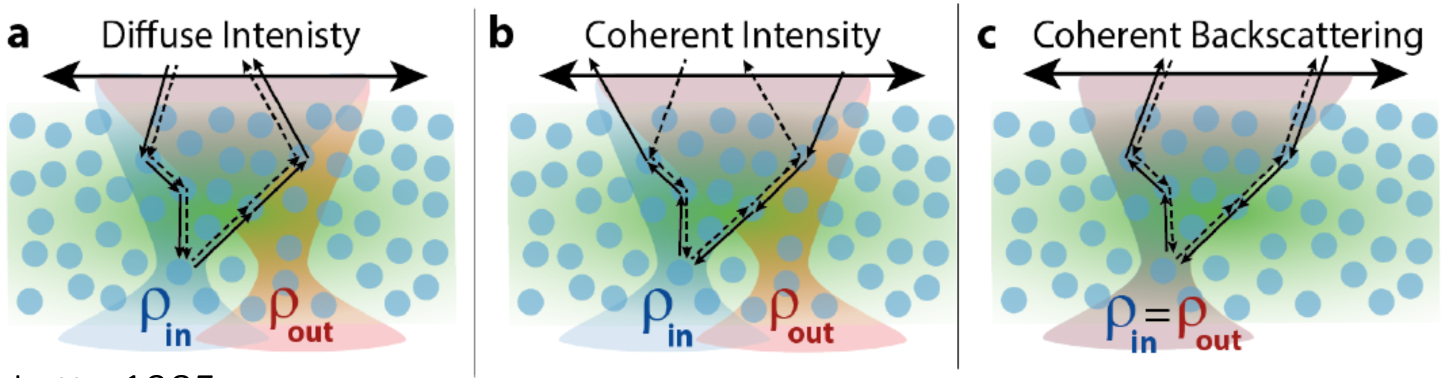

M.P. van Albada and A. Lagendijk., Phys. Rev. Lett., 1985
W. Lambert *et al.*., Phys. Rev. X, 2020

U. Najar *et al.*, Nat. Commun., 2024

Manifestation of Multiple Scattering

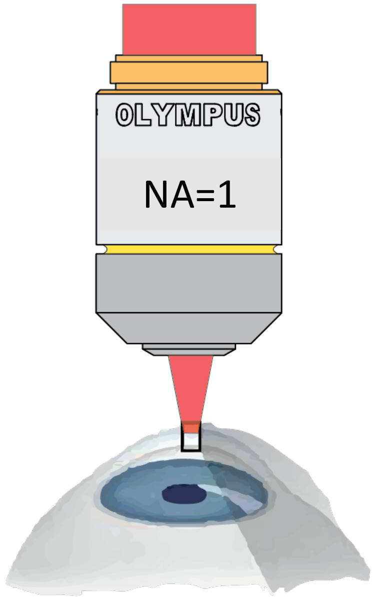

350-µm-thick
extremely opaque
human cornea
$\ell_s \sim 35$ µm

Maps of local RPSFs

Radial average

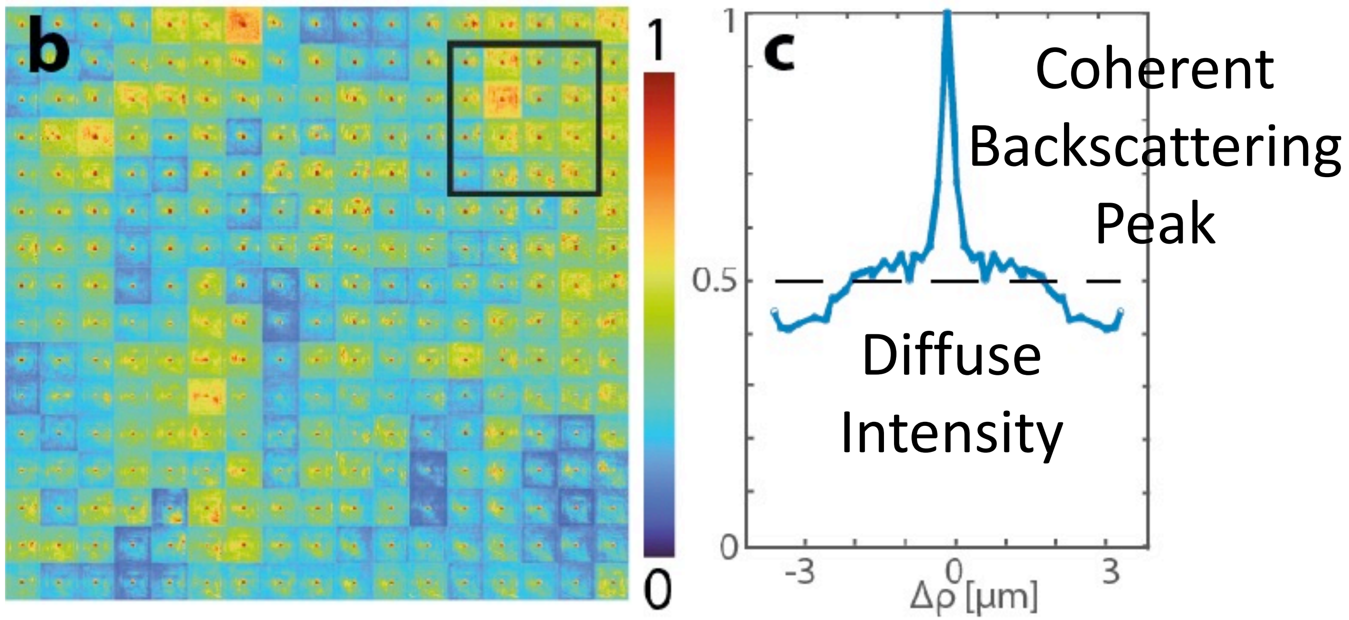

The CBS peak can act a false guide star

M.P. van Albada and A. Lagendijk., Phys. Rev. Lett., 1985
W. Lambert *et al.*., Phys. Rev. X, 2020
U. Najar *et al.*, Nat. Commun., 2024

Multi-Scale Analysis of Wave Distortions

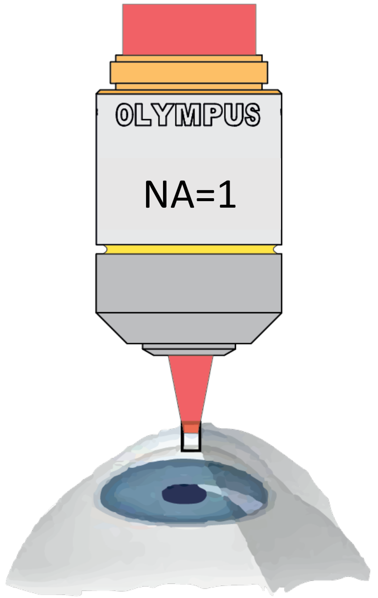

350-µm-thick
extremely opaque
human cornea
ℓ_s~35 µm

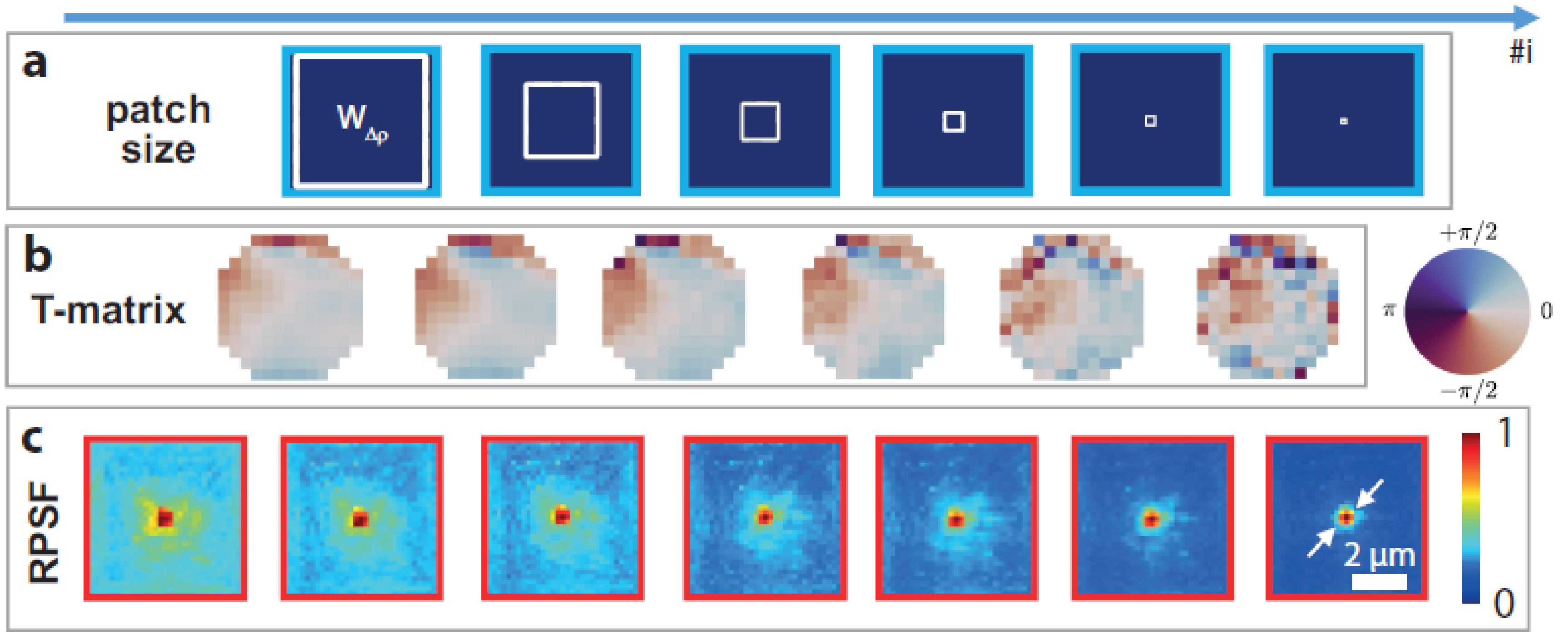

**Gradual reduction of the isoplanatic patch
to guarantee the convergence
of the aberration correction process**

U. Najar *et al.*, Nat. Commun., 2024

T-matrix Focusing

U. Najar

T-matrix

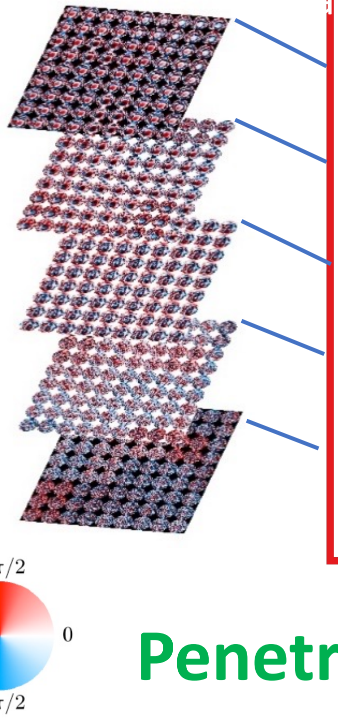

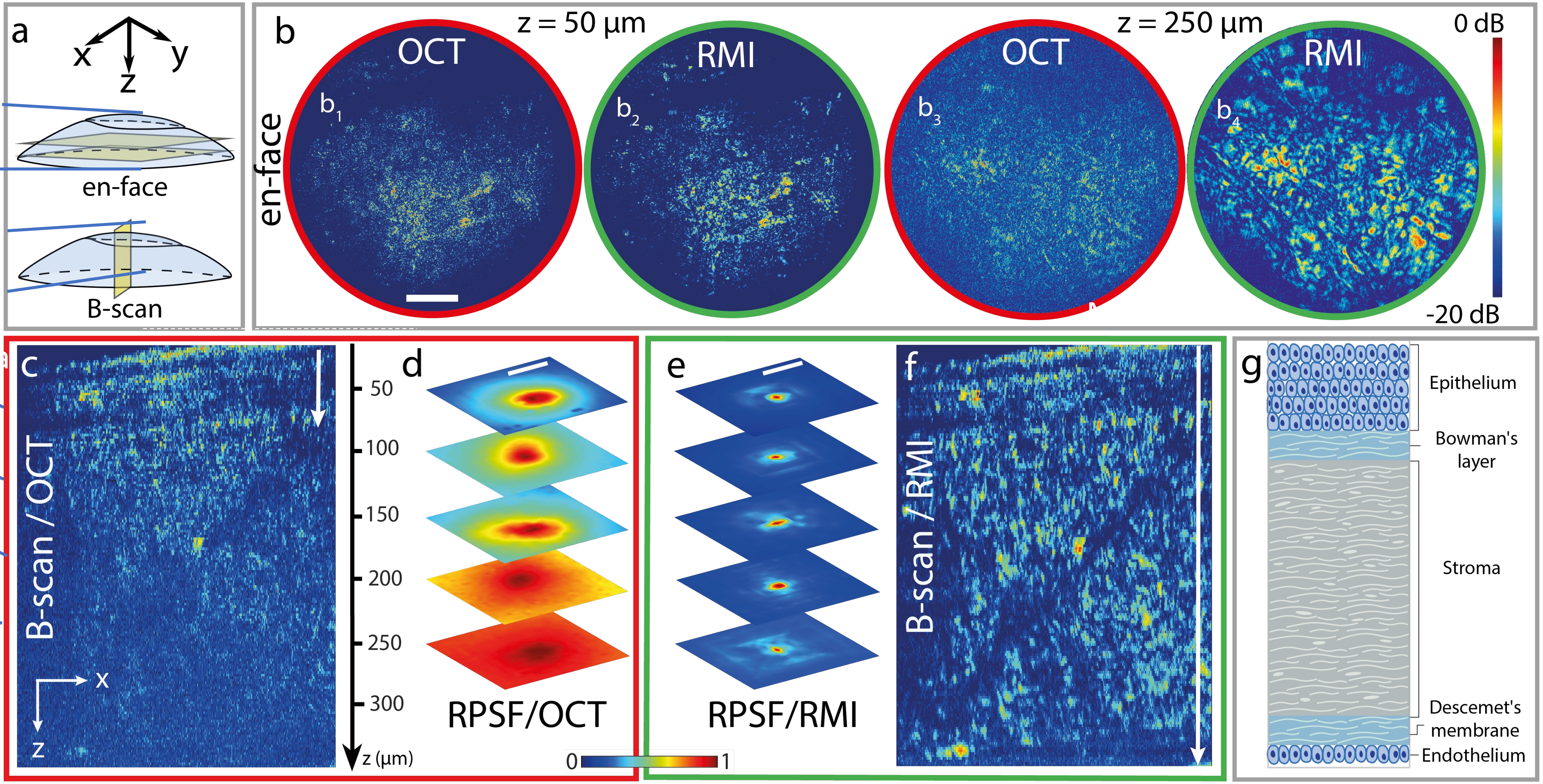

Penetration depth >×5 – Contrast +15 dB & Resolution × 10 in depth

U. Najar *et al.*, Nat. Commun., 2024

Optical Matrix Imaging

Ultra-fast, quantitative, dynamic

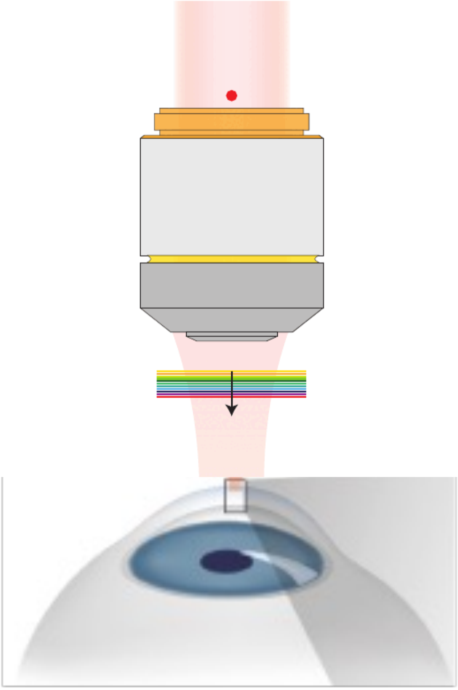

www.owlo.io

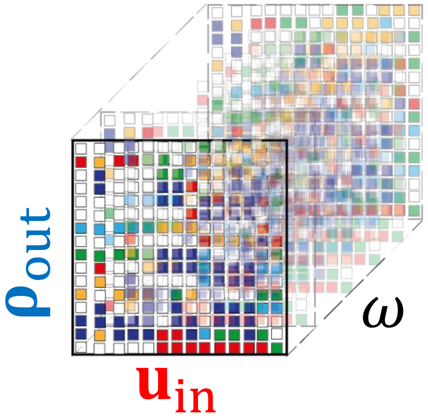

$$R(\boldsymbol{\rho}_{out}, \mathbf{u}_{in}, \omega)$$

Multi-Spectral

Reflection Matrix

Three-dimensional confocal imaging

10^9 voxels, 1 s

Paul Balondrade

Victor Barolle

N. Guigui

P. Balondrade, V. Barolle, N. Guigui, E. Auriant, N. Rougier, C. Boccara, M. Fink, A. Aubry, Nature Photonics, 2024

Embryo Segmentation & Quantification

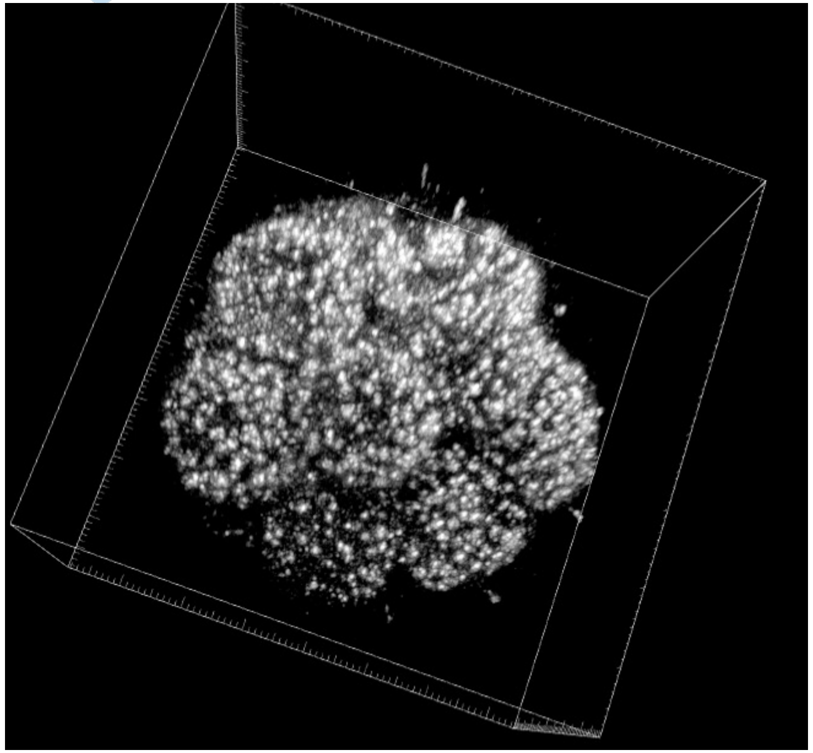

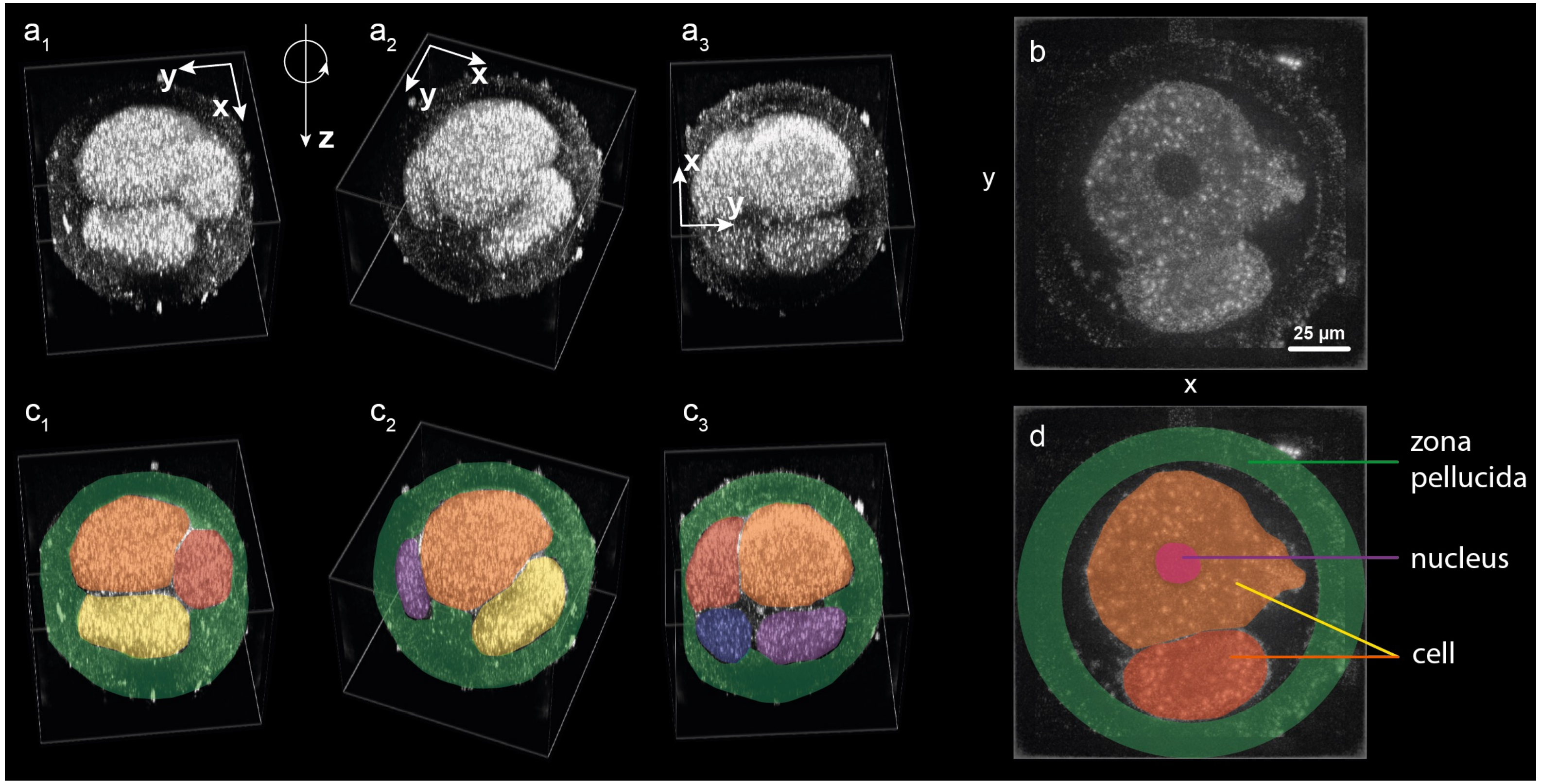

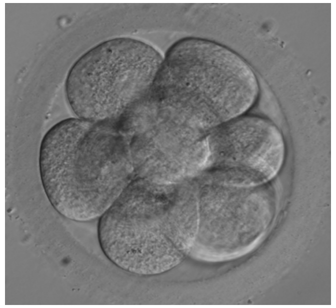

V. Barolle, *et al.*, arXiv:2410,11126 (2024)

Towards Quantitative Imaging

Wave velocity and scattering mfp

Flavien Bureau

Scanning the speed-of-sound

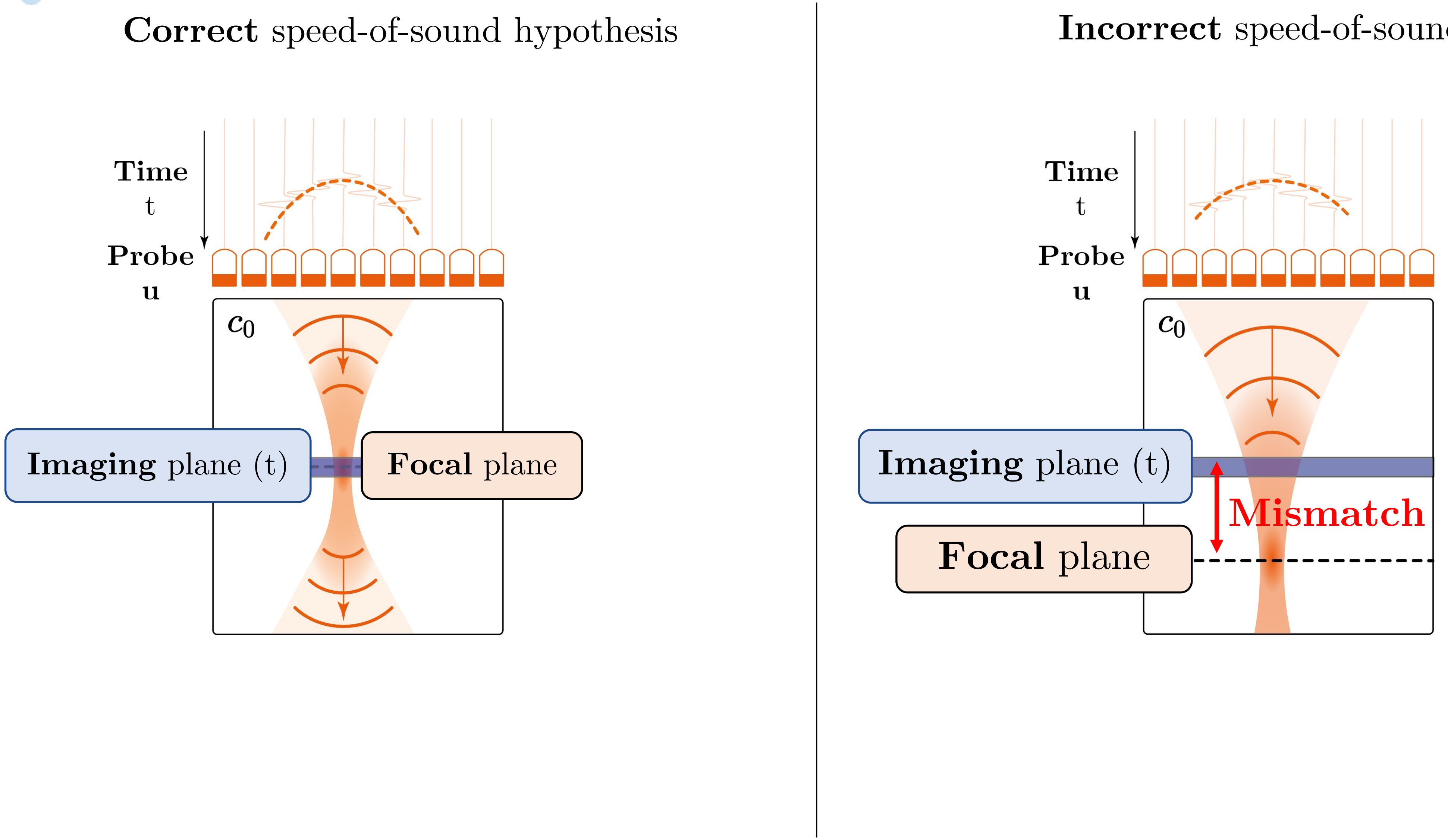

[Bureau et al, 2024] "Reflection matrix imaging for wave velocity tomography", *arXiv:2409.13901*

Scanning the speed-of-sound

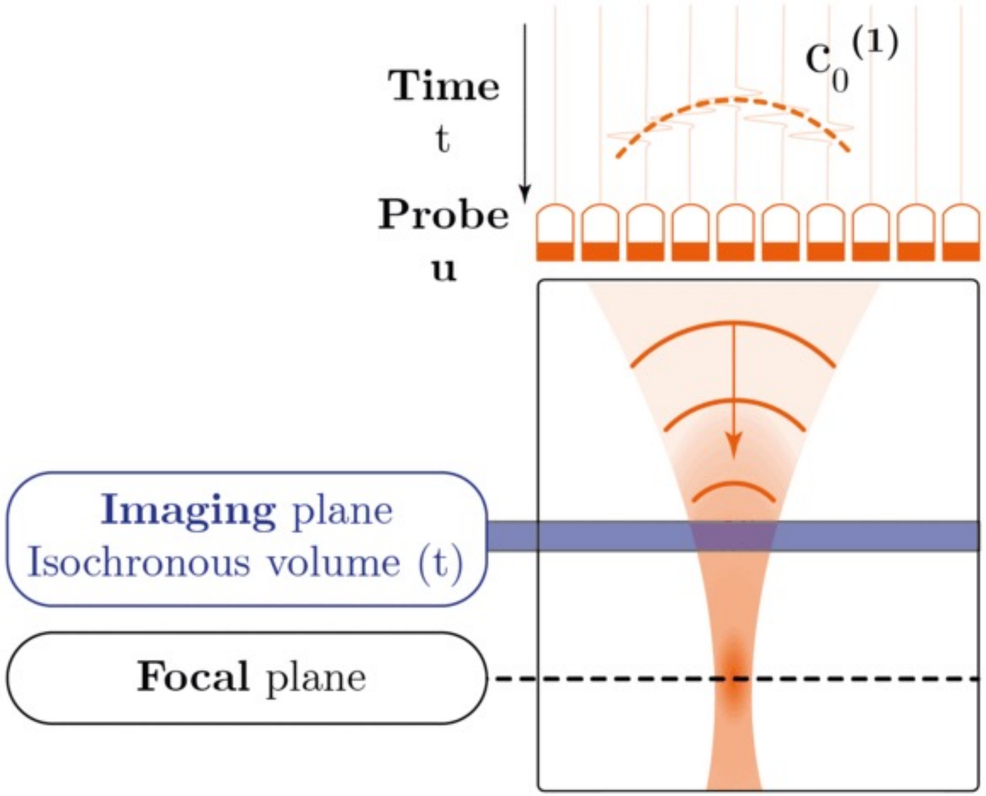

Ultrasound **phantom**

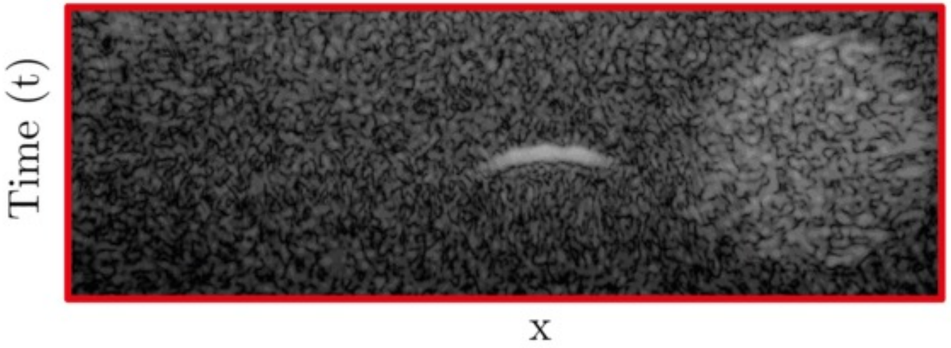

[Bureau et al, 2024] "Reflection matrix imaging for wave velocity tomography", *arXiv:2409.13901*

Speed-of-Sound Estimation

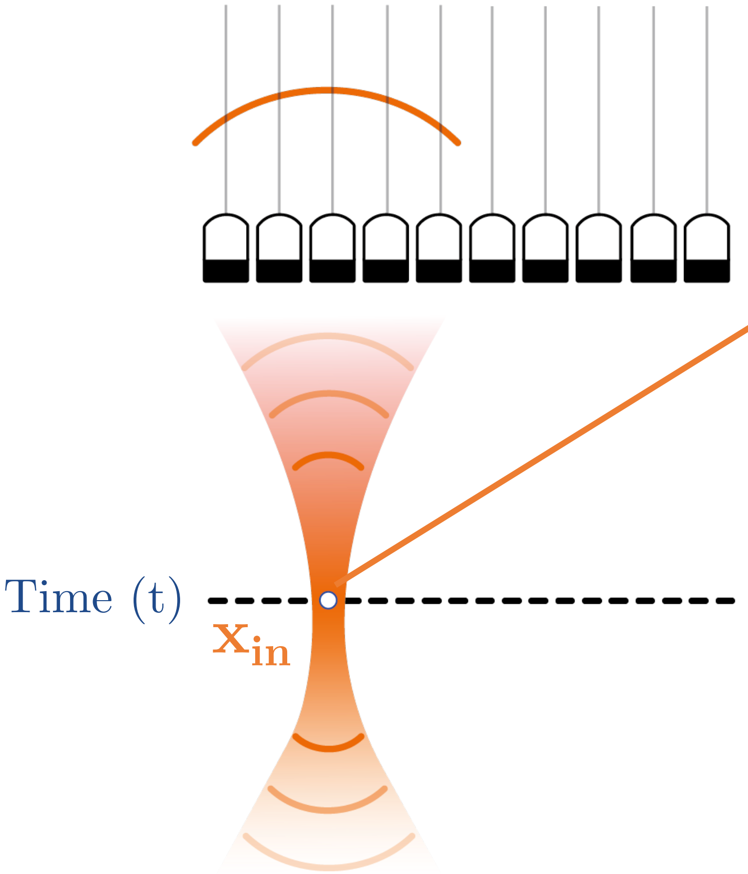

$$R\left(t, x_{\text{in}}, x_{\text{out}}, c_0\right)$$

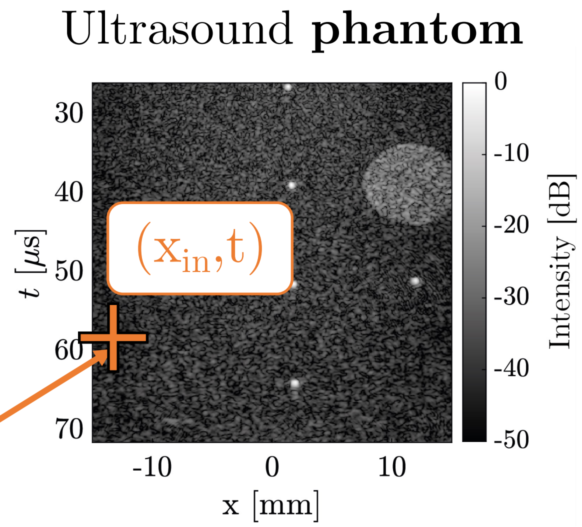

[Bureau et al, 2024] "Reflection matrix imaging for wave velocity tomography", *arXiv:2409.13901*

Speed-of-Sound Estimation

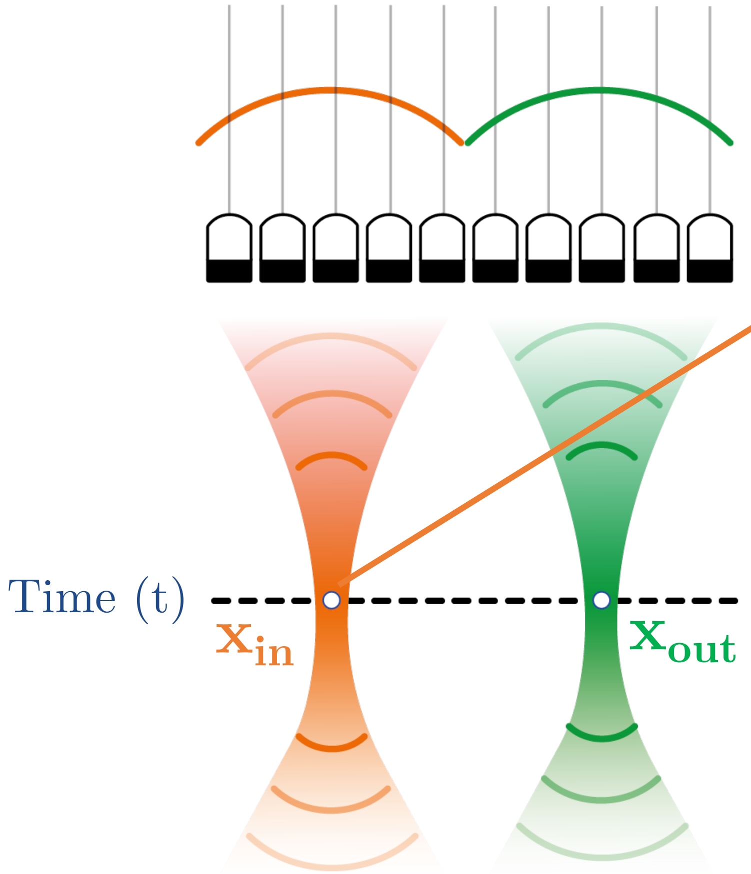

$$R\left(t, x_{in}, x_{out}, c_0\right)$$

Ultrasound **phantom**

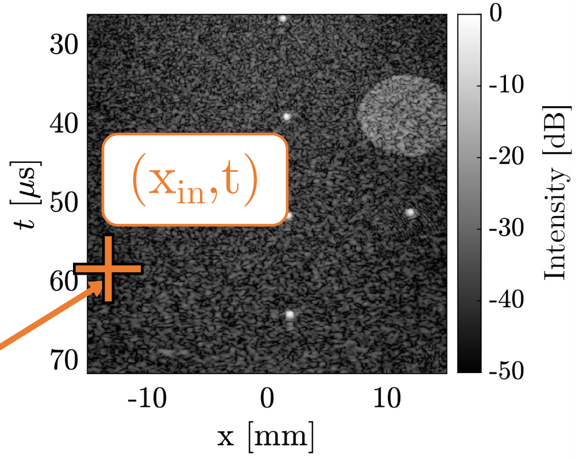

[Bureau et al, 2024] "Reflection matrix imaging for wave velocity tomography", *arXiv:2409.13901*

Speed-of-Sound Estimation

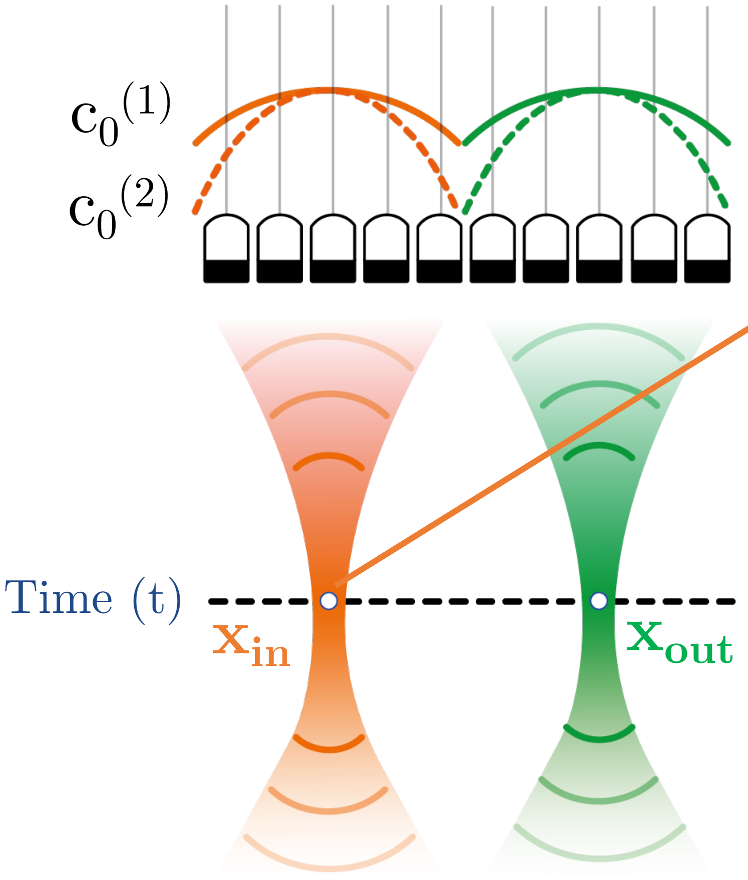

$$R\left(t, x_{in}, x_{out}, c_0\right)$$

Ultrasound **phantom**

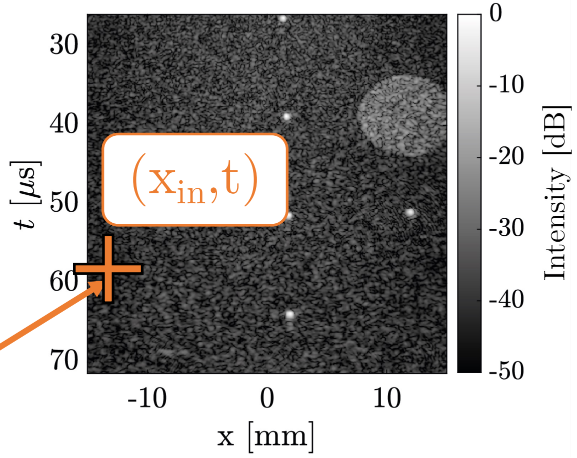

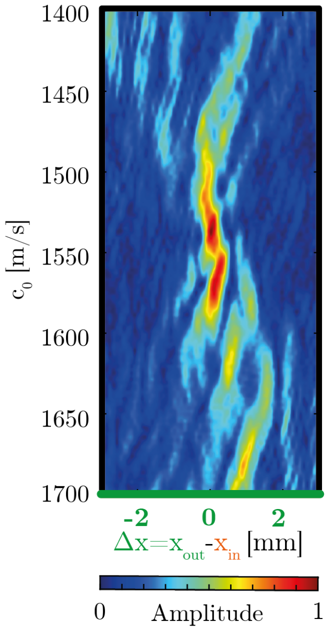

Focal spot

[Bureau et al, 2024] "Reflection matrix imaging for wave velocity tomography", *arXiv:2409.13901*

Speed-of-Sound Estimation

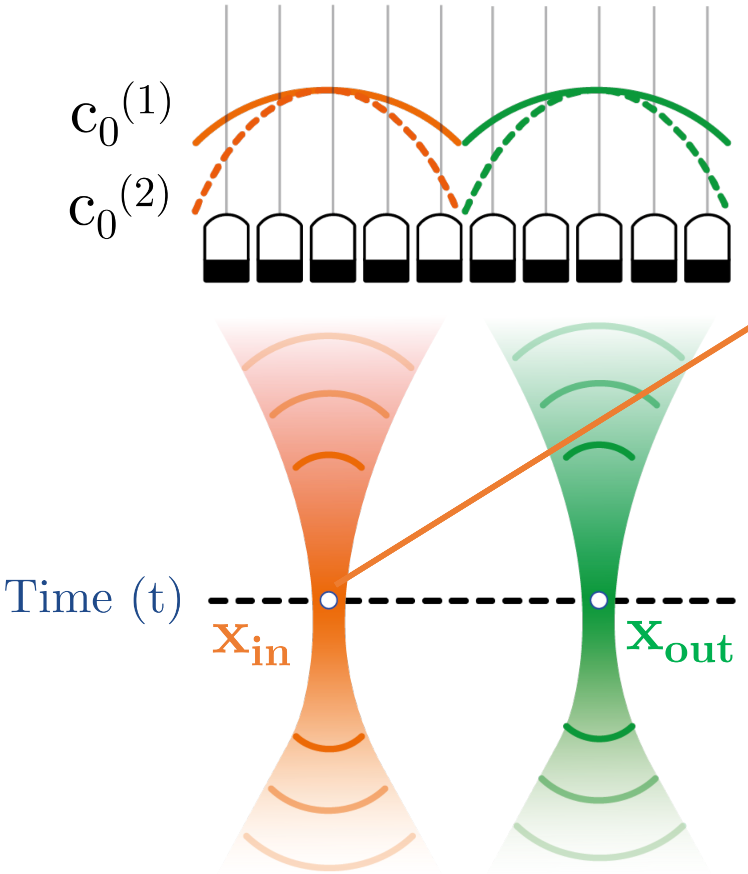

$$R\left(t, x_{in}, x_{out}, c_0\right)$$

Ultrasound **phantom**

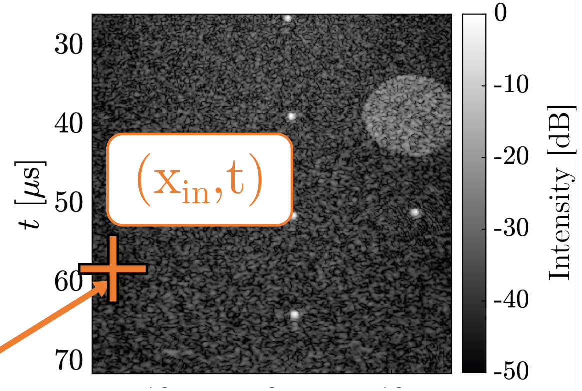

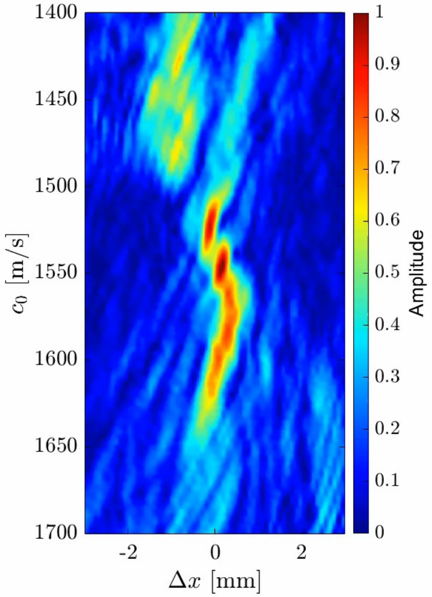

Focal spot

modulated by random reflectivity

[Bureau et al, 2024] "Reflection matrix imaging for wave velocity tomography", *arXiv:2409.13901*

Speed-of-Sound Estimation

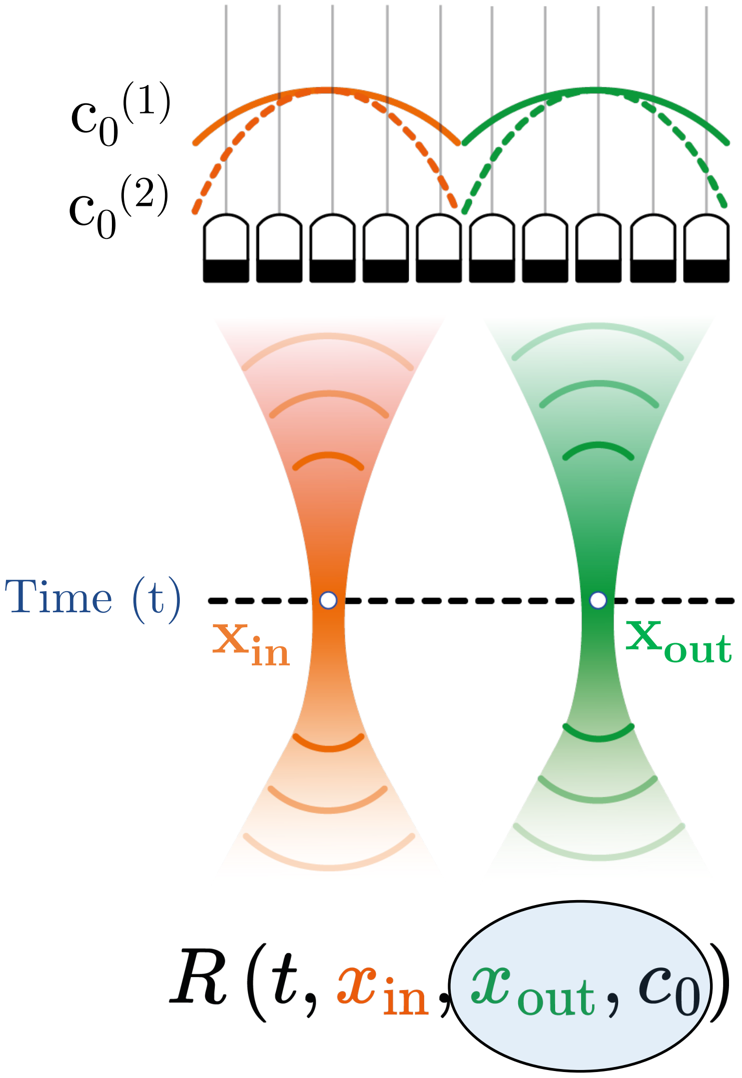

Ultrasound **phantom**

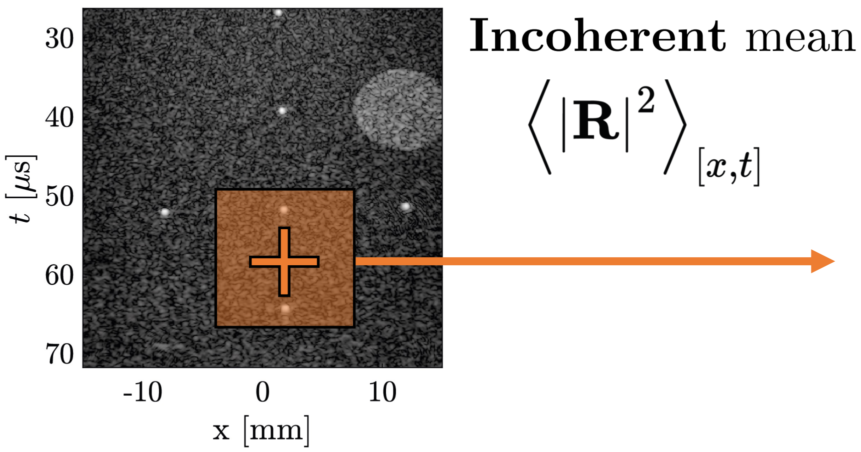

Incoherent mean

$$\left\langle \left|\mathbf{R}\right|^2 \right\rangle_{[x,t]}$$

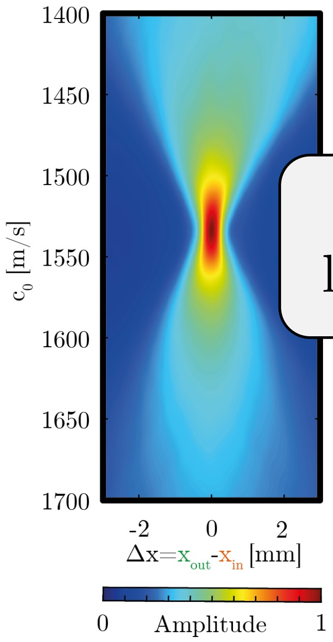

Self portrait of the local focusing process

[Bureau et al, 2024] "Reflection matrix imaging for wave velocity tomography", *arXiv:2409.13901*

Speed-of-Sound Estimation

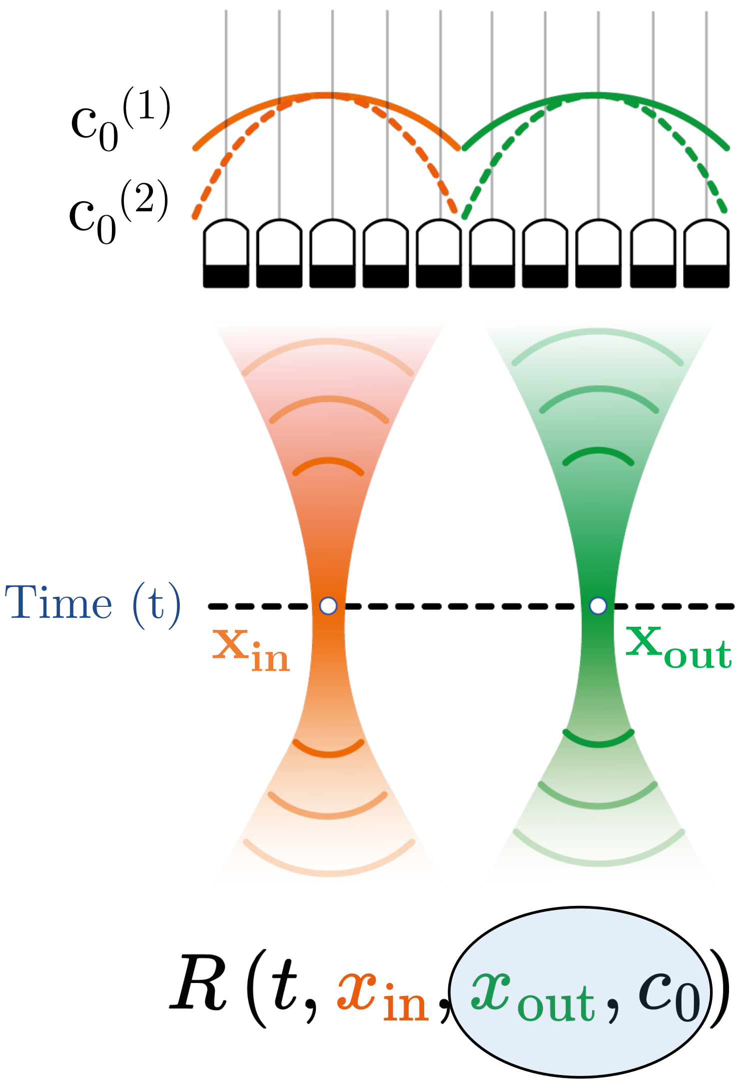

Ultrasound **phantom**

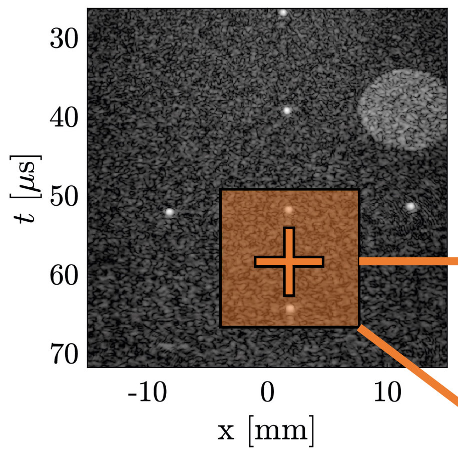

Incoherent mean

$$\left\langle |\mathbf{R}|^2 \right\rangle_{[x,t]}$$

Coherent mean

SVD of $\mathbf{R} \rightarrow U_1(\Delta x, c_0)$

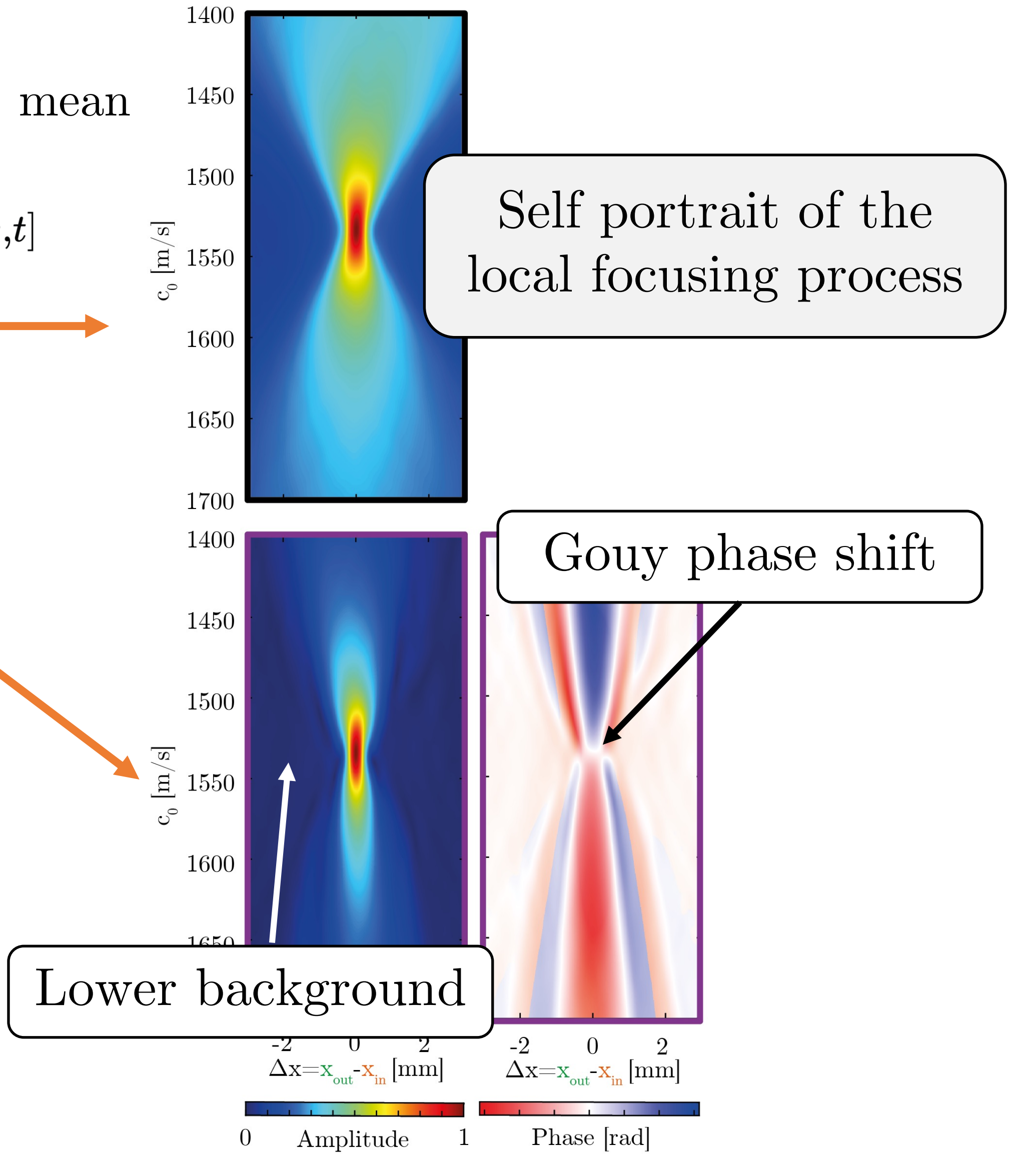

[Bureau et al, 2024] "Reflection matrix imaging for wave velocity tomography", *arXiv:2409.13901*

Speed-of-Sound Estimation

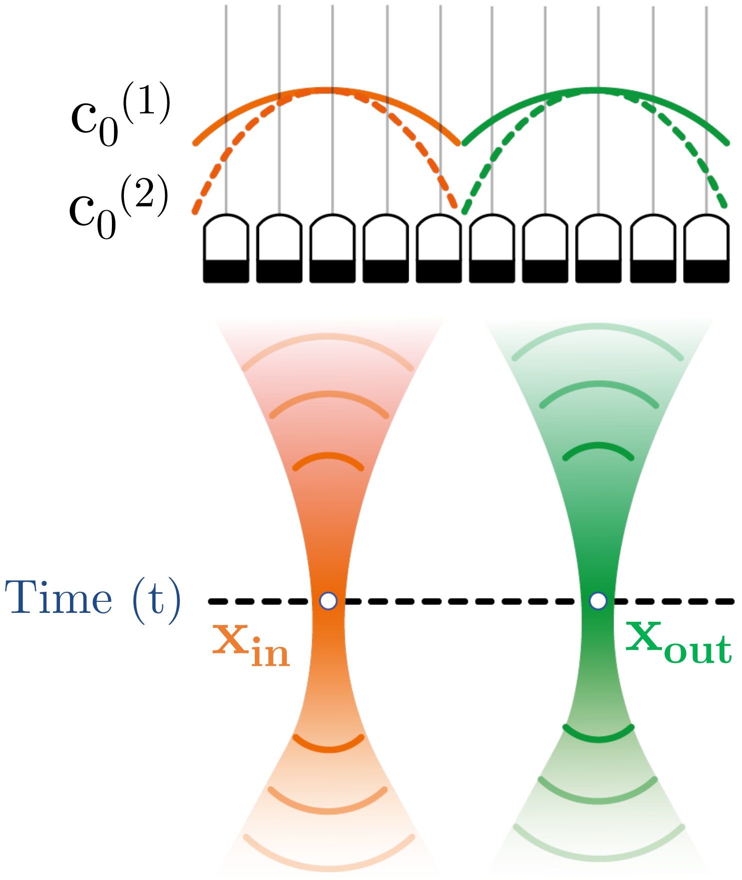

$$R\,(t, x_{\mathrm{in}}, x_{\mathrm{out}}, c_0)$$

Ultrasound **phantom**

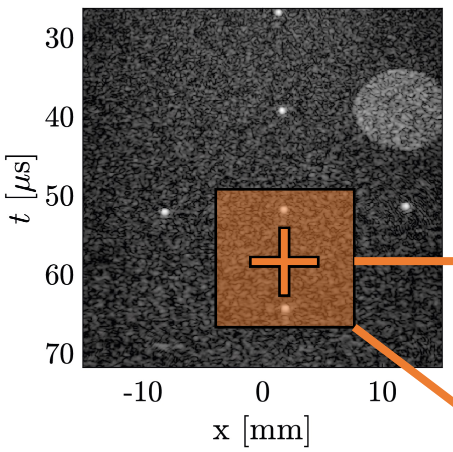

Incoherent mean

$$\left\langle |\mathbf{R}|^2 \right\rangle_{[x,t]}$$

Coherent mean

SVD of $\mathbf{R} \rightarrow U_1(\Delta x, c_0)$

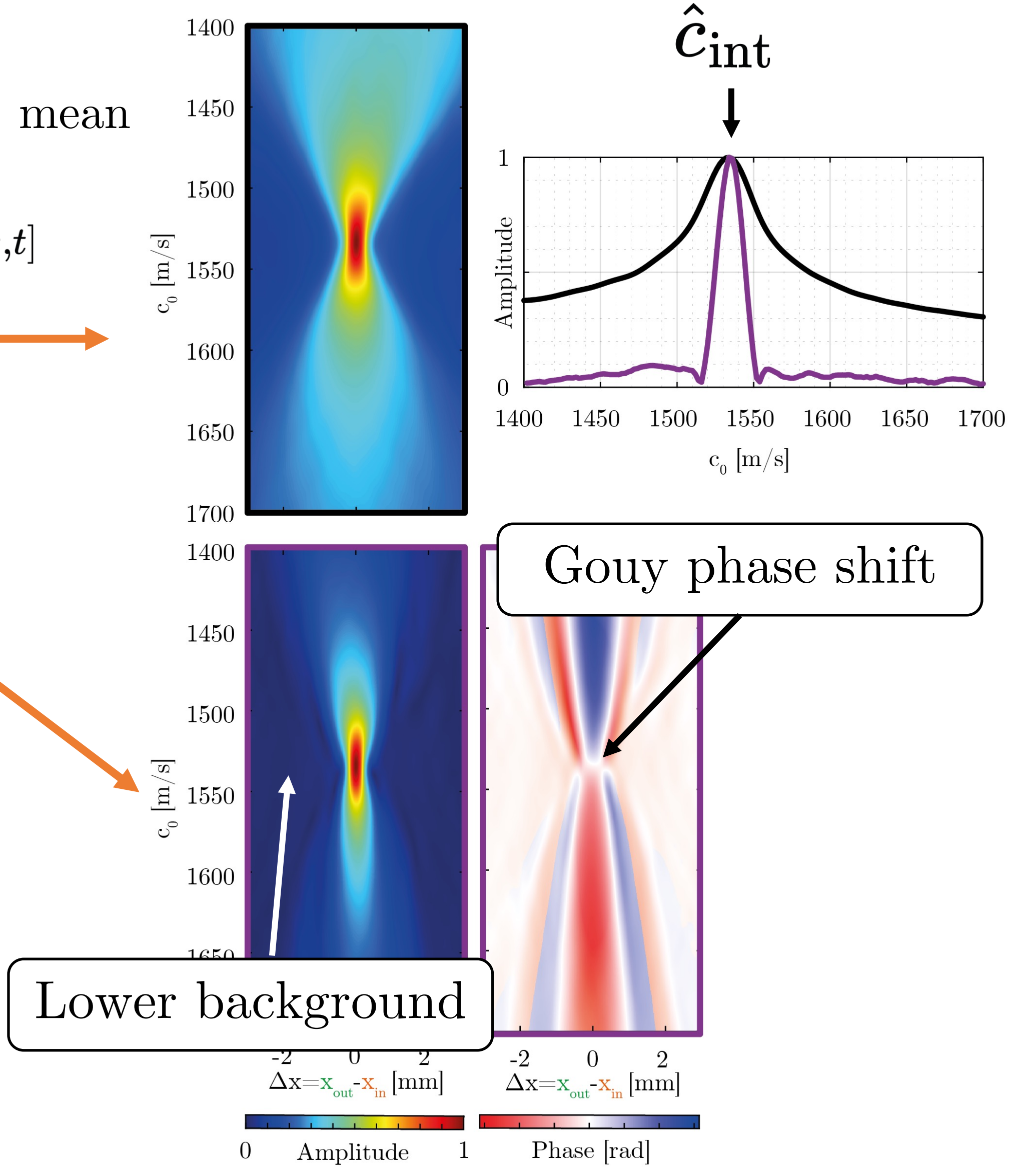

[Bureau et al, 2024] "Reflection matrix imaging for wave velocity tomography", *arXiv:2409.13901*

A difficult-to-image patient liver

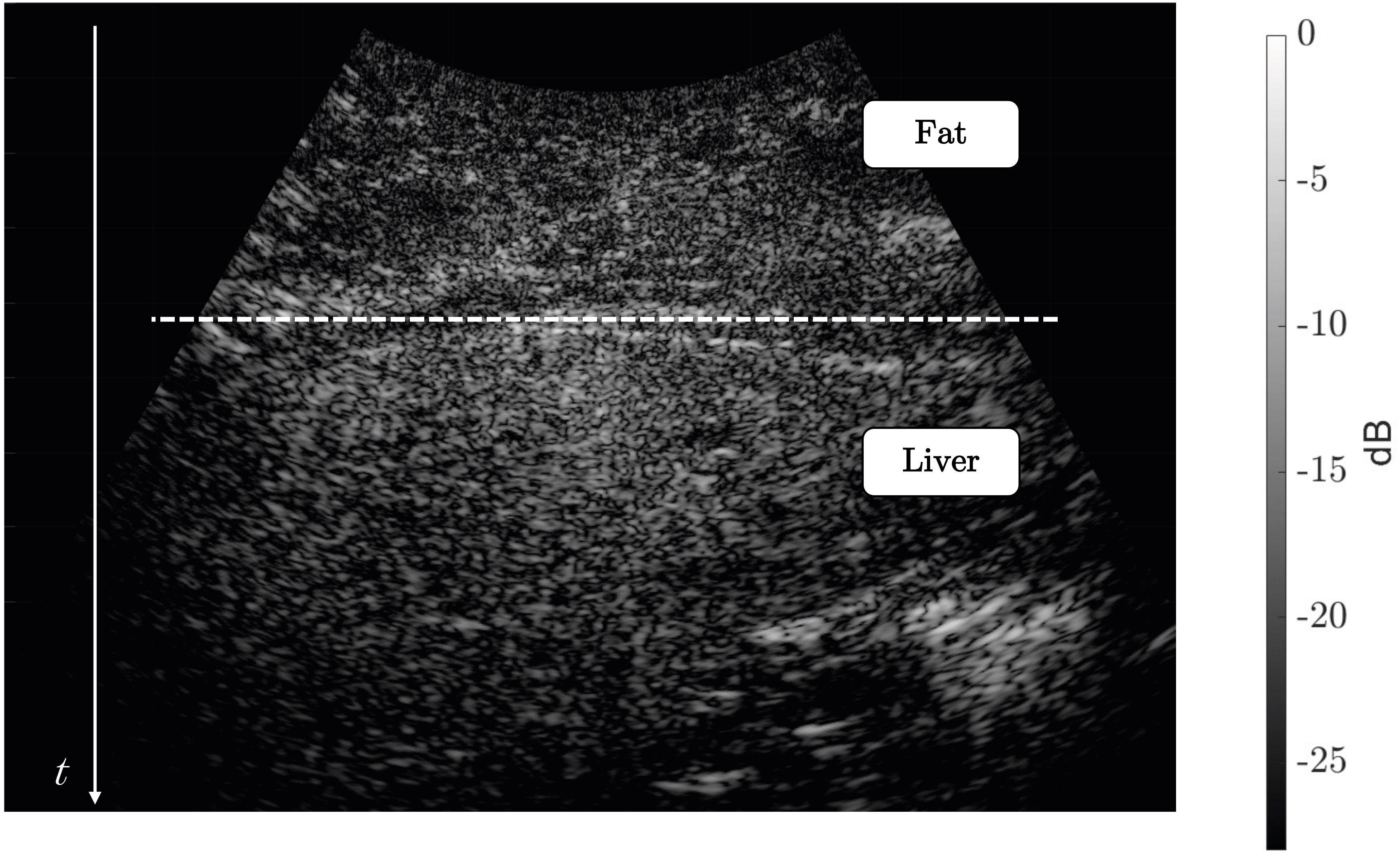

F. Bureau *et al.*, arXiv: 2409.13901 (2024)

Integrated Speed-of-Sound Map

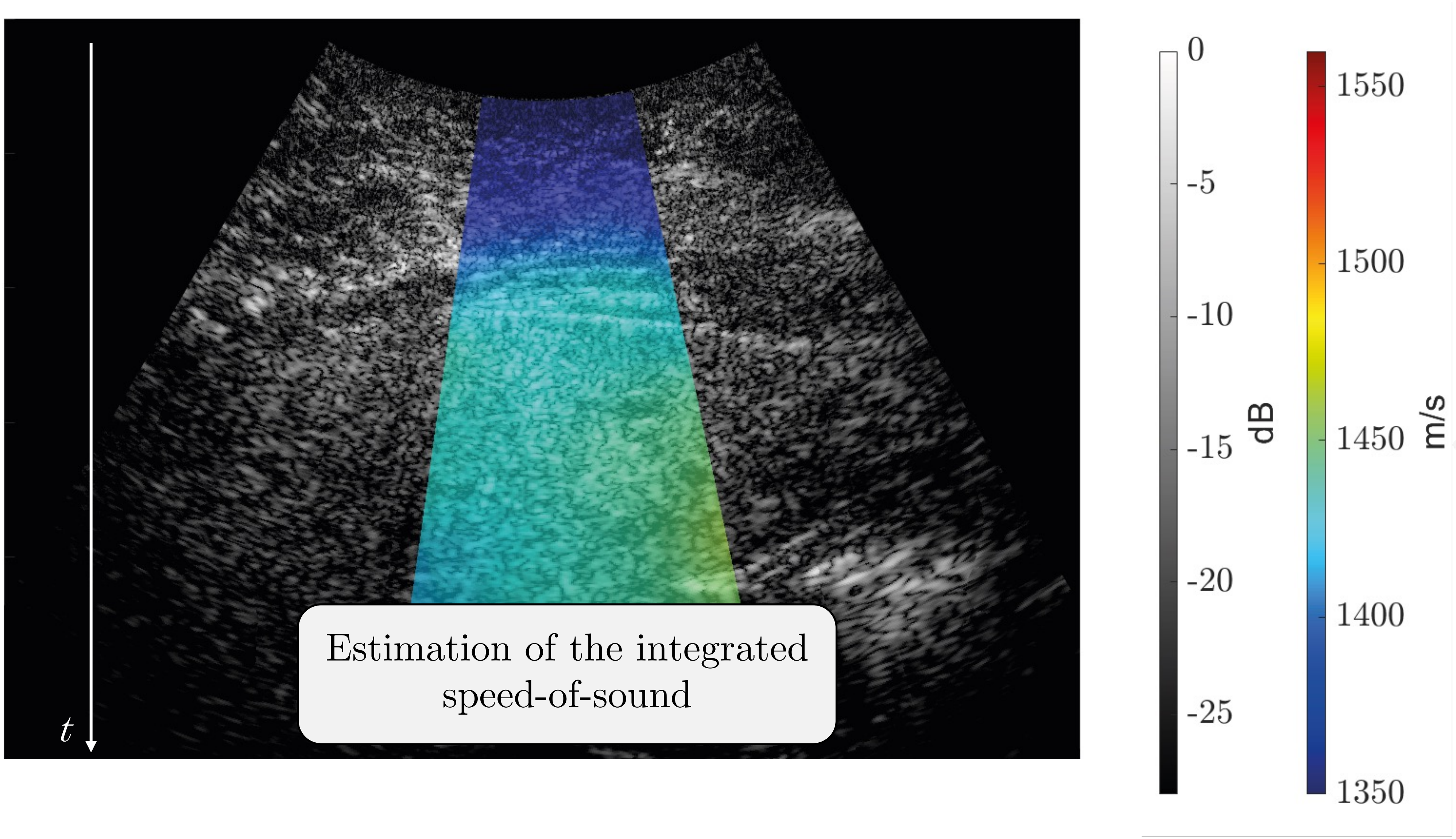

F. Bureau *et al.*, arXiv: 2409.13901 (2024)

Integrated Speed-of-Sound Map

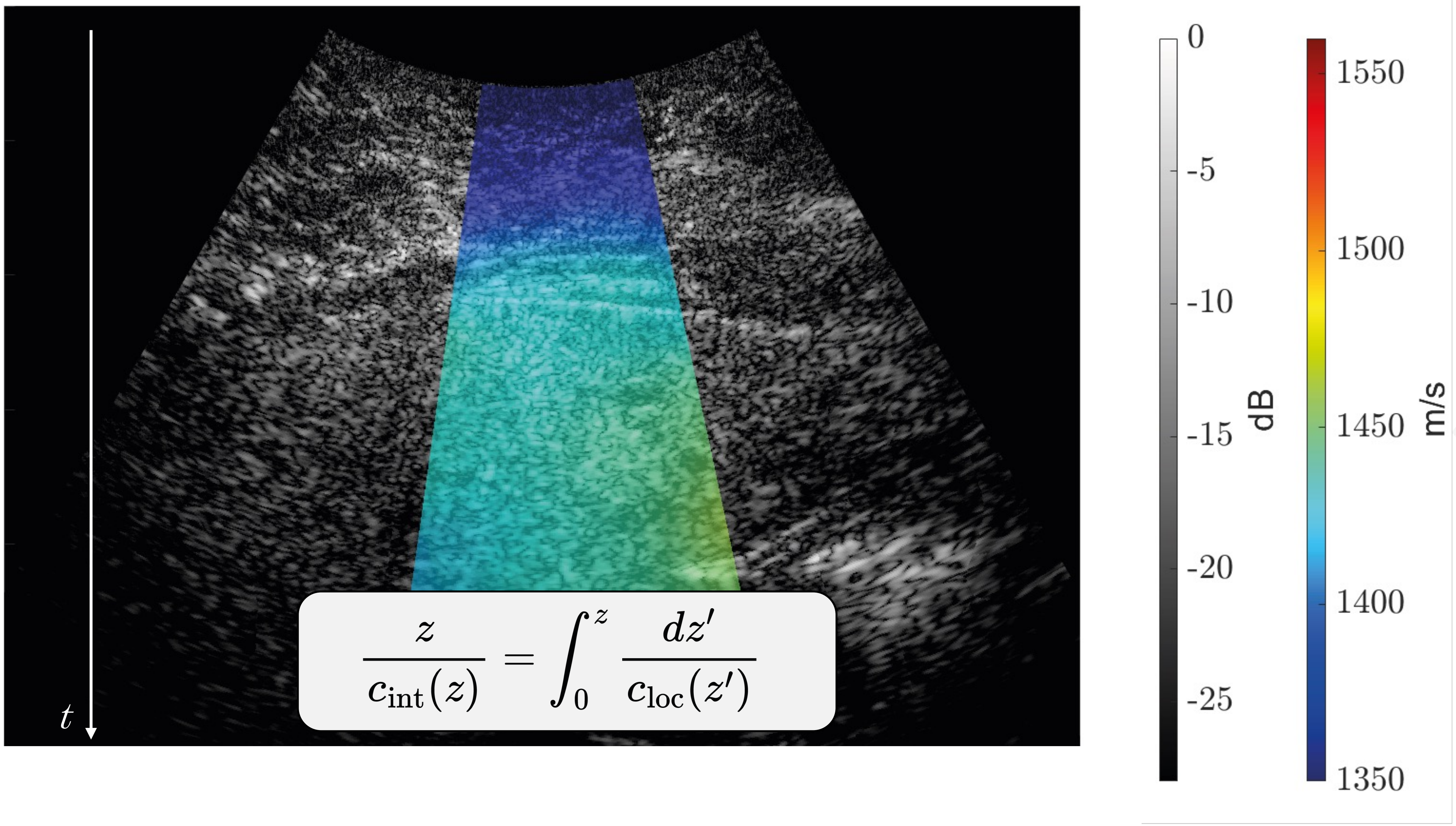

F. Bureau *et al.*, arXiv: 2409.13901 (2024)

M.Jakovljevic *et al.*, J. Acoust. Soc. Am. (2018)

Integrated Speed-of-Sound Map

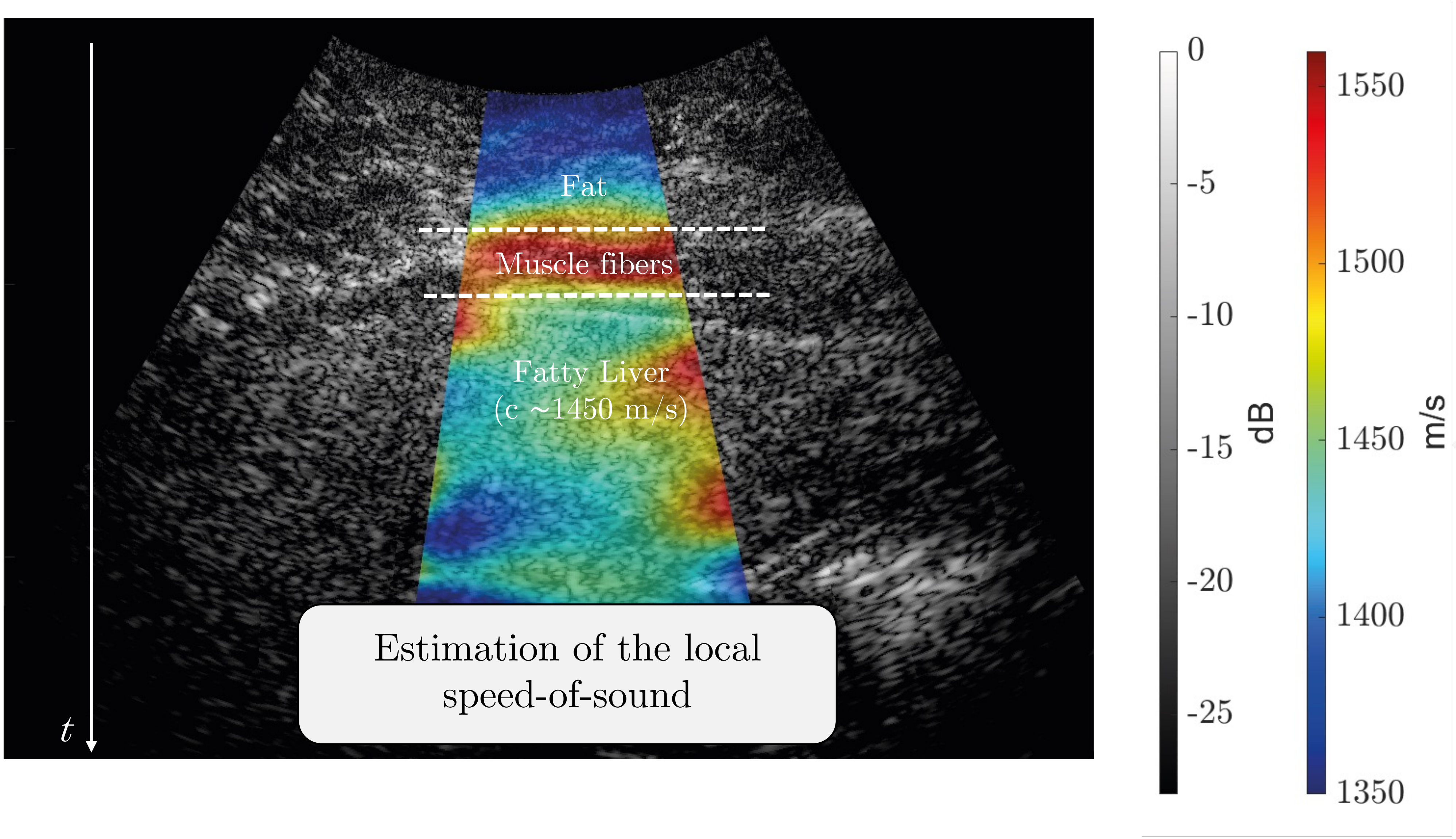

F. Bureau *et al.*, arXiv: 2409.13901 (2024)

Quantitative Matrix Imaging

Speed-of-sound Tomography
(in reflection)

Liver US image

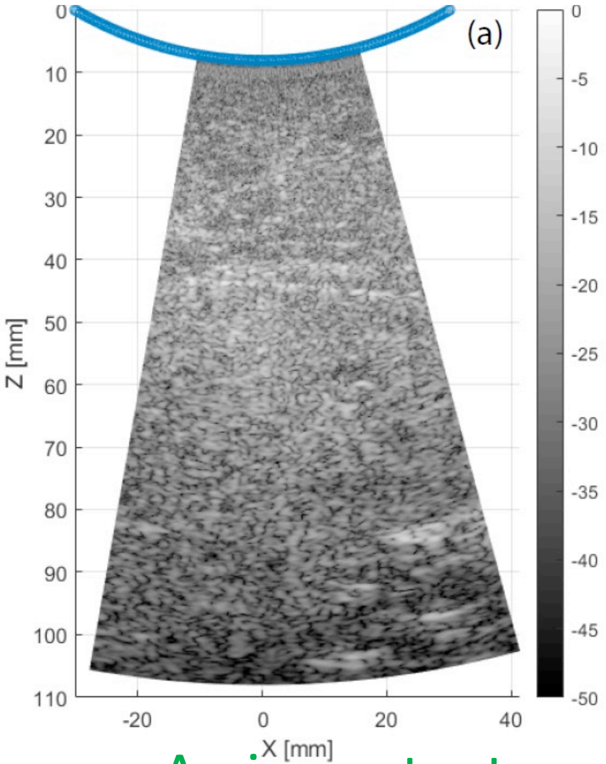

Speed-of-sound

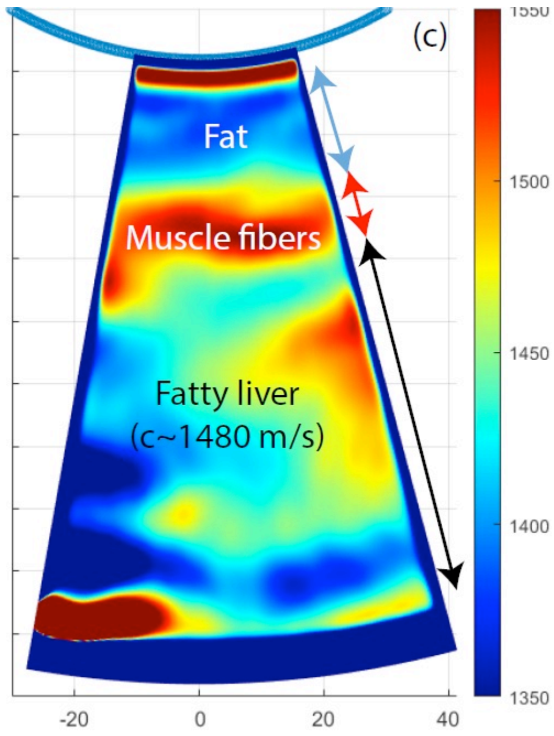

An important parameter bio-marker
for steatosis diagnosis
(accumulation of fat droplets)

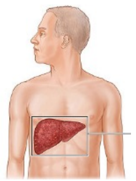

A crucial bio-marker
for breast cancer

Standard B-mode

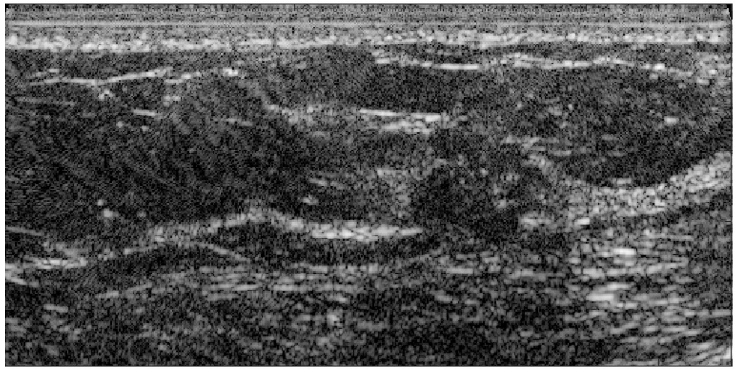

Speed-of-sound

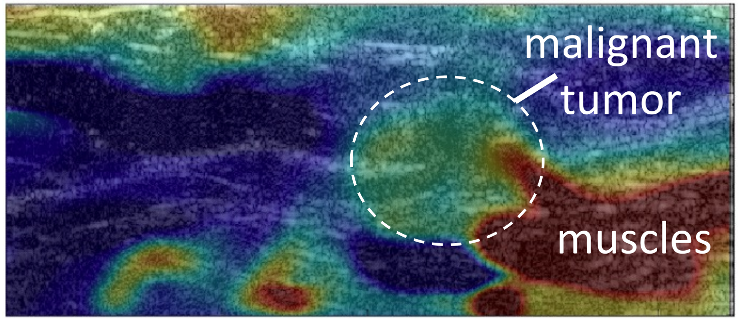

Emma Brenner,
PhD thesis

[Bureau et al, 2024] "Reflection matrix imaging for wave velocity tomography", *arXiv:2409.13901*

Single Scattering Projection

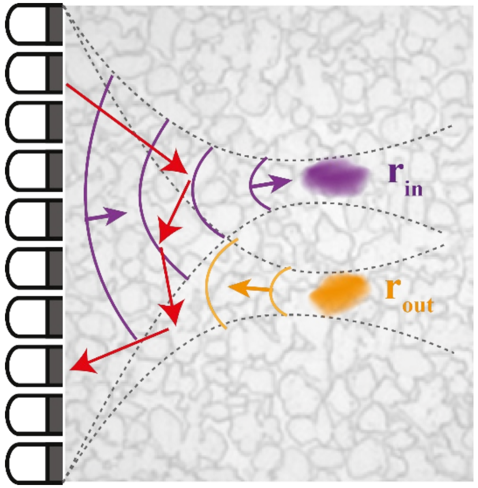

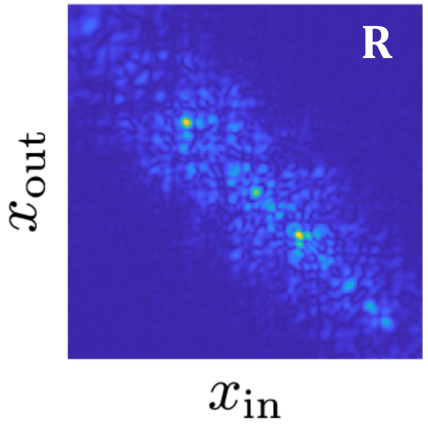

Projection onto a characteristic single scattering subspace

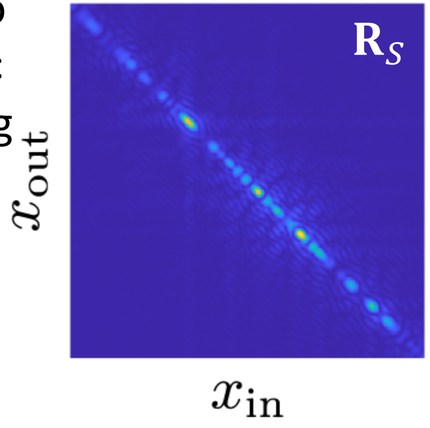

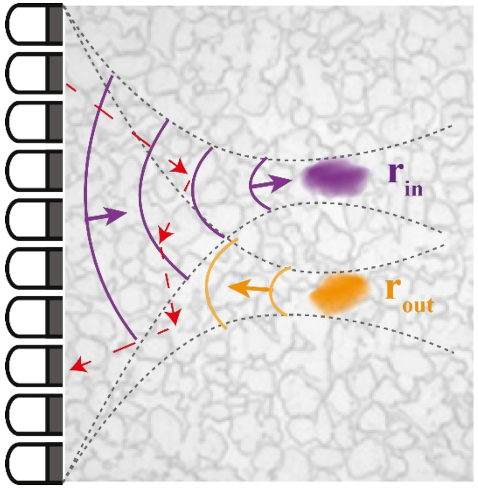

Total intensity

$$I(t) = \mathrm{Tr}\left[\mathbf{R}(t)\mathbf{R}^{\dagger}(t)\right]$$

Single scattering intensity

$$I_S(t) = \mathrm{Tr}\left[\mathbf{R}_S(t){\mathbf{R}_S}^{\dagger}(t)\right]$$

Single scattering rate → $$\boxed{\rho_S(t) = \frac{I_S(t)}{I(t)} = 1 - \rho_M(t)}$$ ← Multiple scattering rate

C. Brütt *et al.*, Phys. Rev. E (2022)

A. Goicoechea *et al.*, Phys. Rev. Lett. (2024)

Local Multiple Scattering Rate

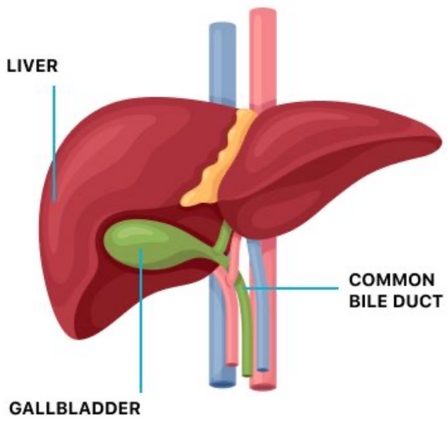

US Image

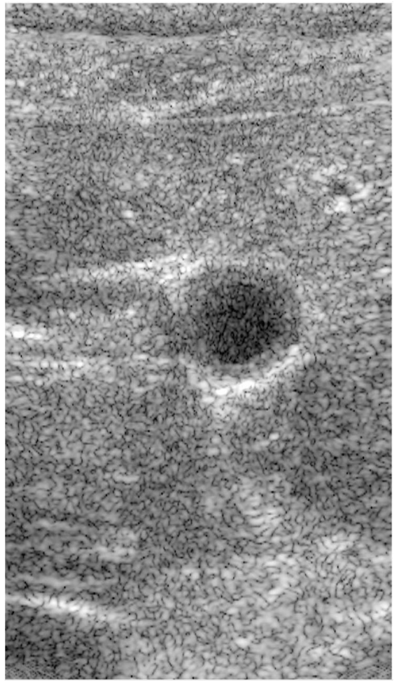

W. Lambert, *et al.*, IEEE Trans. Med. Imag. (2022)

Quantitative Ultrasound Imaging

Local Multiple Scattering Rate

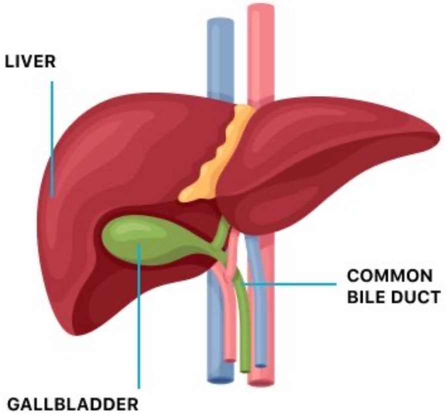

US Image

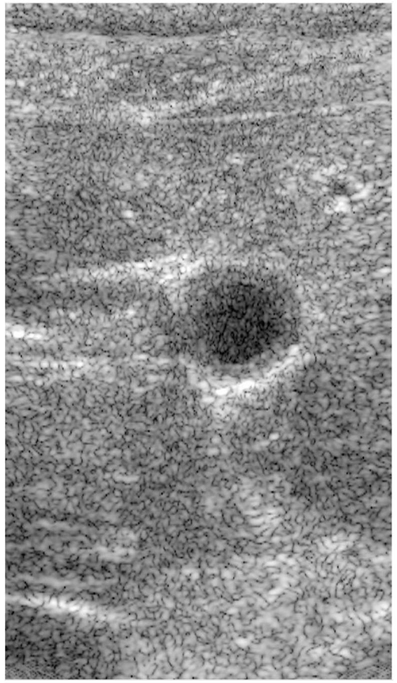

Multiple Scattering

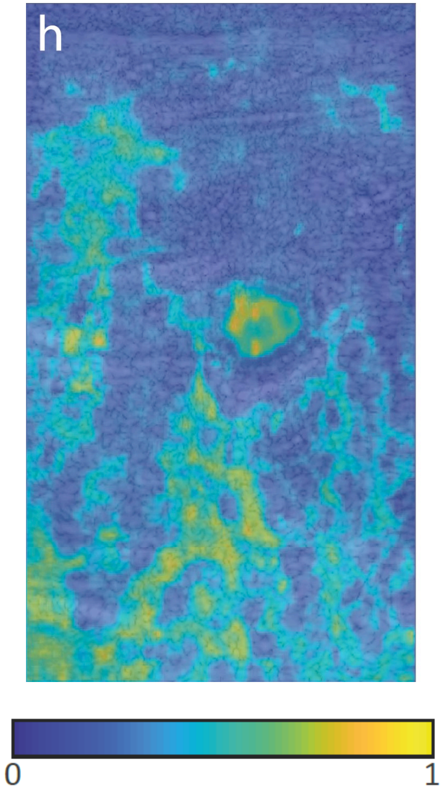

Reliability index of the US image

W. Lambert, *et al.*, IEEE Trans. Med. Imag. (2022)

Local Multiple Scattering Rate

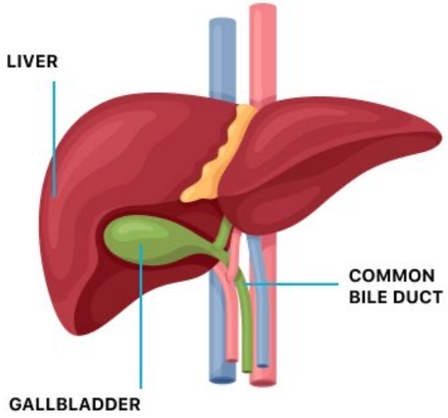

HOLOGIC® The Science of Sure

SUPERSONIC imagine

US Image

Multiple Scattering

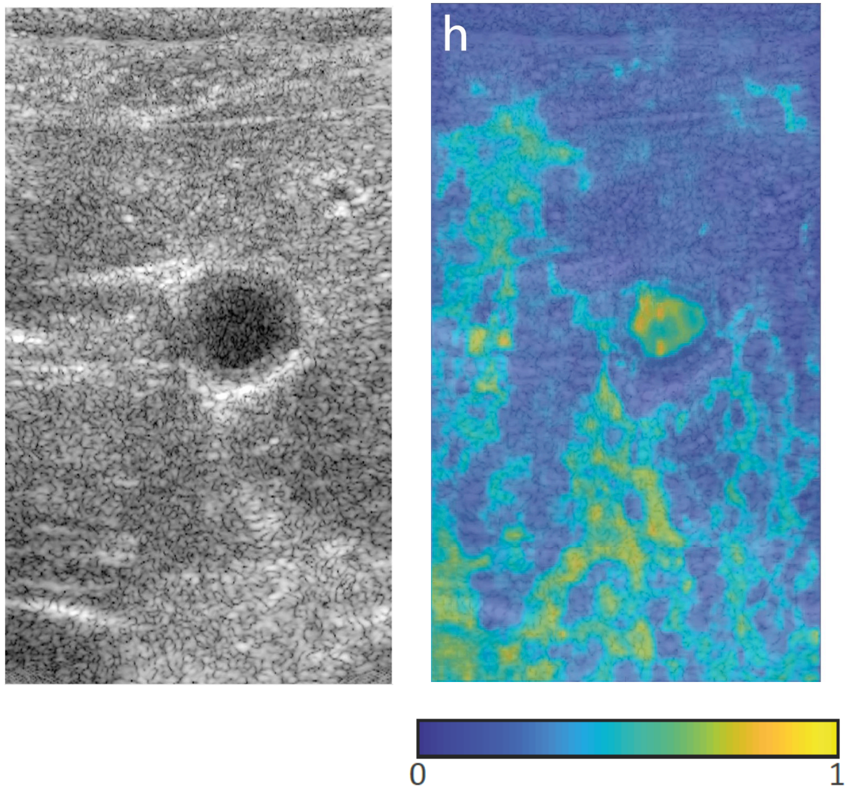

Reliability index of the US image

W. Lambert, *et al.*, IEEE Trans. Med. Imag. (2022)

A novel characterization tool

Discrimination Scattering/Absorption

attenuation

$$\ell_{ext}^{-1} = \ell_s^{-1} + \ell_a^{-1}$$

scattering

absorption

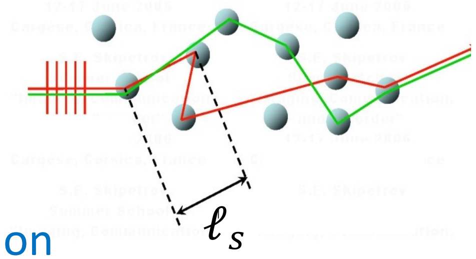

A. Aubry and A. Derode, JASA (2011)

Discrete Model (dilute regime) $\ell_s = 1/(n\sigma_s)$

particle concentration

scattering Cross-section

Continuous Model $\ell_s \sim 2(\sigma_c/c_0)^{-2} k_0^{-3} \ell_c^{-2}$

SoS Fluctuations

Correlation Length

Potential bio-marker for diagnosis (liver disease, breast tumor etc.)

What about our mesurement?

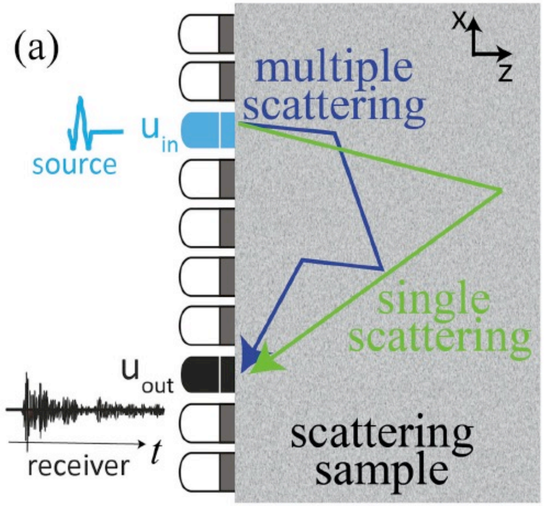

Semi-infinite medium
Integration over the medium surface

single scattering

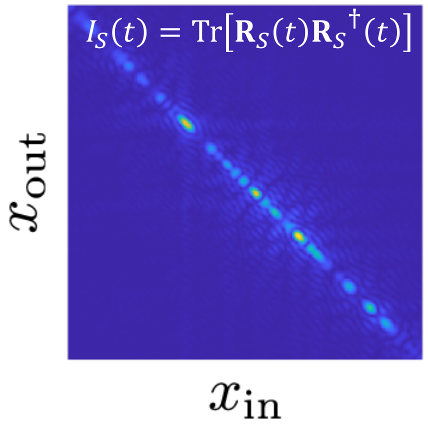

Radiative transfer

$$I_S(t) = \frac{e^{-ct/\ell_{\mathrm{ext}}}}{4l_s}$$

total intensity

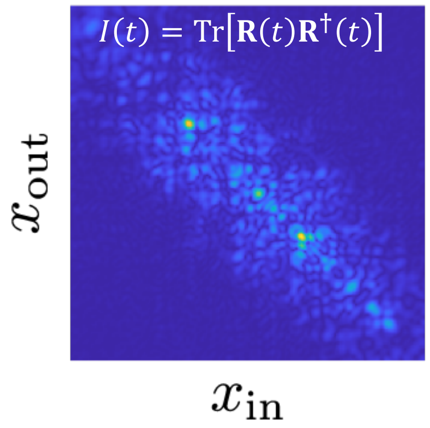

Radiative transfer ($ct < \ell_s$)

$$I(t) \cong \frac{1}{4l_s} e^{-ct/\ell_a} e^{-ct/(4\ell_s)}$$

Exponential time-decay of the single scattering rate: $\rho_S(t) \sim e^{-3ct/4\ell_s}$

Independent measurement of absorption and scattering losses!

A. Goicoechea *et al.*, Phys. Rev. Lett. (2024)

In-vivo measurement of ℓ_S in liver

Multiple scattering is far from being negligible in liver

256 transducers
5-10 MHz
pitch 0.2 mm

A. Goicoechea

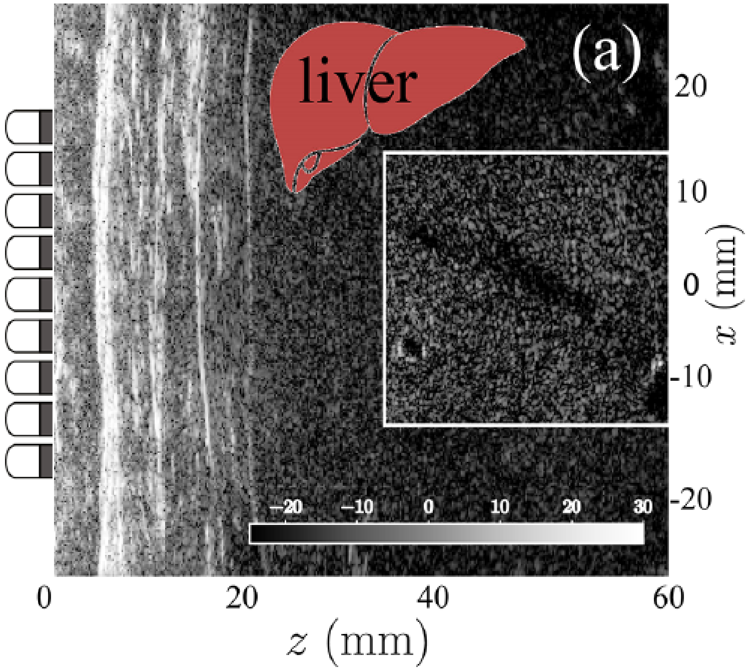

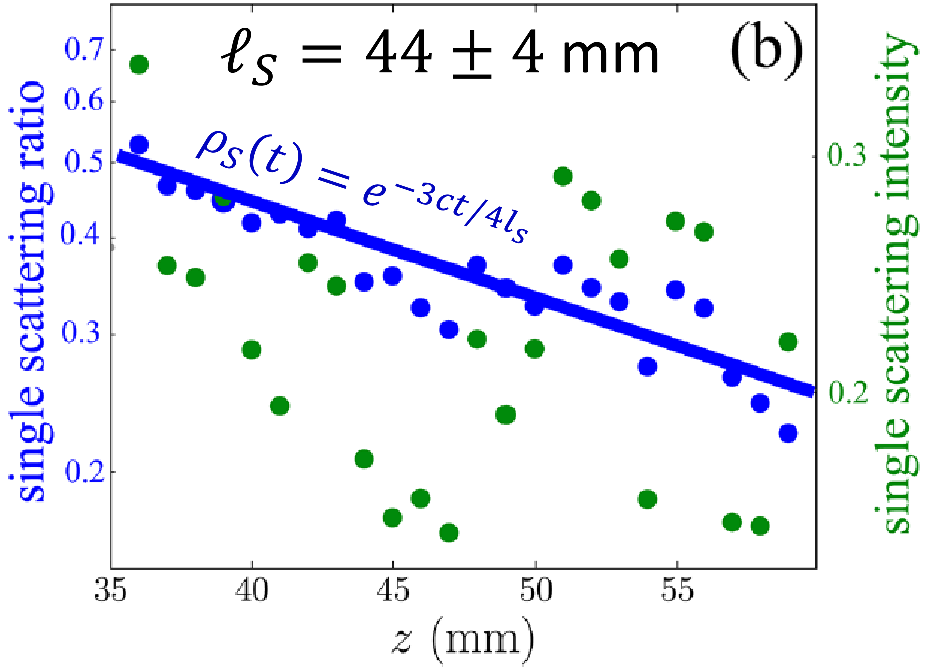

Single scattering rate robust to reflectivity fluctuations

Potential bio-marker of liver disease !

A. Goicoechea *et al.*, Phys. Rev. Lett. (2024)

Conclusion
& Perspectives

Going Beyond ℓ_t

Multi-Conjugate Adaptive Focusing

Address complex wave trajectories

Retrieve a highly-resolved map
of refractive index

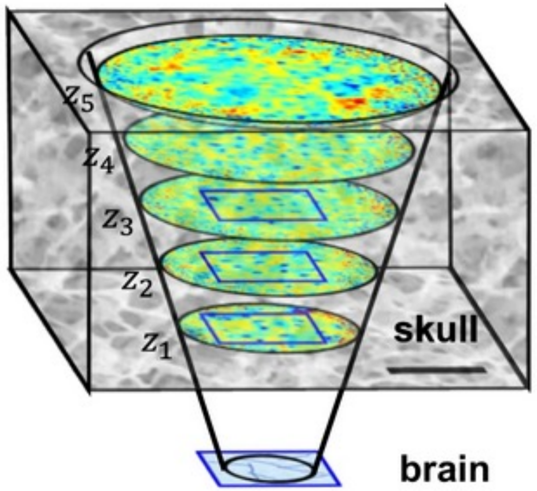

S. Kang, *et al.*, Nat. Commun. (2023)

Exploit time/frequency degrees of freedom

Harness wave diffusion

Exploit multiple scattering for high resolution and
deeper imaging

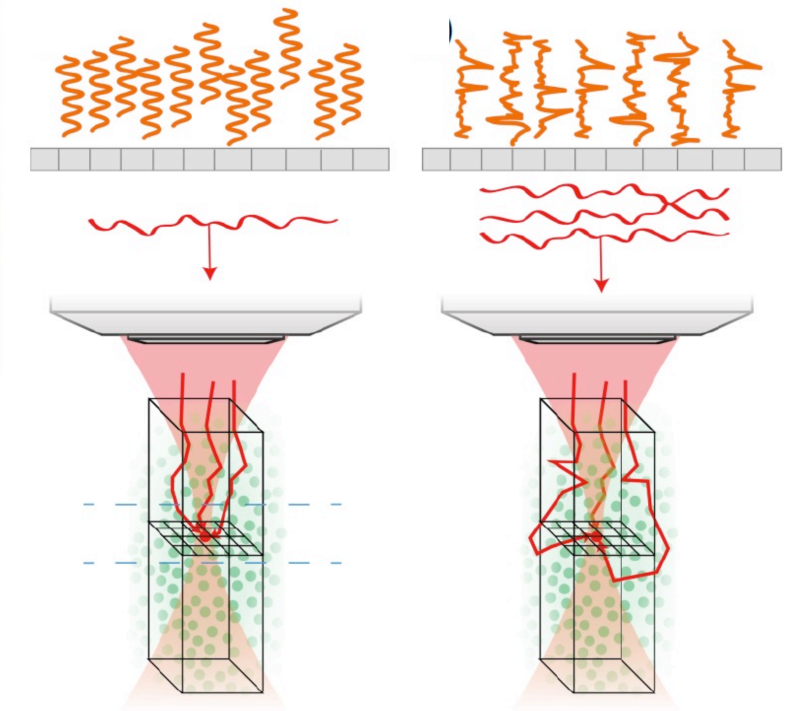

Going beyond Isoplanicity

Exploit Medium Dynamics

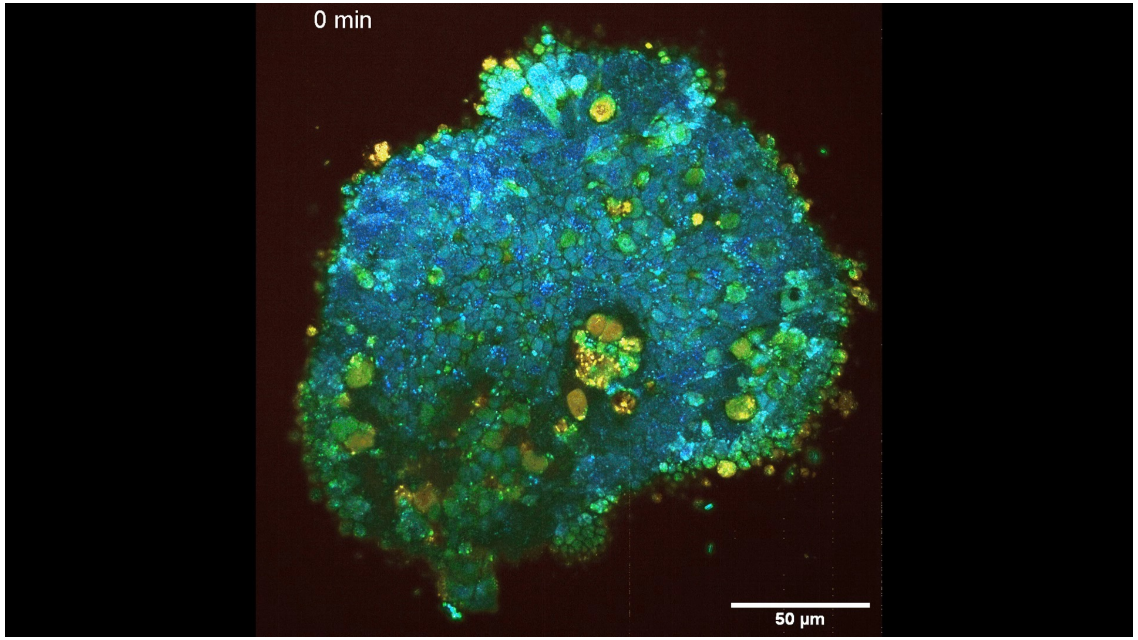

J. Scholler *et al.*, Light Sci. Appl., 2019

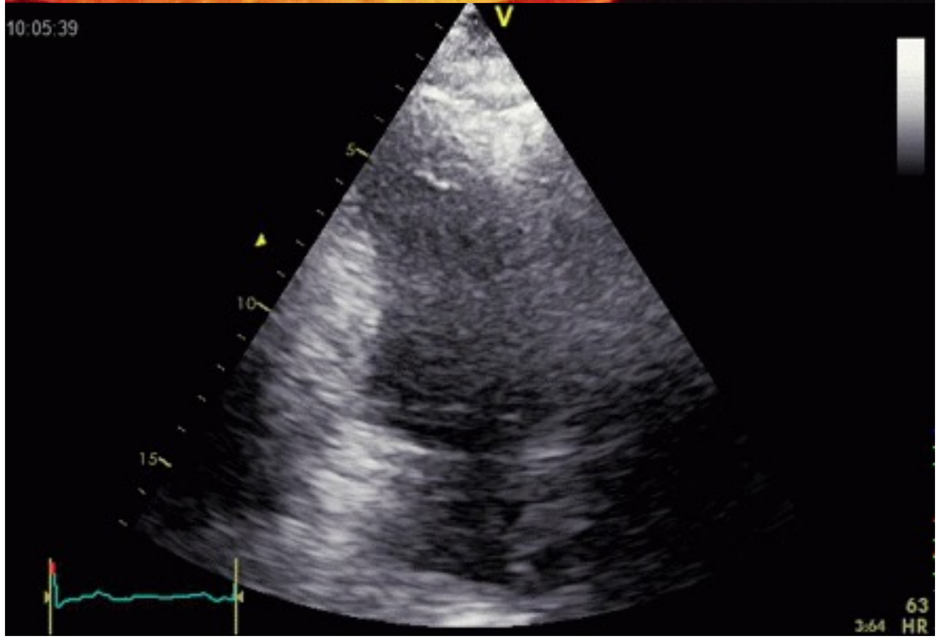

Going beyond isoplanicity

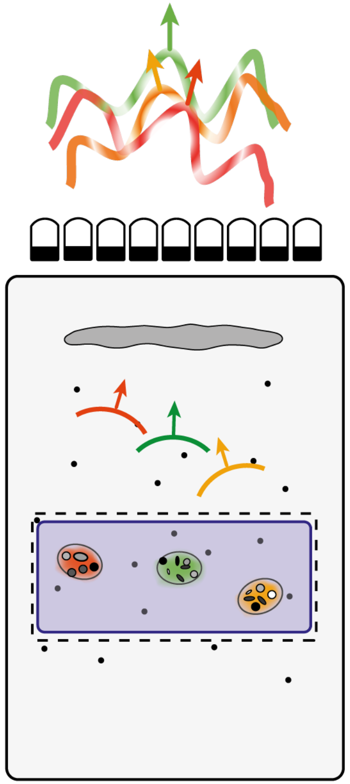

Spatial correlations ✓

Un-correlated
wave-front distortions

⇓

Aberration law

Virtual coherent reflector

Isoplanatic patch ~ Correlation area

Elsa Giraudat

Going beyond isoplanicity

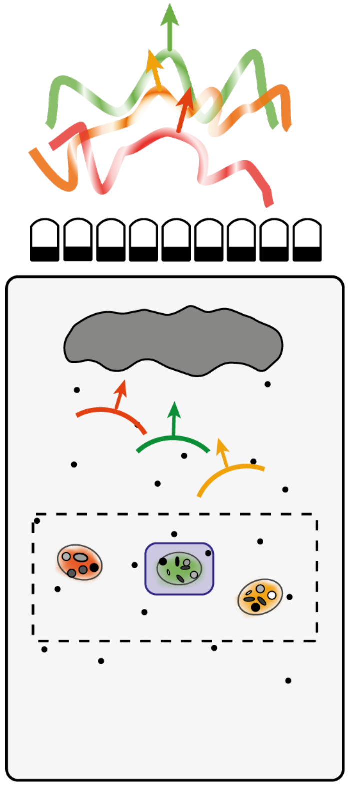

Spatial correlations

Un-correlated
wave-front distortions

⇓

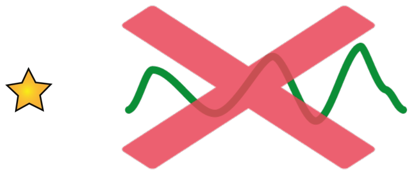

Isoplanatic patch < Correlation area

Elsa Giraudat

Lack of isoplanatism makes adaptive focusing and matrix imaging fail

Going beyond isoplanicity

Spatial correlations

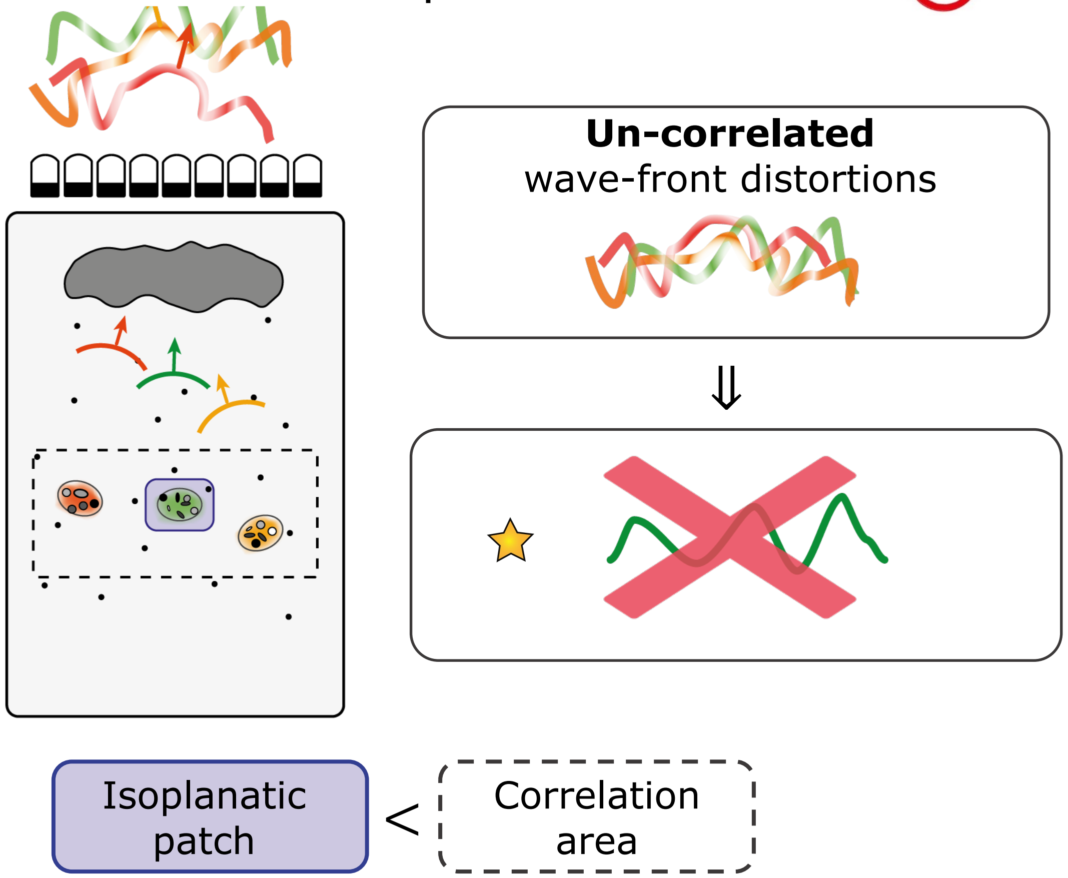

Temporal correlations

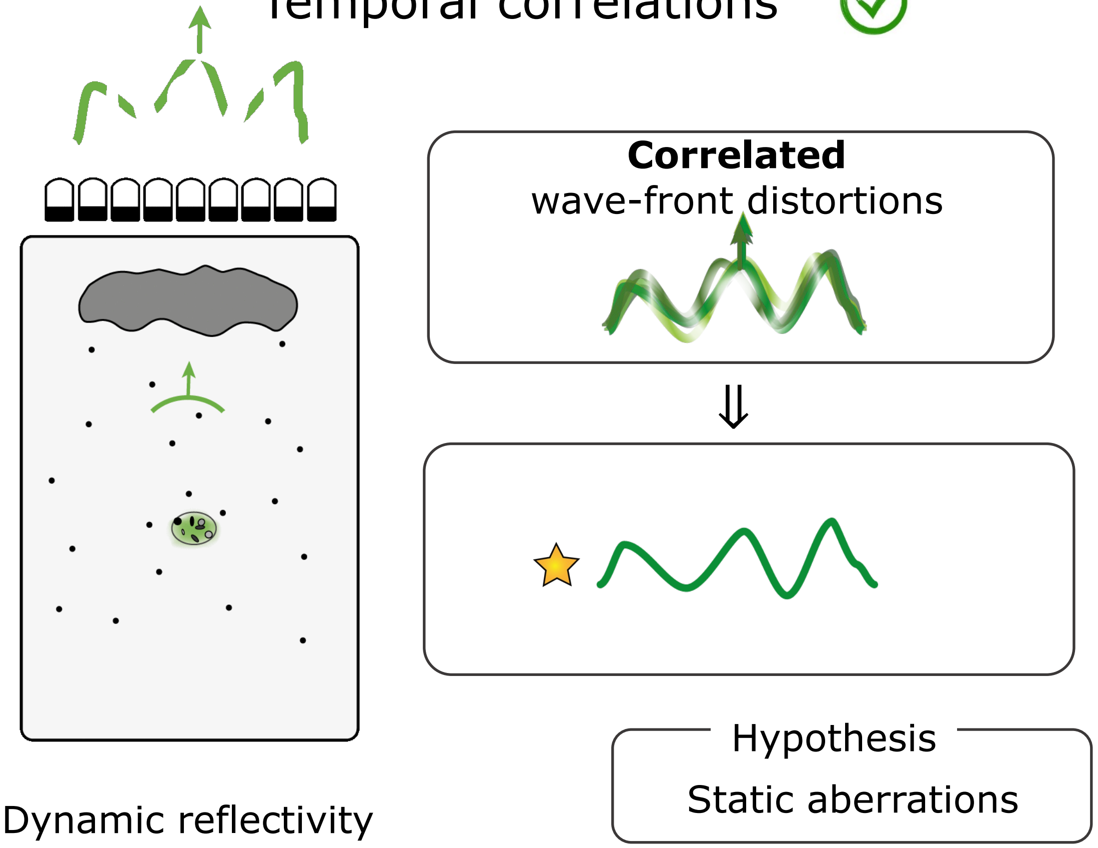

[Zhao et al., 1992] "Phase Aberration Correction Using Echo Signals from Moving Targets I: Description and Theory". *Ultrasonic Imaging*
[Osmanksi et al., 2012] "Aberration correction by time reversal of moving speckle noise". *IEEE TUFFC*

Going beyond Isoplanicity

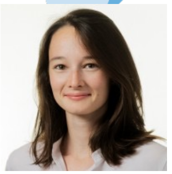

Elsa Giraudat

Yichen Sun

Spatial correlations

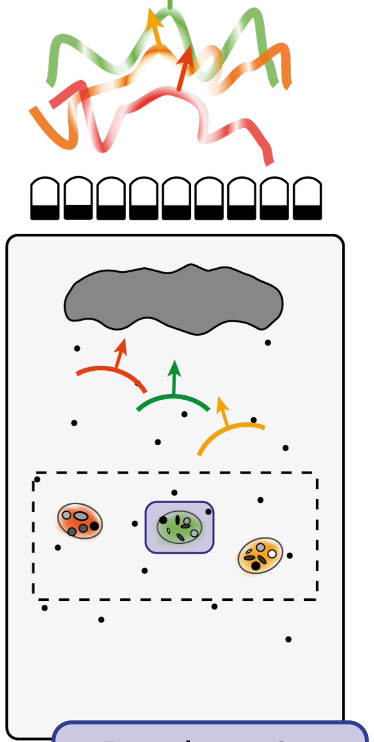

Un-correlated
wave-front distortions

⇓

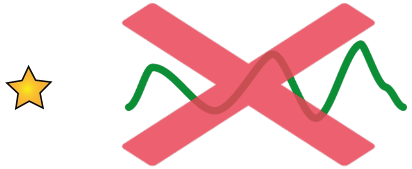

Isoplanatic patch < Correlation area

Temporal correlations

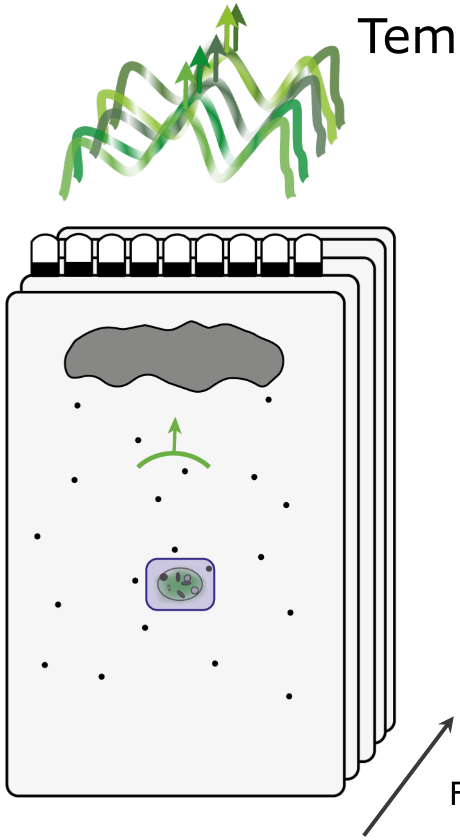

Correlated
wave-front distortions

⇓

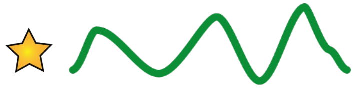

Hypothesis
Static aberrations

Exploit temporal decorrelation of speckle to obtain independent focusing laws for each point of the medium

Acknowledgements

Reminiscence

Jad Aoun
Paul Balondrade
Victor Barolle
Emma Brenner
Cécile Brütt
Flavien Bureau
Gatien Clément
Laura Cobus
Elsa Giraudat
Antton Goïcoechea
Nicolas Guigui
Hussam Hanouni
William Lambert
Arthur Le Ber
Ulysse Najar
Justine Robin
Yichen Sun
Rita Touma
Thibaud Vernier
Thomas Wasik

Collaborators

Mathias Fink
Michel Campillo
Claire Prada
Arnaud Derode
Claude Boccara
Arnaud Burtin
Olivier Couture
Jean-Christophe Komorowski

Institut Langevin ONDES ET IMAGES
Supersonic imagine
IPGP INSTITUT DE PHYSIQUE DU GLOBE DE PARIS
OVSG
LIB Laboratoire d'Imagerie Biomédicale
ESPCI PARIS
cnrs
PSL UNIVERSITÉ PARIS

Harnessing Spatio-Temporal d.o.f

Towards a compensation of multiples

Elsa Giraudat

Academic Experiment

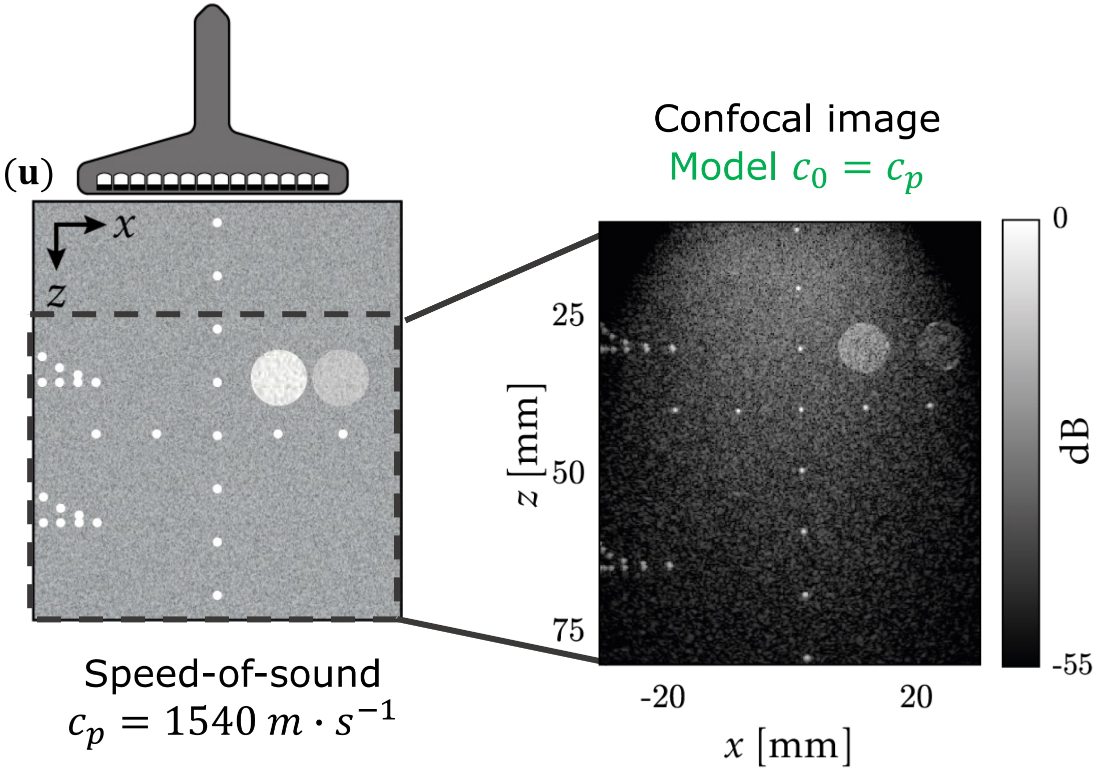

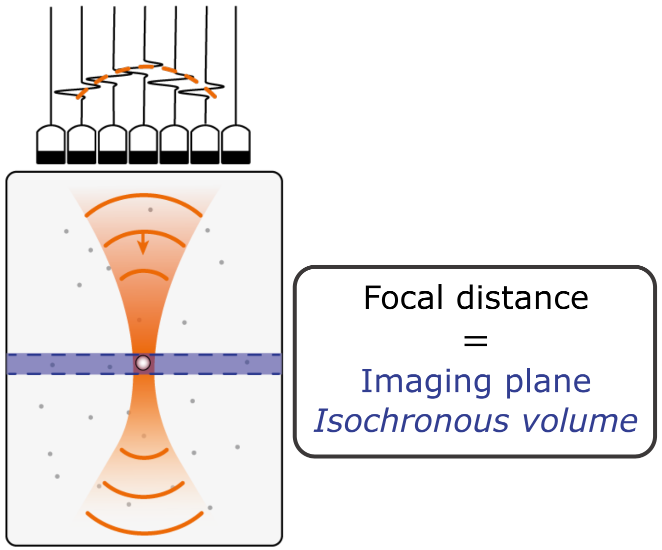

The confocal image is a correct estimator of the medium reflectivity

Academic Experiment

Linear array

Plexiglas

Tissue-mimicking phantom

$c_{\mathbf{plexi}}$
$\sim \mathbf{2800\ m \cdot s^{-1}}$

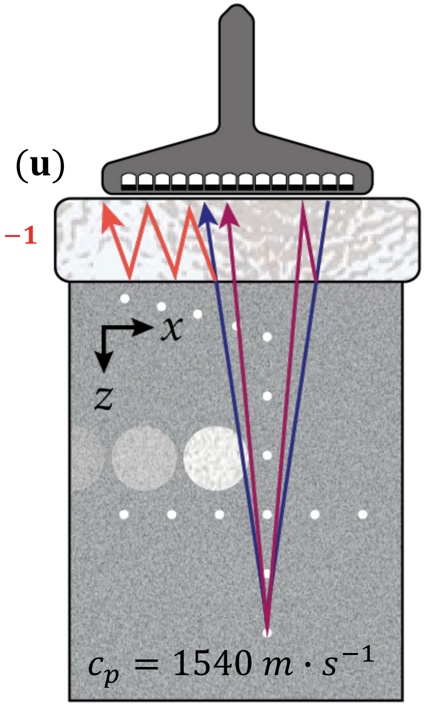

confocal image
Model $c_0 = c_p$

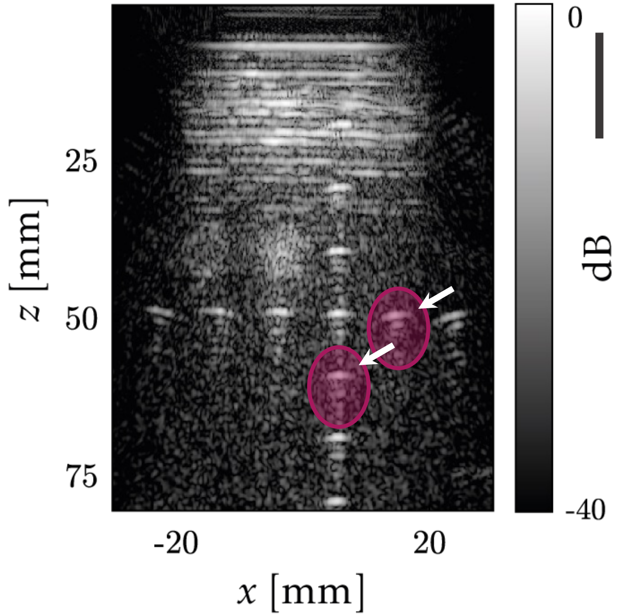

multiple reflections

wrong wave velocity model c_0
+ reverberations

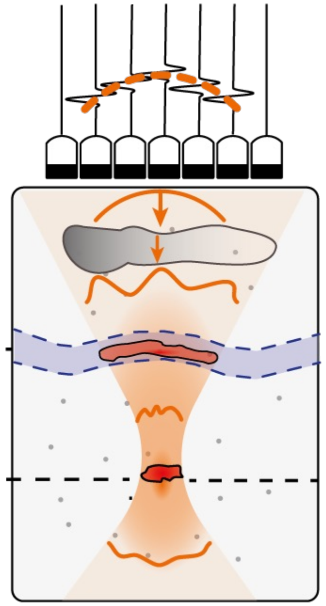

imaging plane
defocus
focal distance

Ballistic	
Multiple reflections	

- ✗ wave velocity mismatch ⇒ defocus
- ✗ Impédance discontinuities ⇒ reverberations

Revereberations drastically degrade the ultrasound image
To compensate for this detrimental effect, an adapted spatio-temporal focusing law shall be tailored

Probing the temporal dispersion of echoes

Focused Reflection Matrix

$\overline{\mathbf{R}}_{\mathbf{rr}} = [\mathrm{R}(x_{\mathrm{out}}, \boldsymbol{x}_{\mathrm{in}}, z)]$

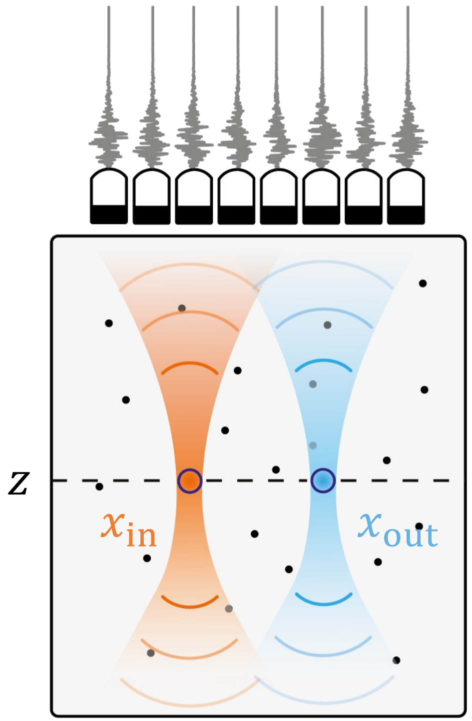

$z_{in} = z_{out}$

Spatial spreading of focal spots

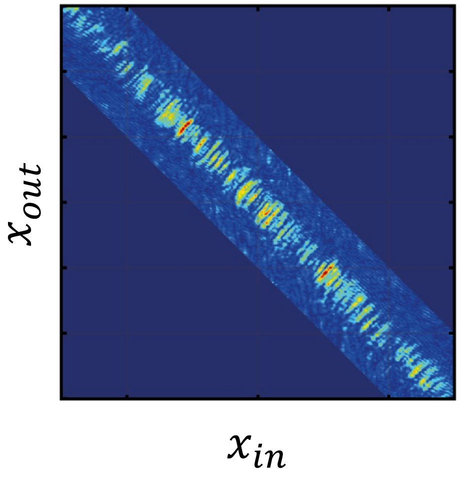

Beamforming process

$$R(\mathbf{r}_{\mathrm{out}}, \mathbf{r}_{\mathrm{in}}, \tau) = \sum_{\mathbf{u}_{\mathrm{in}}} \sum_{\mathbf{u}_{\mathrm{out}}} R\big(\mathbf{u}_{\mathrm{out}}, \mathbf{u}_{\mathrm{in}}, \underline{\Delta t(\mathbf{u}_{\mathrm{in}} \to \mathbf{r}_{\mathrm{in}}) + \Delta t\,(\mathbf{r}_{\mathrm{out}} \to \mathbf{u}_{\mathrm{out}})}\big)$$

way-and-return travel time
= **ballistic** time

Probing the temporal dispersion of echoes

Focused Reflection Matrix

$\overline{\mathbf{R}}_{\mathbf{rr}} = [\mathrm{R}(x_{\mathrm{out}}, x_{\mathrm{in}}, z)]$

Time-resolved Focused **R**-matrix

$\mathbf{R}_{\mathbf{rr}}(\tau) = [\mathrm{R}(\mathbf{r}_{\mathrm{out}}, \mathbf{r}_{\mathrm{in}}, \tau)]$

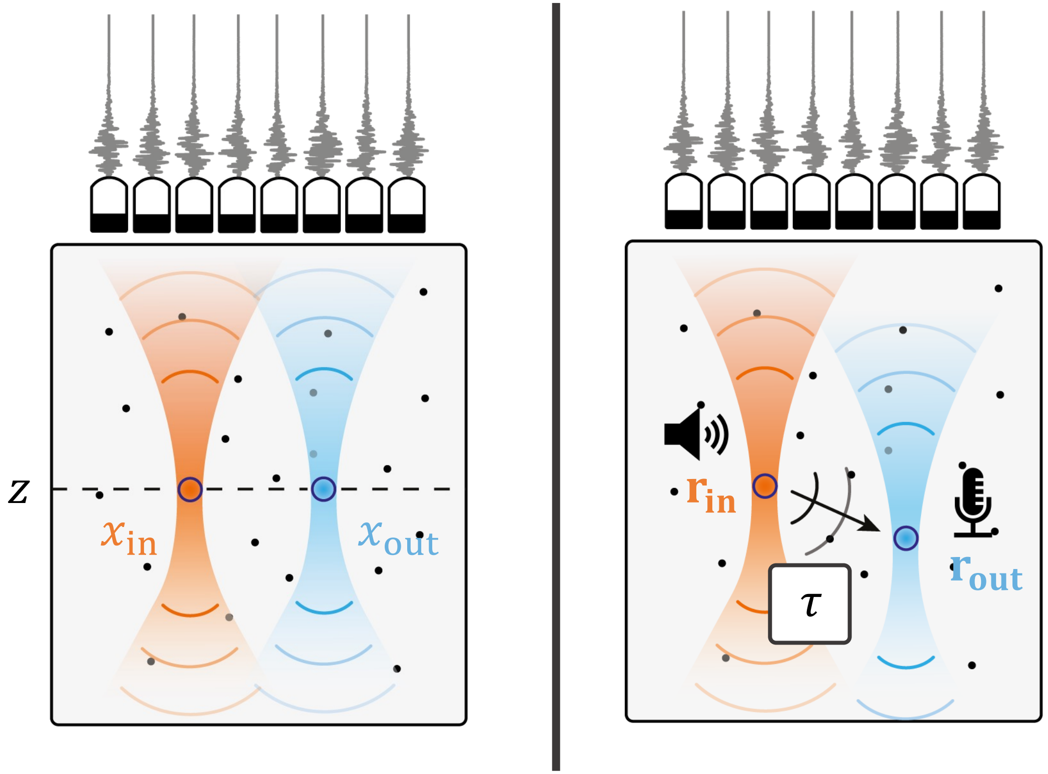

Ballistic time

Beyond ballistic time

$z_{in} \neq z_{out}$

Time-resolved responses between each couple of virtual sources and detectors

Probing the temporal dispersion of echoes

Focused Reflection Matrix

$\overline{\mathbf{R}}_{\mathbf{rr}} = [\mathrm{R}(x_{\mathrm{out}}, x_{\mathrm{in}}, z)]$

Time-resolved Focused **R**-matrix

$\mathbf{R}_{\mathbf{rr}}(\tau) = [\mathrm{R}(\mathbf{r}_{\mathrm{out}}, \mathbf{r}_{\mathrm{in}}, \tau)]$

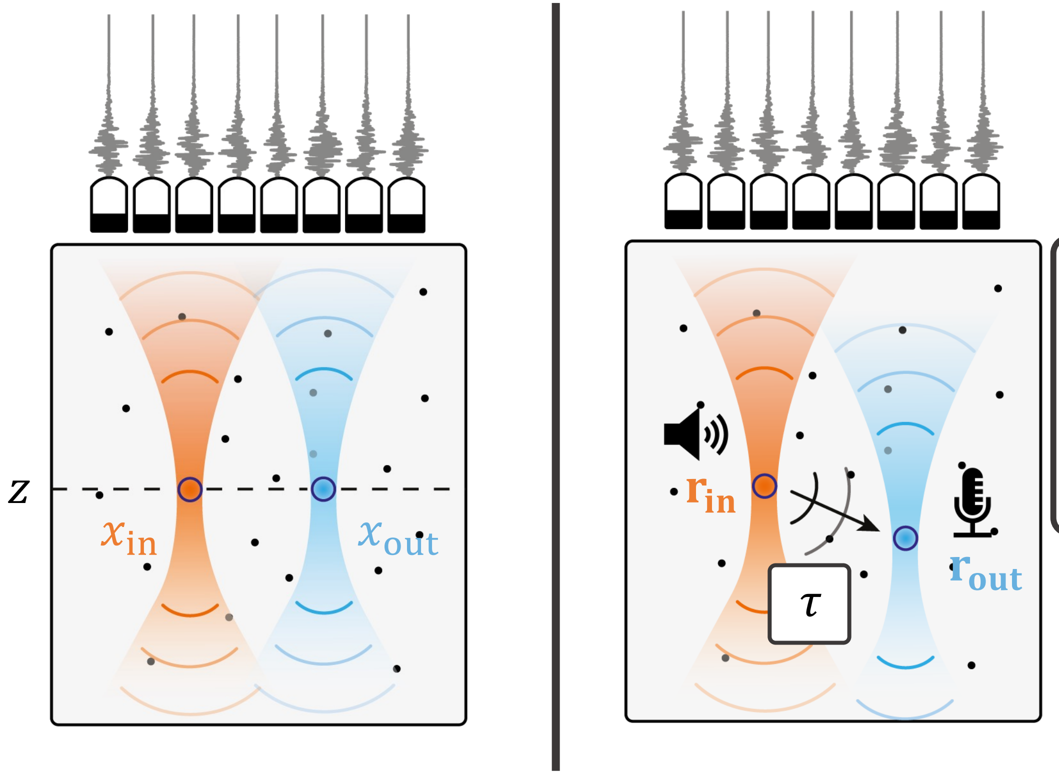

Ballistic time

Beyond ballistic time

Generalized beamforming process

$$R(\mathbf{r}_{\mathrm{out}}, \mathbf{r}_{\mathrm{in}}, \tau) = \sum_{\mathbf{u}_{\mathrm{in}}} \sum_{\mathbf{u}_{\mathrm{out}}} R\Big(\mathbf{u}_{\mathrm{out}}, \mathbf{u}_{\mathrm{in}}, \underbrace{\Delta t(\mathbf{u}_{\mathrm{in}} \to \mathbf{r}_{\mathrm{in}}) + \Delta t\,(\mathbf{r}_{\mathrm{out}} \to \mathbf{u}_{\mathrm{out}})}_{\text{Ballistic time}} + \tau\Big)$$

Time lapse

Time-resolved responses between each couple of virtual sources and detectors

[Lambert, 2020] " Matrix Approach for Ultrasound Imaging and Quantification." *Thèse de Doctorat, Université PSL*

Self-Portrait of the Focusing Process

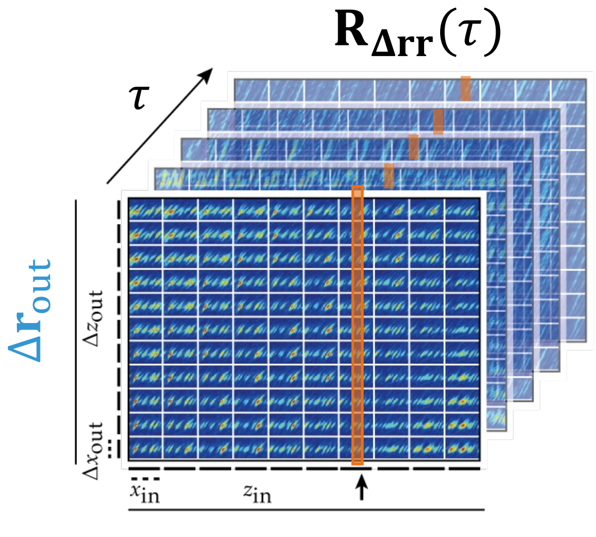

Tissue-mimicking Phantom
Right model c_0

Bright Scatterer

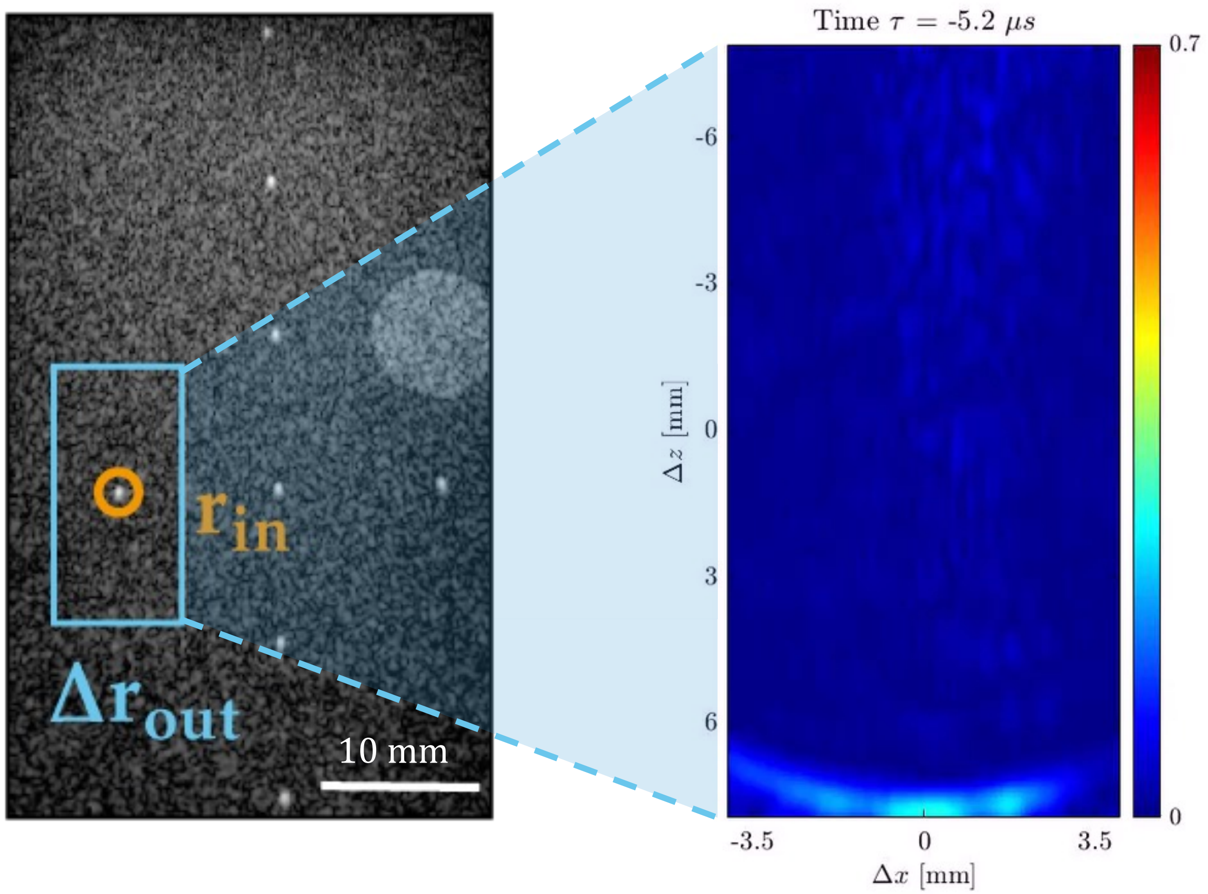

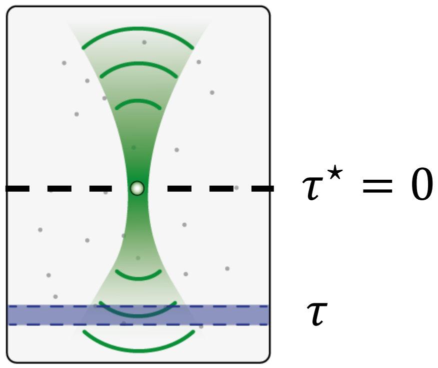

Focusing at the expected ballistic time $\tau^\star = 0\ \mu s$

No temporal dispersion

The time-resolved reflection matrix provides propagation movie associated with the echo reflected by the scatterer at point $\mathbf{r}_{in}$

Self-Portrait of the Focusing Process

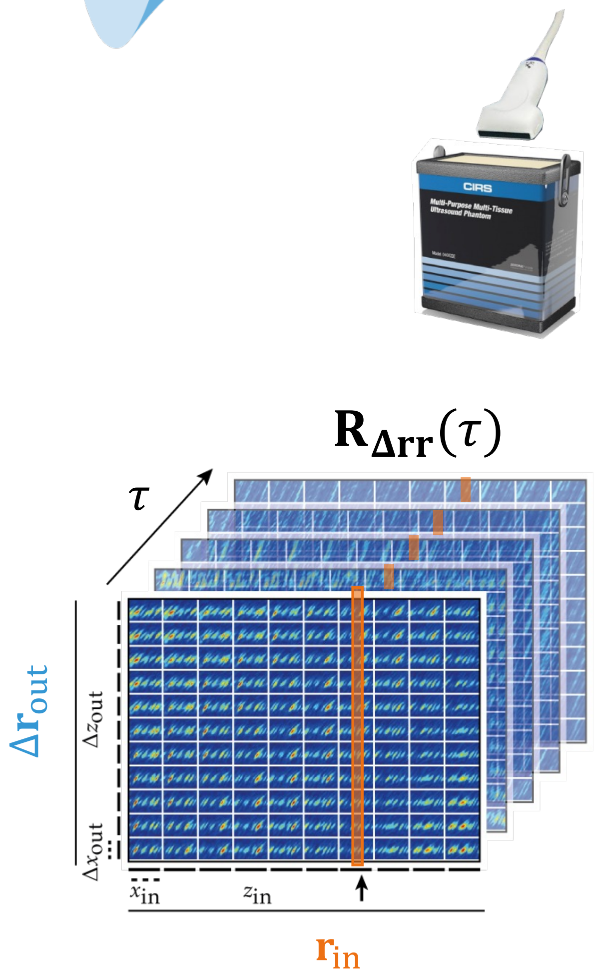

Tissue-mimicking Phantom

Right model c_0

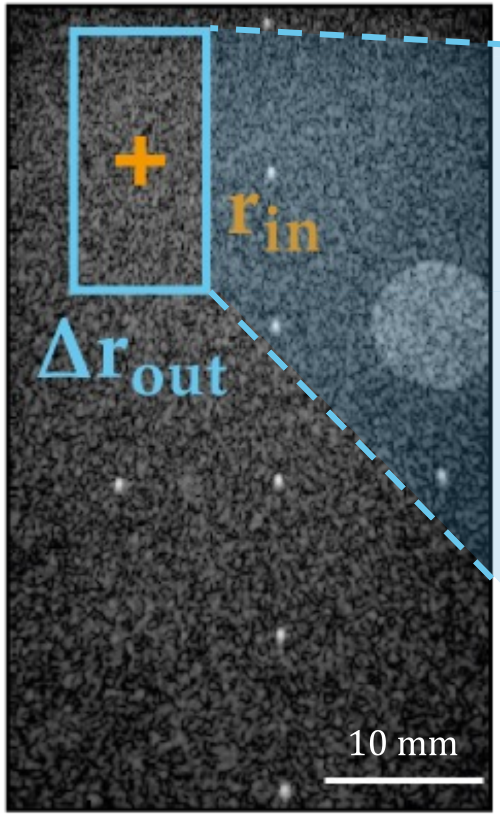

Speckle

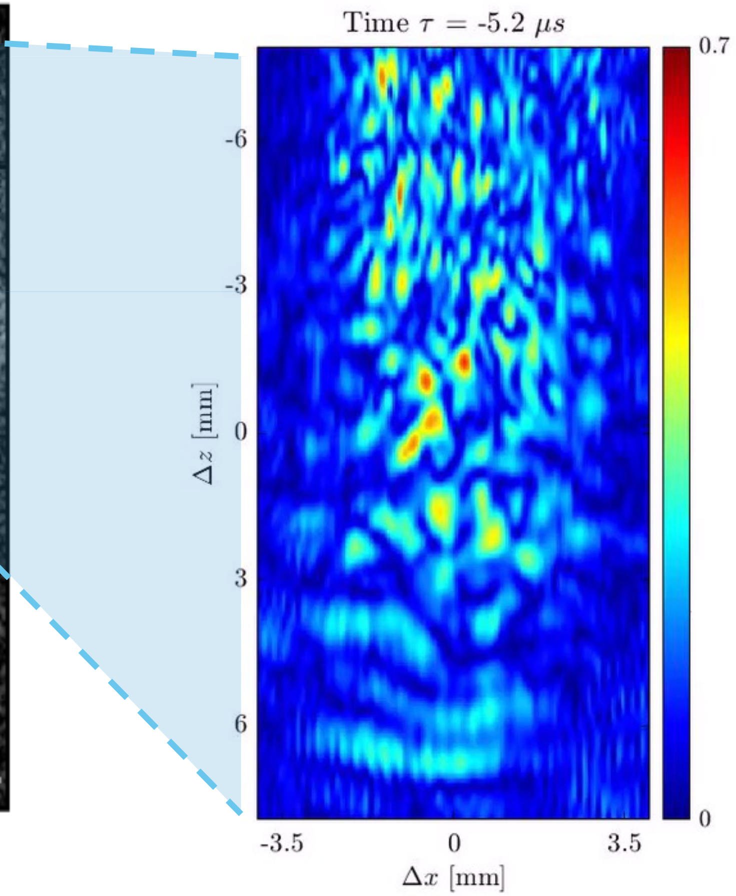

The coherent wave is hidden by random fluctuations due to ultrasound speckle and multiple scattering

Self-Portrait of the Focusing Process

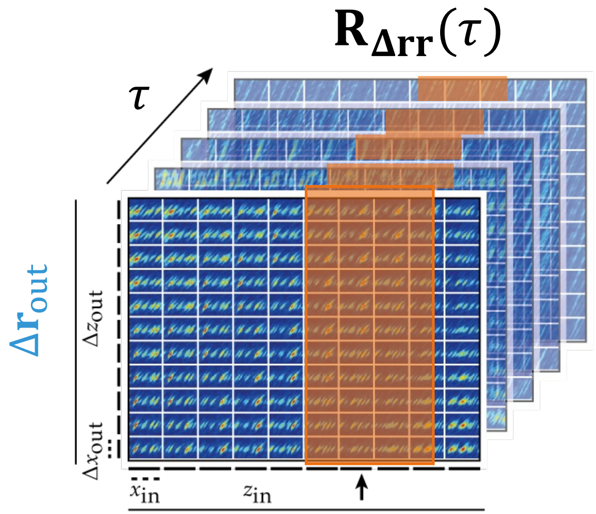

Set of points $\mathbf{r}_{in}$

Tissue-mimicking Phantom
Right model c_0

Correlation of movies between different speckle grains

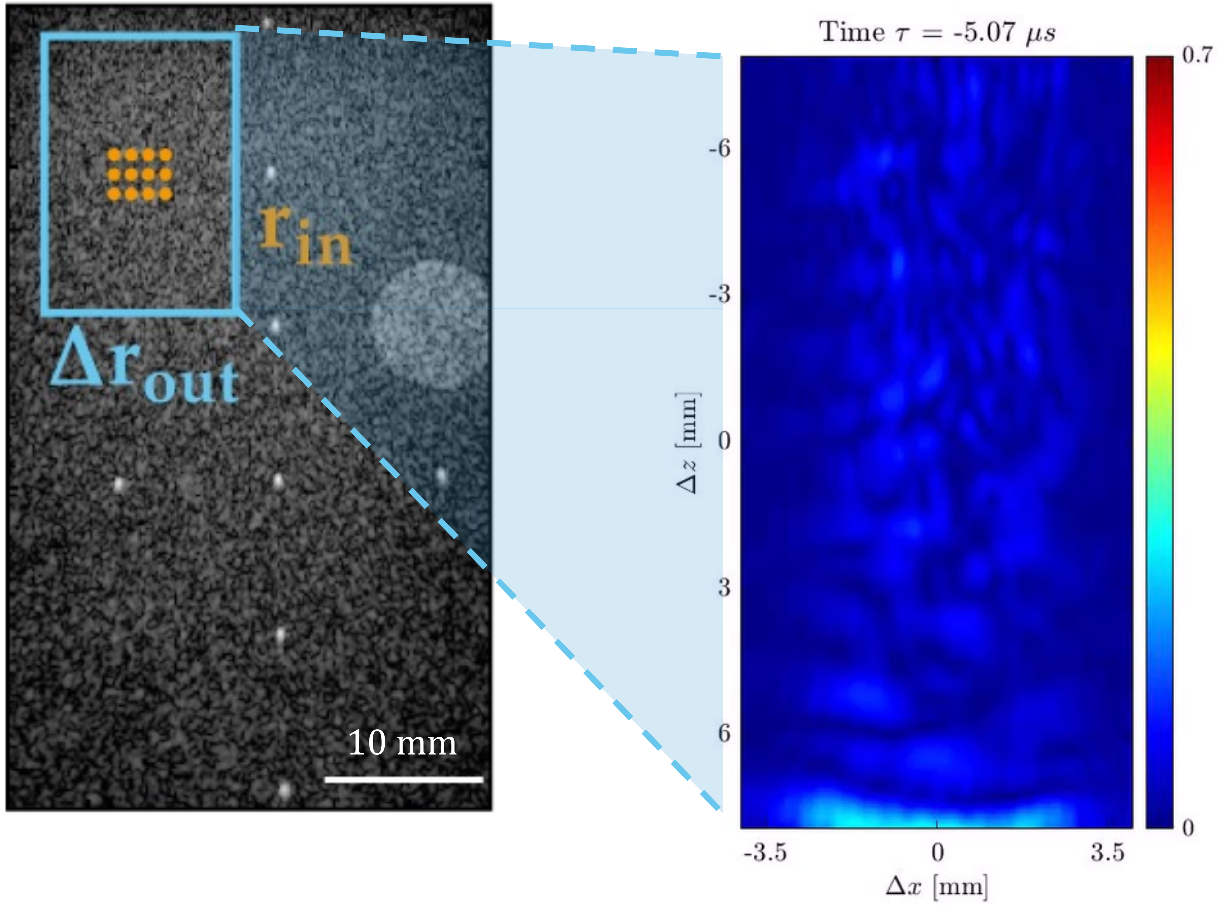

Focusing at the expected ballistic time $\tau^\star = 0\ \mu s$

No temporal dispersion

The coherent average over several realizations of disorder provides the coherent wave in ultrasound speckle

Self-Portrait of the Focusing Process

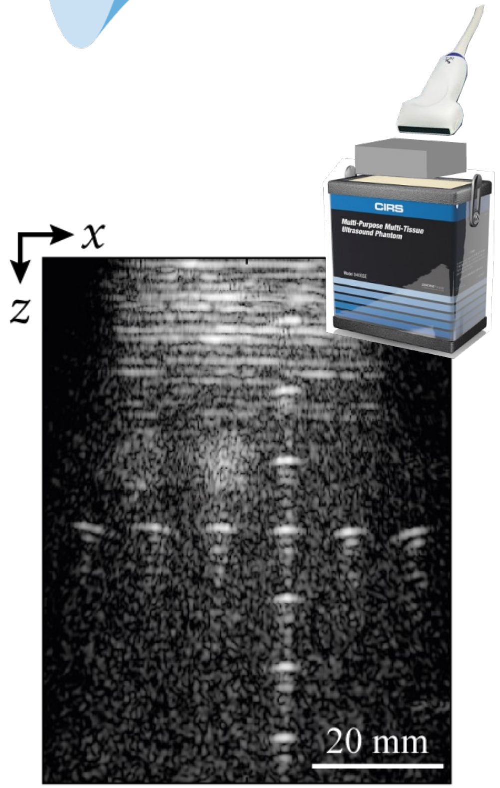

Phantom + **Plexiglass**
Wrong propagation model

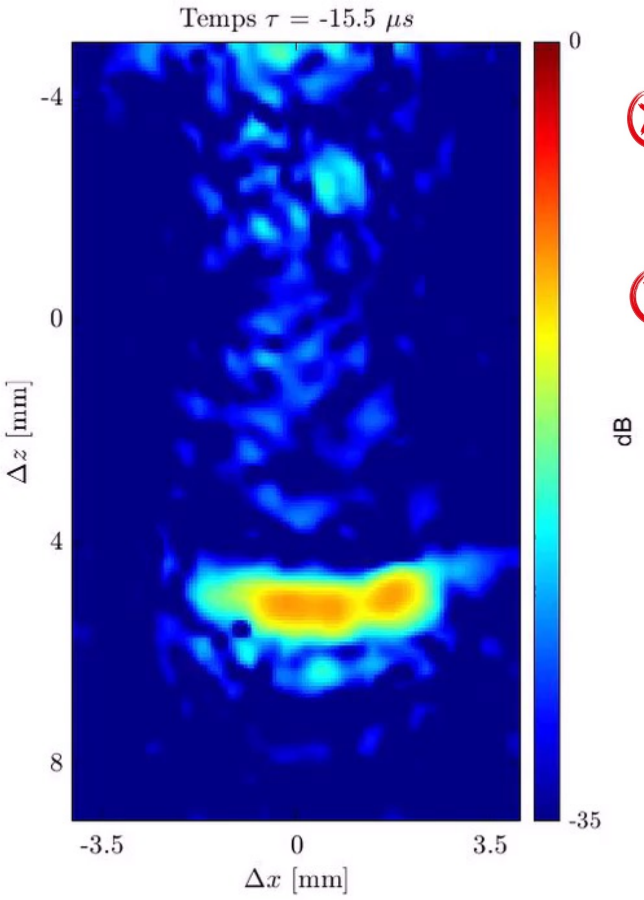

- Focusing of the ballistic wave at time $\tau^\star \sim -12\ \mu s$ ⇒ defocus
- Temporal tail of echoes ⇒ reverberations

Self-Portrait of the Focusing Process

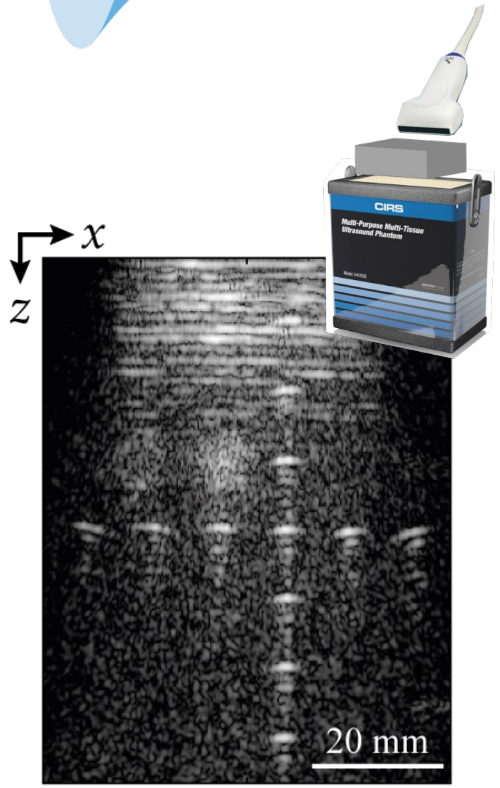

Phantom + **Plexiglass**
Wrong propagation model

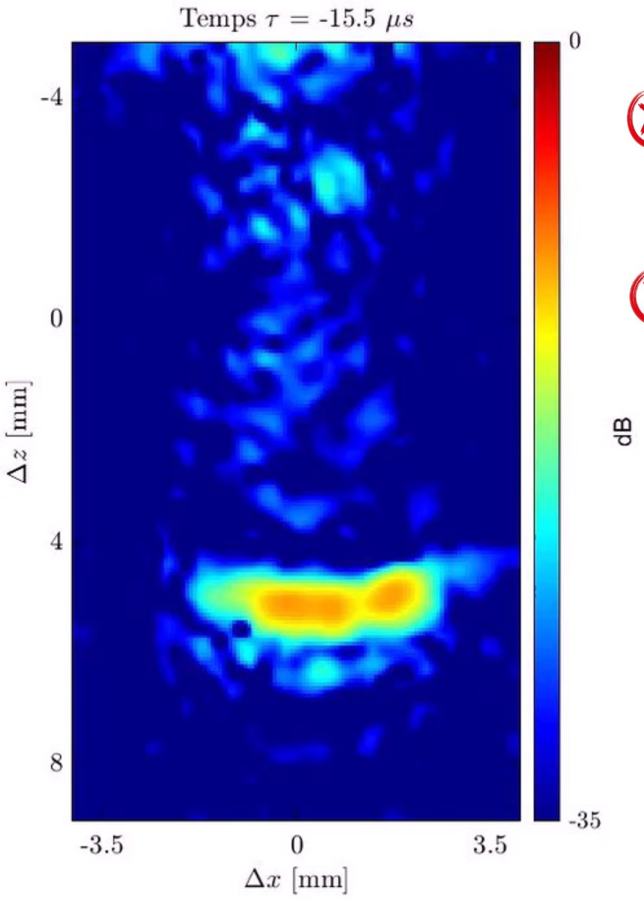

- Focusing of the ballistic wave at time $\tau^\star \sim -12\ \mu s$
  $\Rightarrow$ defocus
- Temporal tail of echoes
  $\Rightarrow$ reverberations

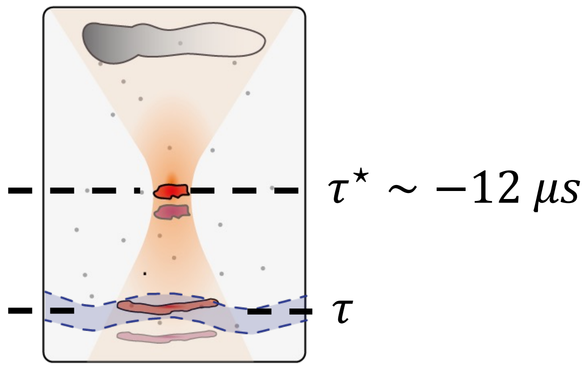

The time-resolved reflection matrix enables us to probe the temporal dispersion of echoes induced by the reverberating layer

How to use this information to compensate for this detrimental effect ?

Time compensation of reverberations

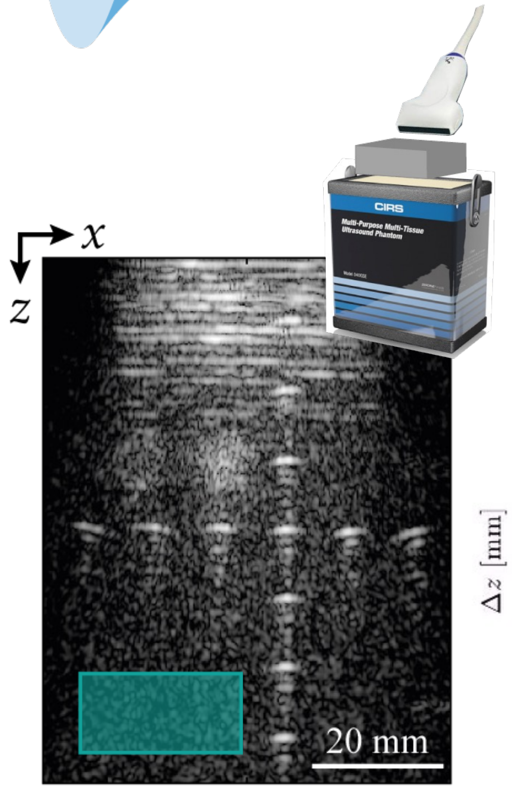

Estimation area of the focusing law in speckle

Phantom + **Plexiglass**

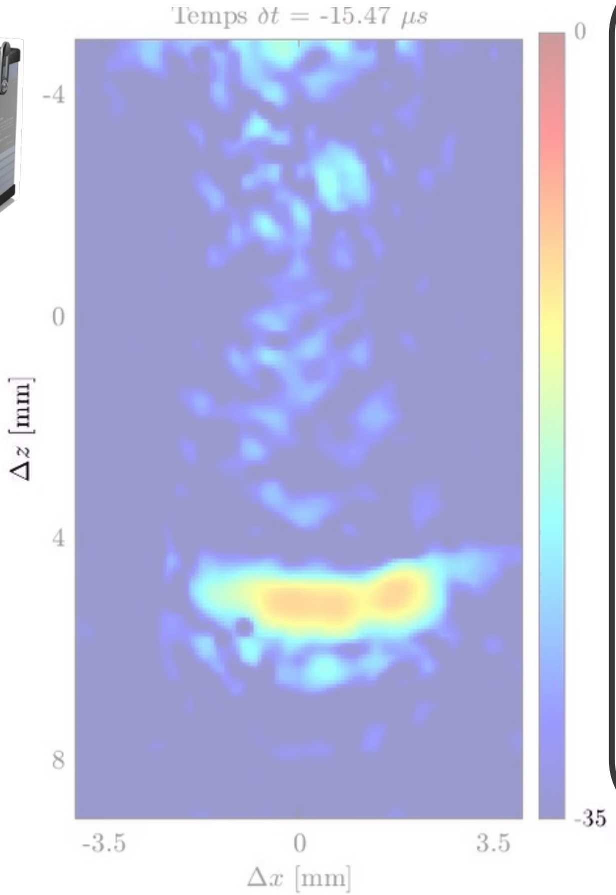

Time response of the virtual coherent reflector in speckle ☆

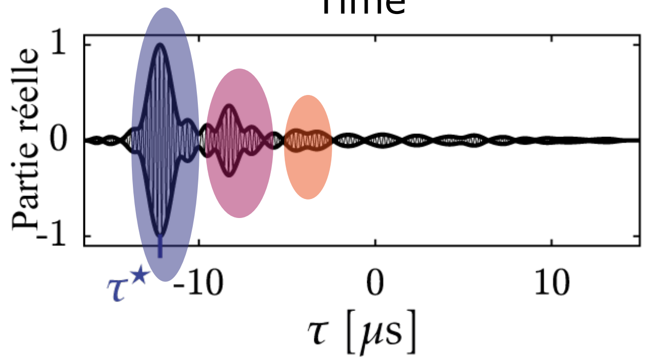

Ballistic echo

Multiple 1

Multiple 2

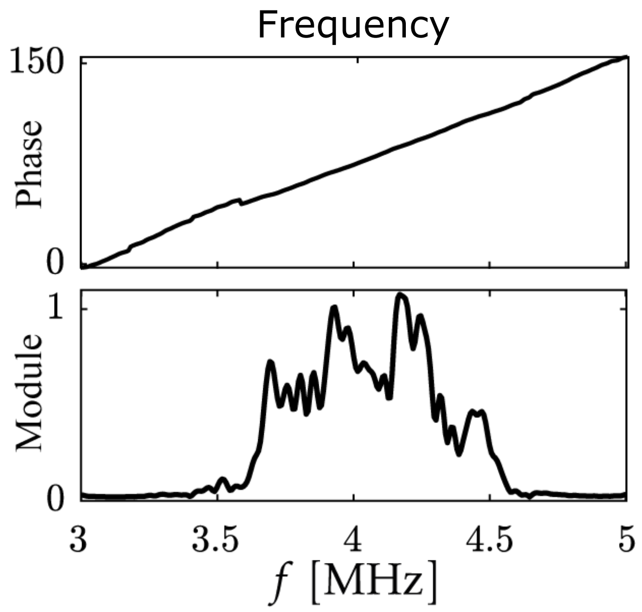

Time reversal of the temporal dispersion law can be leveraged to compensate for defocus and reverberations induced by the plexiglass layer

Time compensation of reverberations

Experiment
Plexiglass - Phantom

Conventional Image
$c_0 = 1540\ m \cdot s^{-1}$

Matrix Image
Full-field Correction

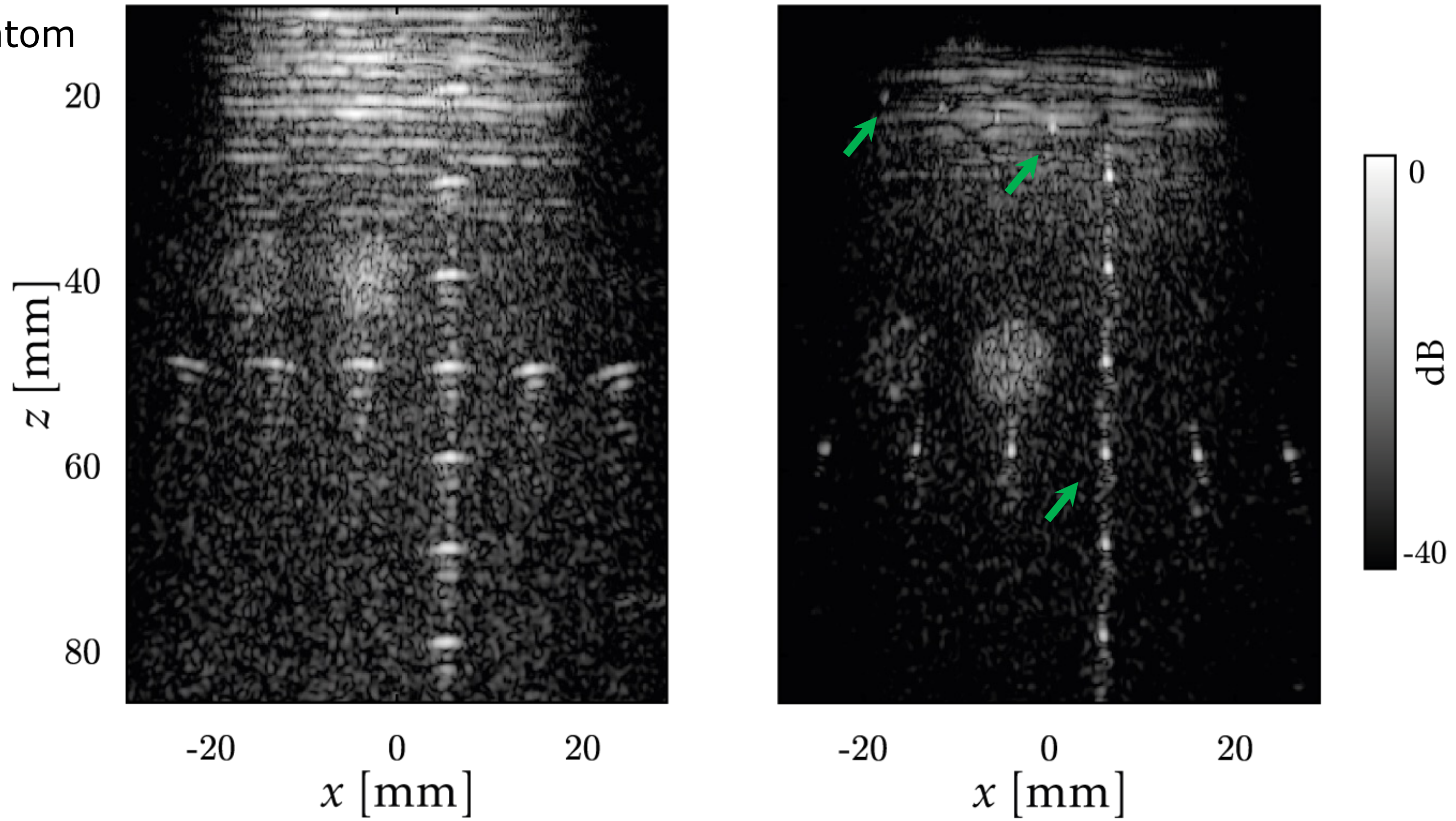

Corrected defocus

Multiples partially compensated

Residual anisoplanatic aberrations

Time reversal allows us to recompress in time the backscattered echoes.

Spatio-Temporal Focusing Laws

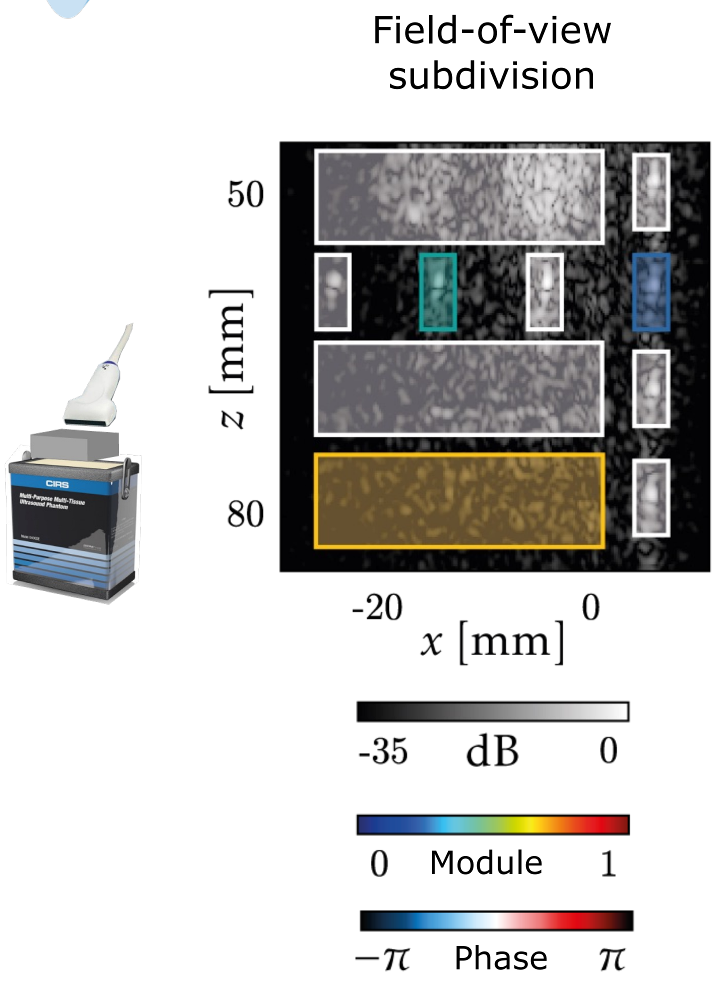

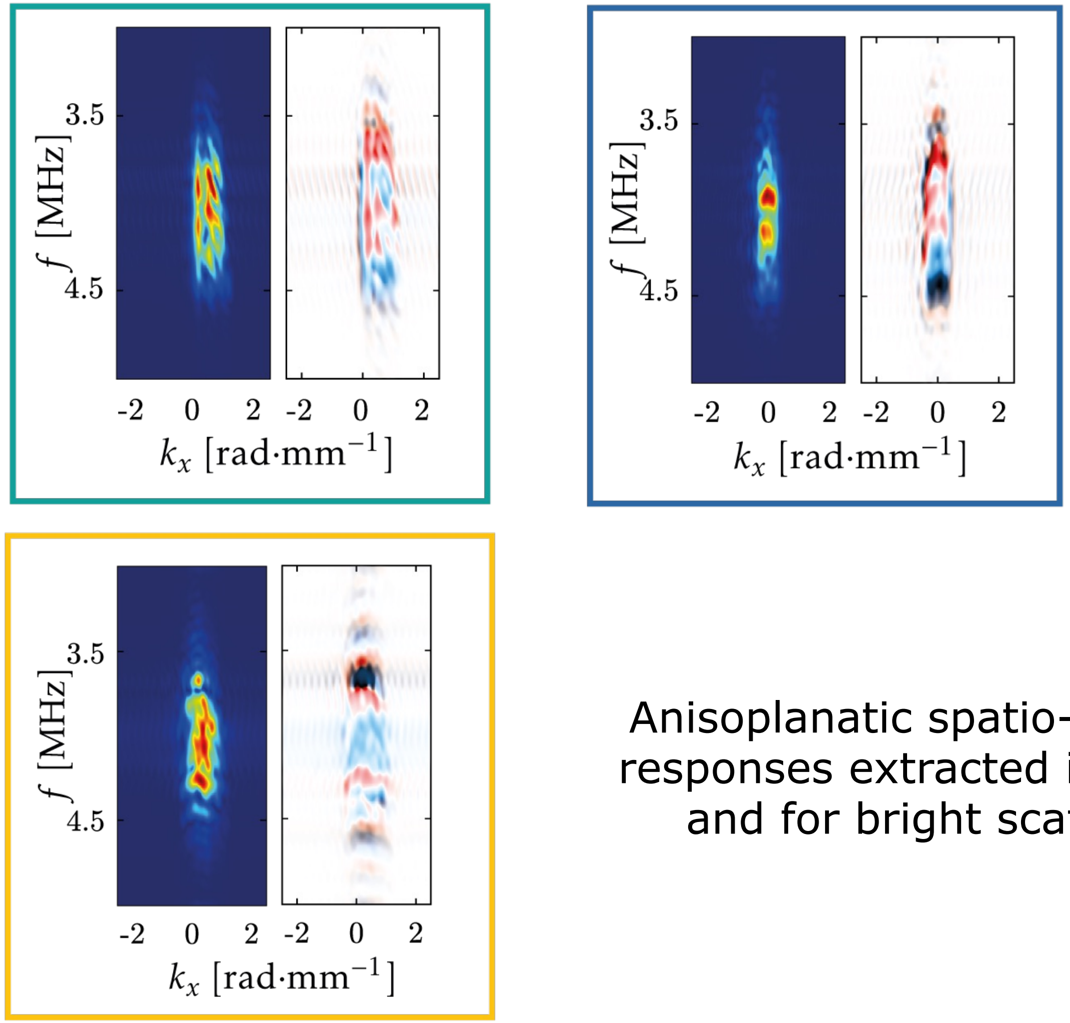

Anisoplanatic spatio-temporal responses extracted in speckle and for bright scatterers

Independent correction of each frequency component of the wave-field

Local Spatio-Temporal Focusing Laws

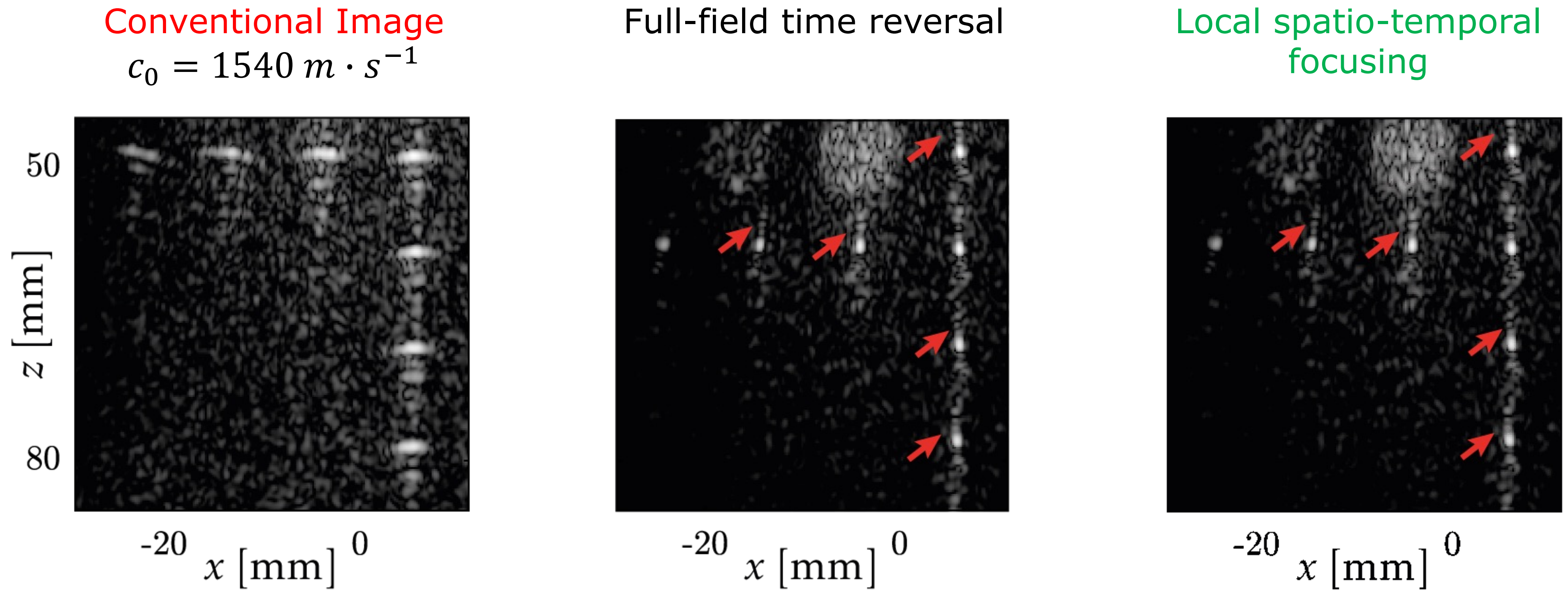

Local spatio-temporal focusing laws allows a fine compensation of multiple reflections and improves the image contrast

Transcranial imaging

Head phantom experiment

Linear probe
Phased array

Heterogeneous skull

- Strong attenuation
- Strong aberrations
- Reverberations

Spatio-Temporal Focusing Laws (Bright Scatterers)

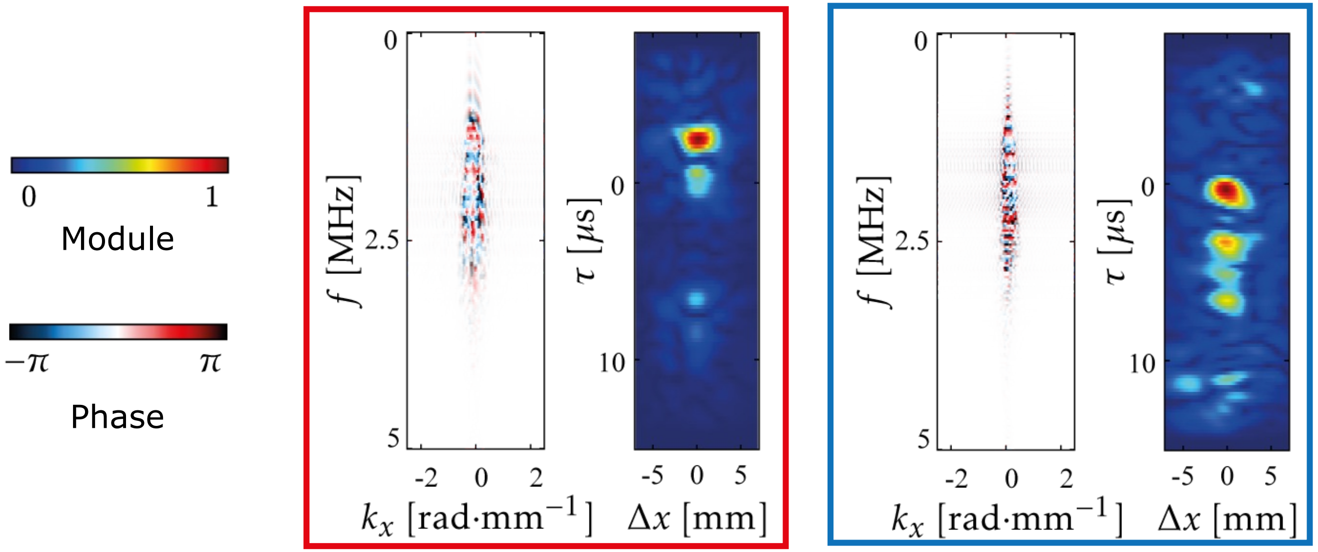

Spatio-temporal focusing

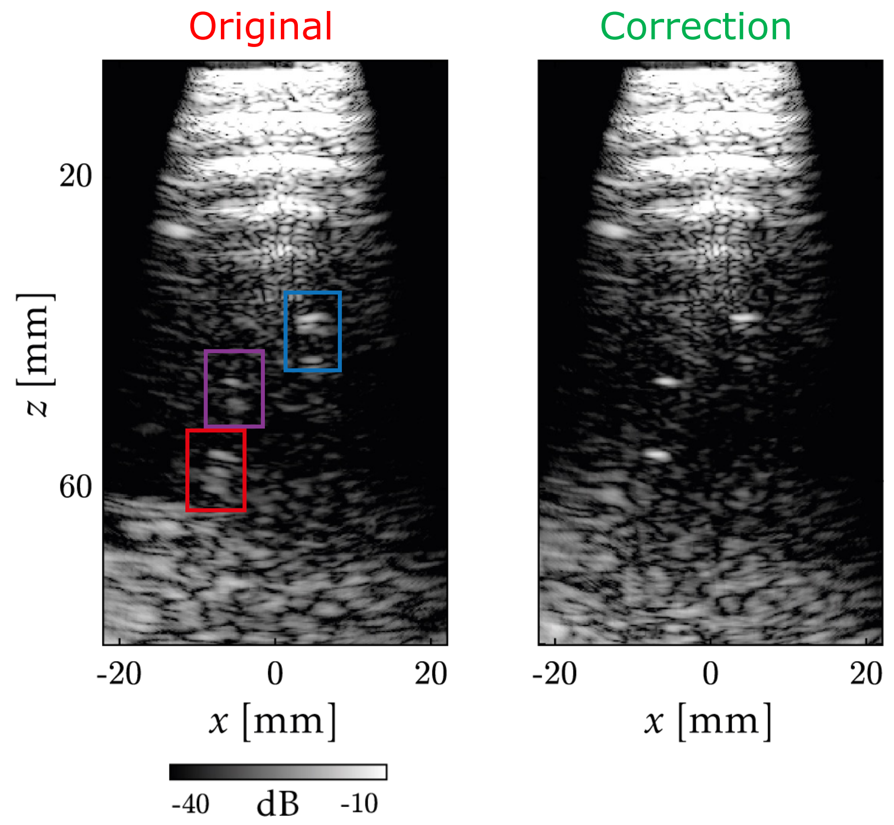

✓ Bright scatterers

✗ Speckle

Lack of isoplanicity to ensure the convergence towards a satisfying spatio-temporal focusing law in speckle

The isoplanatic limit

- In strongly heterogeneous media, the convergence towards a satisfying focusing law is not guaranteed
  ⇒ The range of the memory effect is too small

$\mathbf{r}_{\text{in}}^{1}$

$\mathbf{r}_{\text{in}}^{2}$

$\mathbf{r}_{\text{in}}^{3}$

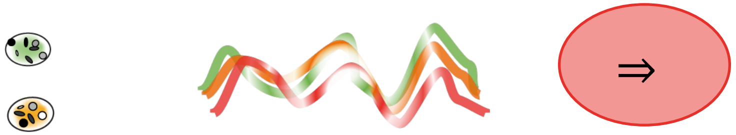

Coherent average over several speckle grains

Virtual coherent reflector

Loi d’aberration

Requires a sufficient number of focusing points $\mathbf{r}_{\text{in}}$ located in the same **isoplanatic patch**

Dynamic Matrix Imaging

Towards an ultra-local compensation of aberrations

Elsa Giraudat

Isoplanatic aberrations

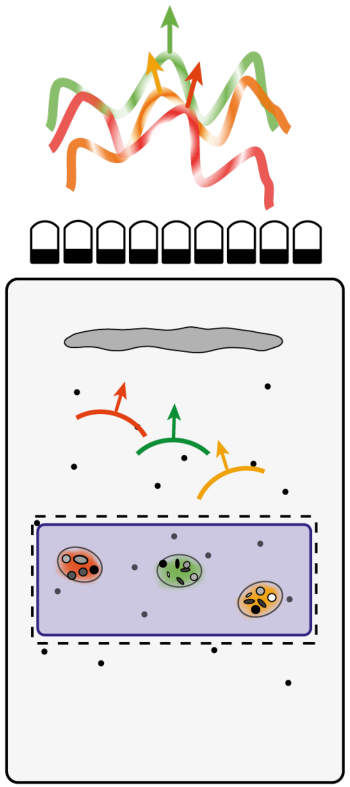

Spatial Correlations

Correlated
wave-front distortions

⇓

Aberration law

Virtual coherent reflector

Isoplanatic patch ~ Correlation area

Anisoplanatic Aberrations

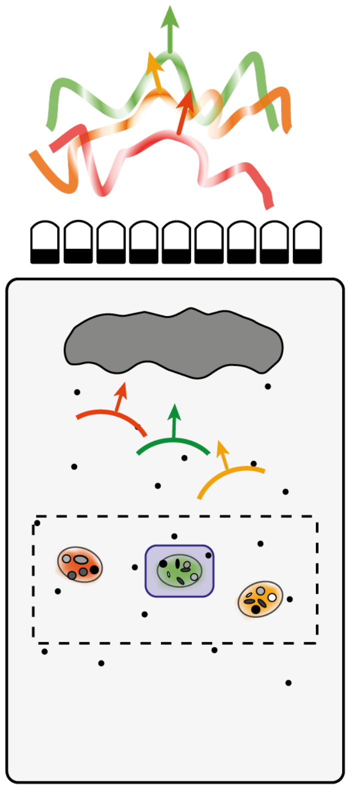

Spatial Correlations

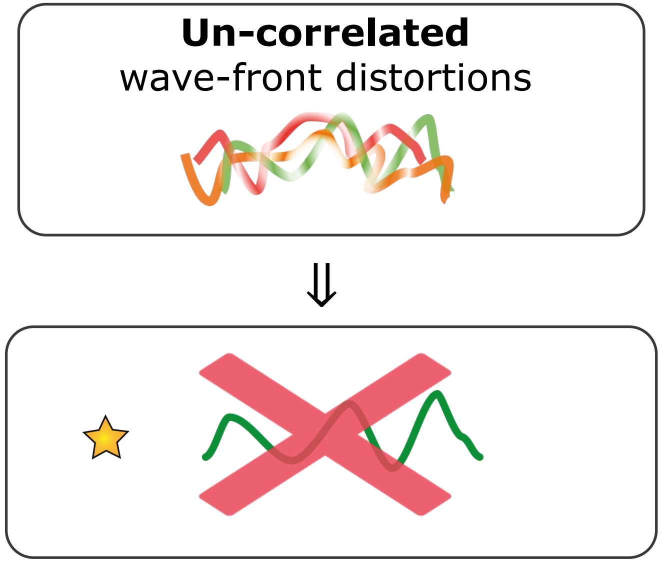

Isoplanatic patch < Correlation area

Lack of isoplanicity makes adaptive focusing and matrix imaging fail

Anisoplanatic Aberrations

Spatial correlations

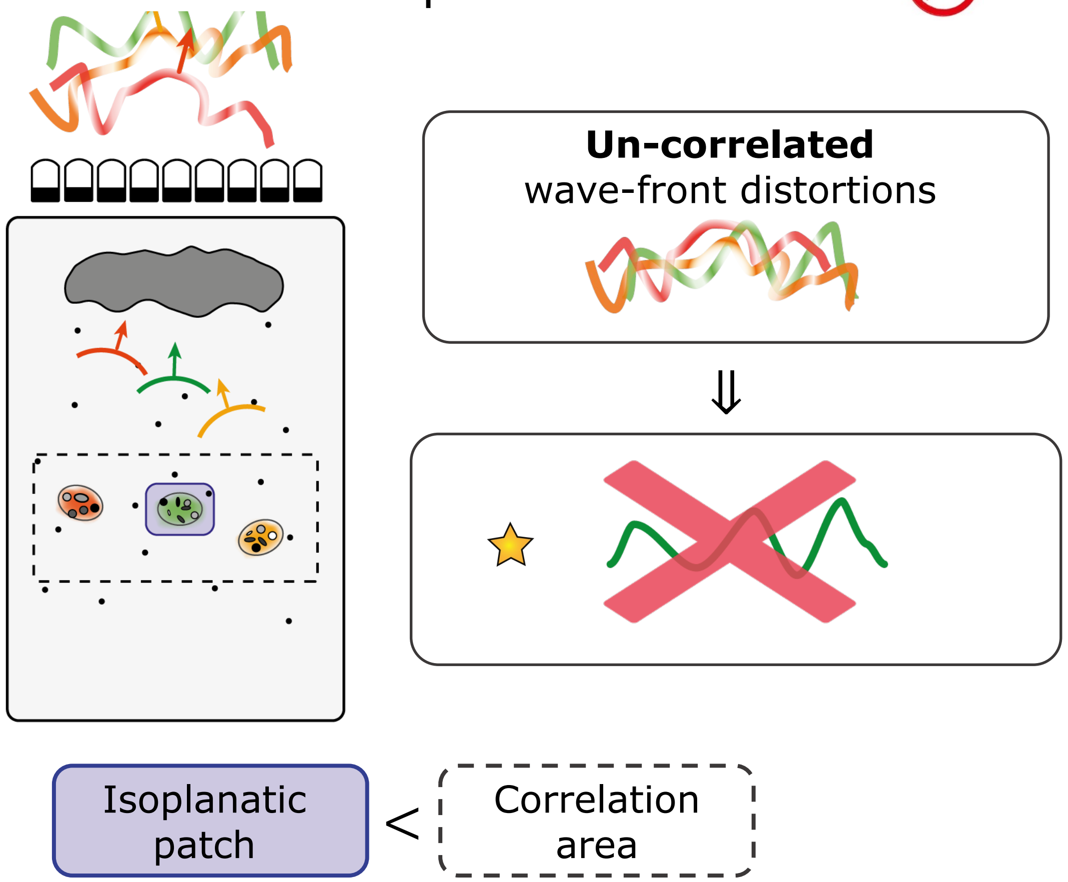

Temporal correlations

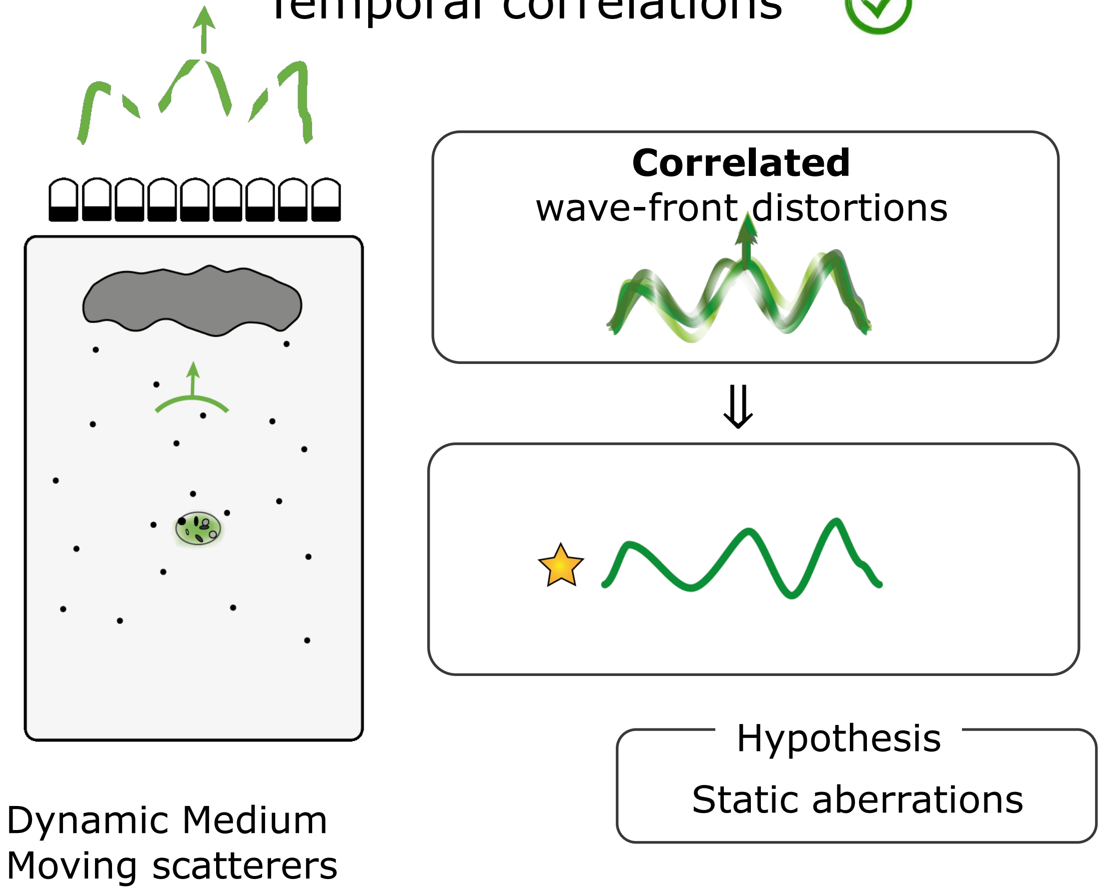

[Zhao et al., 1992] "Phase Aberration Correction Using Echo Signals from Moving Targets I: Description and Theory". *Ultrasonic Imaging*

[Osmanksi et al., 2012] "Aberration correction by time reversal of moving speckle noise". *IEEE TUFFC*

Anisoplanatic Aberrations

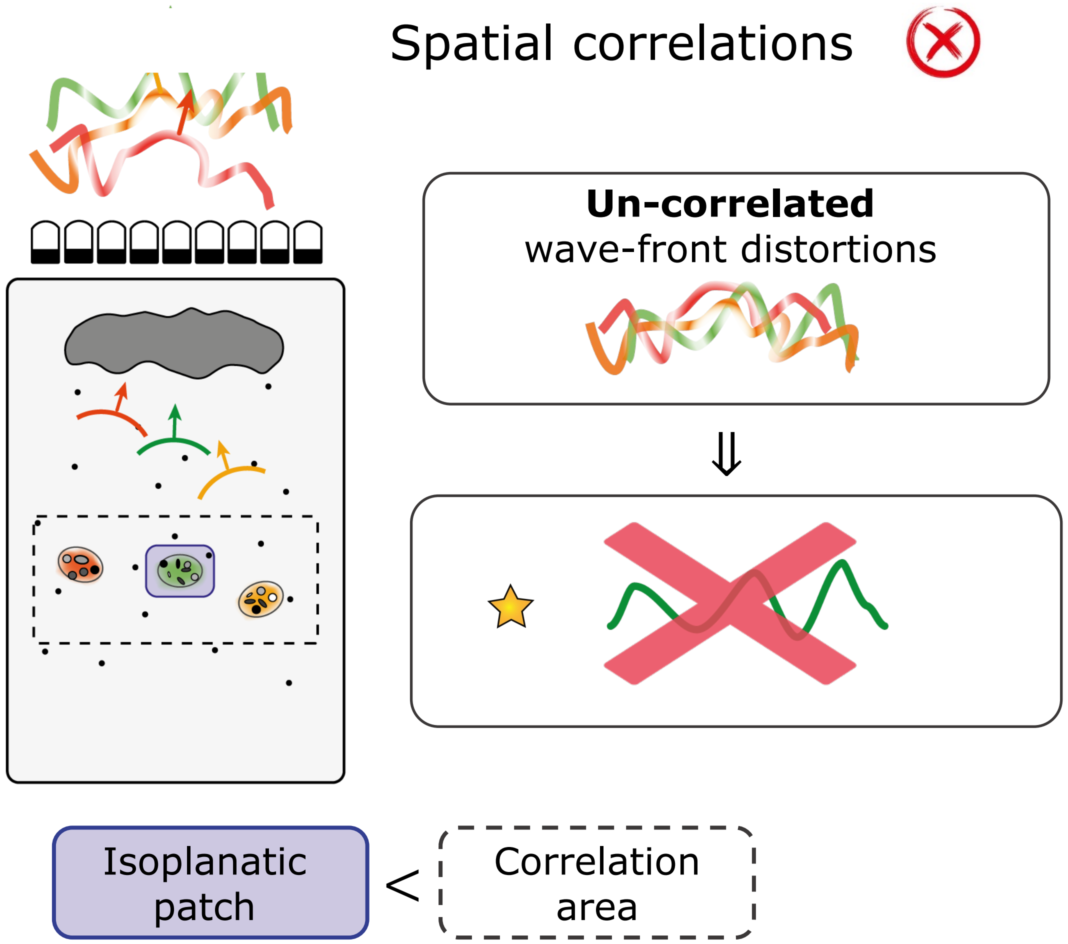

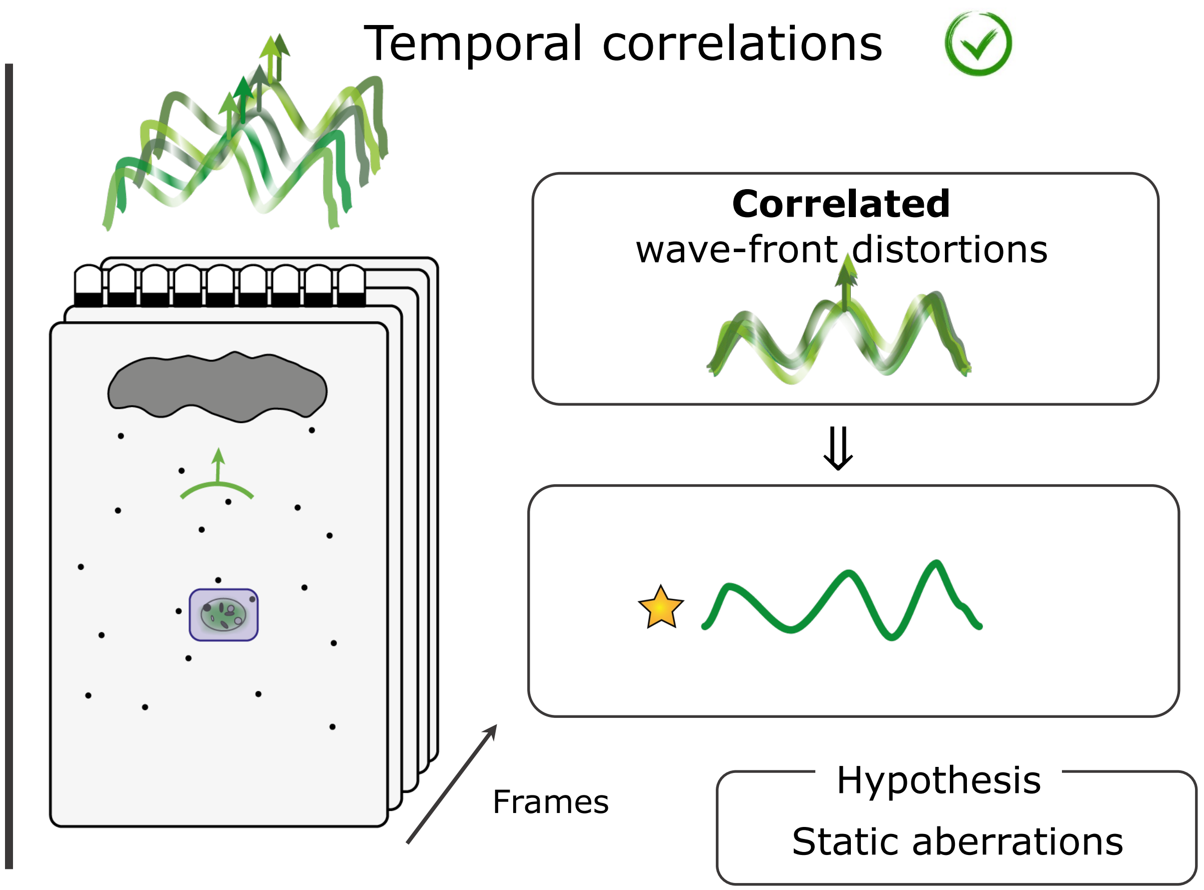

Exploit temporal decorrelation of speckle to obtain independent focusing laws for each point of the medium

[Zhao et al., 1992] "Phase Aberration Correction Using Echo Signals from Moving Targets I: Description and Theory". *Ultrasonic Imaging*
[Osmanksi et al., 2012] "Aberration correction by time reversal of moving speckle noise". *IEEE TUFFC*

Dynamic Transcranial Imaging

Collaboration with Antoine Coudert & Oliver Couture

Laboratoire d'Imagerie Biomédicale

Pre-clinical experiment

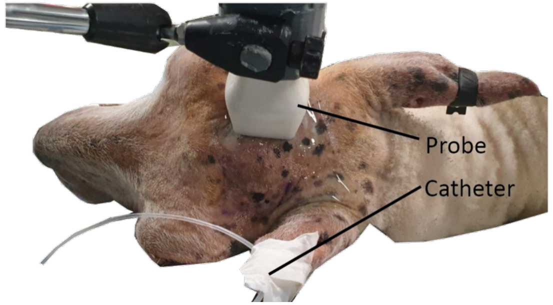

Voumetric imaging

Matrix probe

Dynamic : Repeated acquisition of the reflection matrix

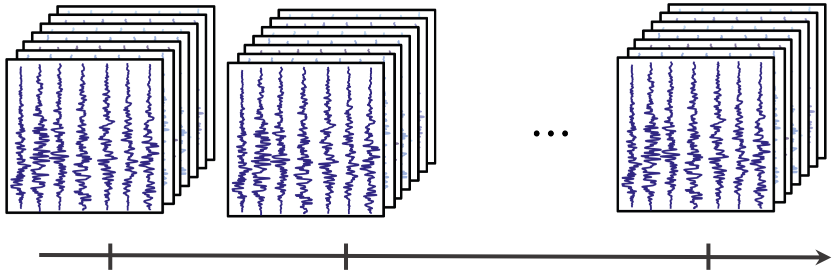

$\mathbf{R}_{\mathbf{u}\theta}(t, \#)$

Time

Frame #

Ultra-fast imaging constraints

Frame rate

~ 200 Hz

5 emissions

Diverging waves

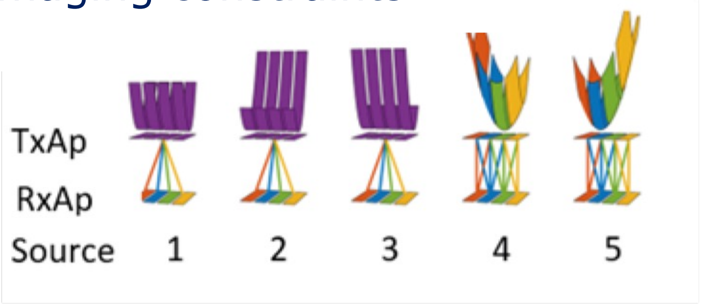

Objective

Dynamic focused reflection matrix $\overline{\mathbf{R}}_{\mathbf{rr}}\ (\#)$

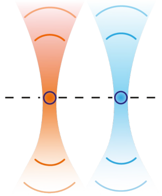

Ultra-local compensation of wave-distortions

Extraction of dynamic signals

Original Image

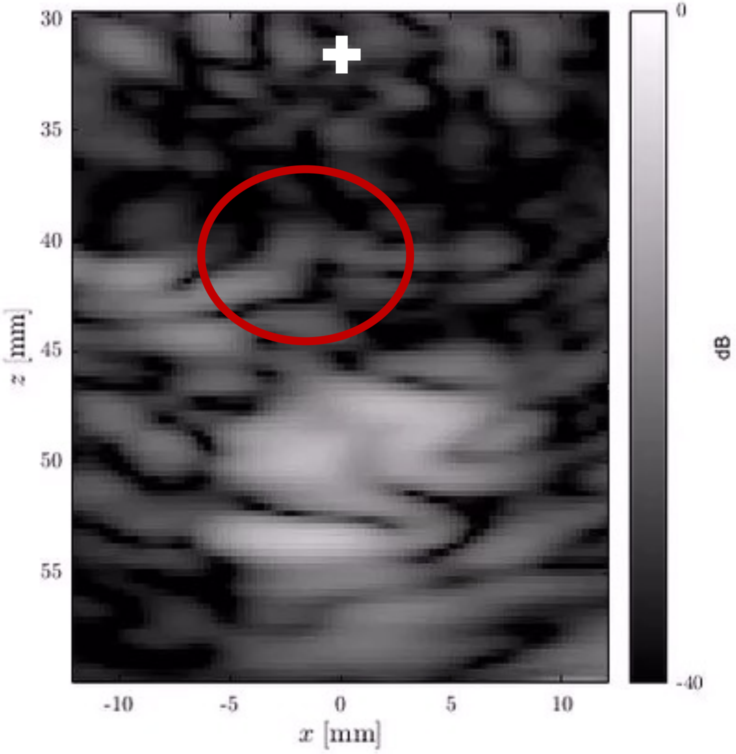

Pixel reflectivity at each frame #

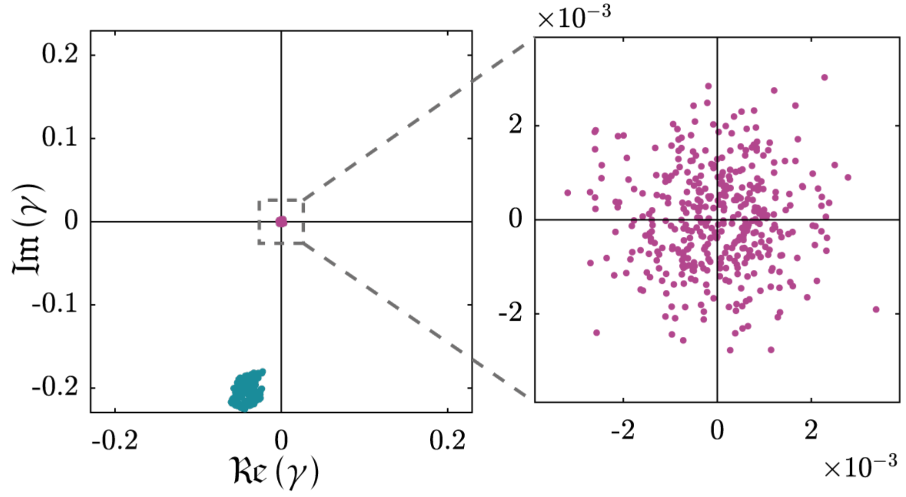

Before extraction

After extraction

~ random

Dynamic Image

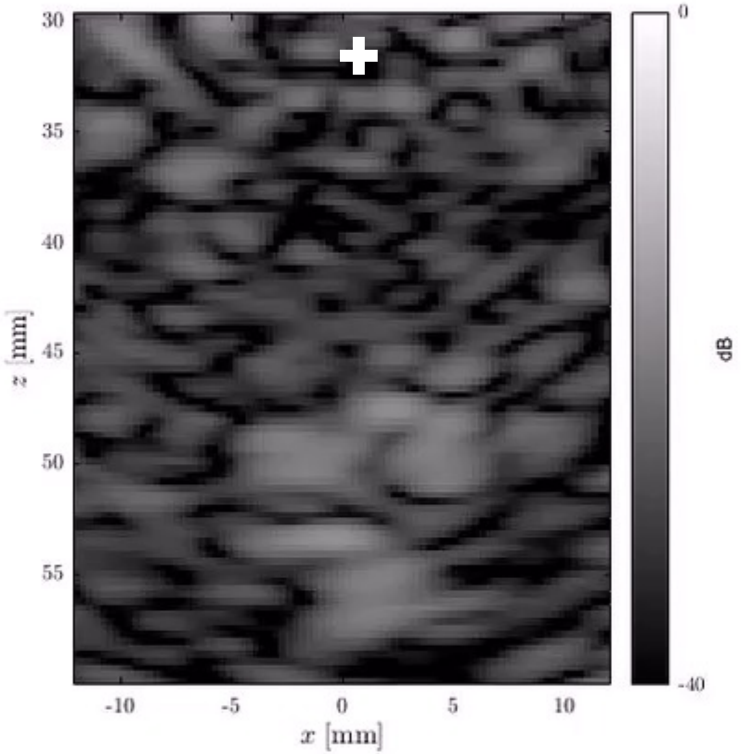

Filtering static component

$$\bar{R}_{\text{dyn}}(\mathbf{r}_{\text{out}}, \mathbf{r}_{\text{in}}, \#_n) = \bar{R}(\mathbf{r}_{\text{out}}, \mathbf{r}_{\text{in}}, \#_n) - \langle \bar{R}(\mathbf{r}_{\text{out}}, \mathbf{r}_{\text{in}}, \#_m) \rangle_{m \in [n-2:n+2]}$$

[Coudert, 2023] « Développement de la microscopie de localisation ultrasonore volumétrique et transcrânienne adaptée pour l'humain ». *Thèse de "Doctorat, Sorbonne Université*

Aberration Matrix

Extraction of aberration laws in speckle

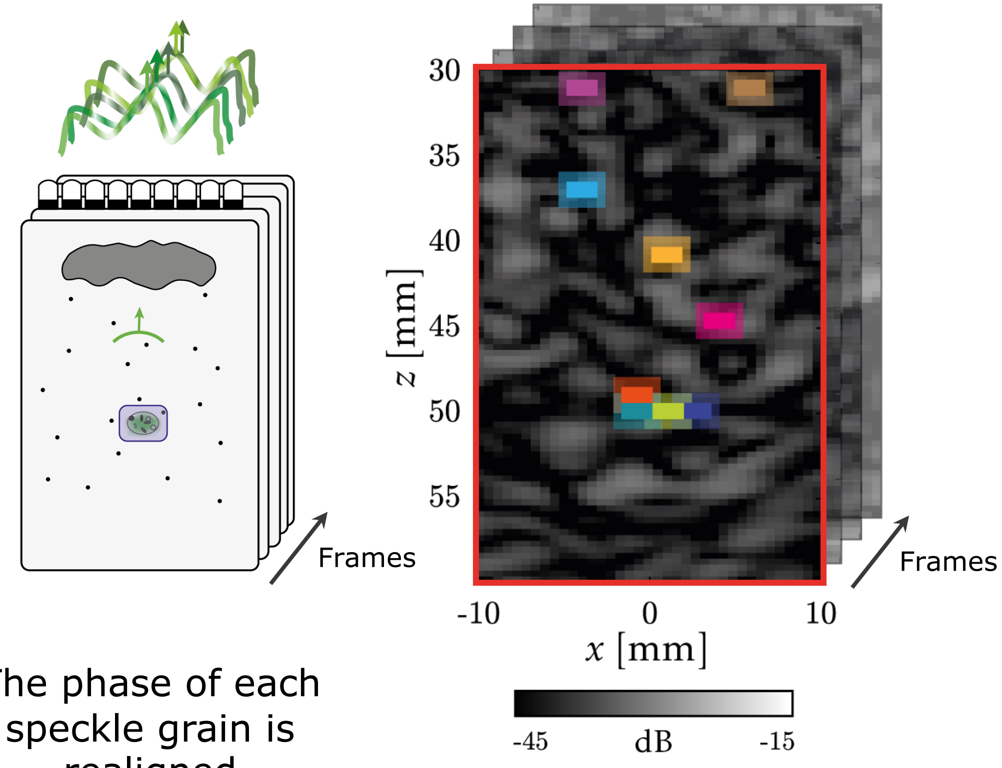

The phase of each speckle grain is realigned

Map of aberration laws

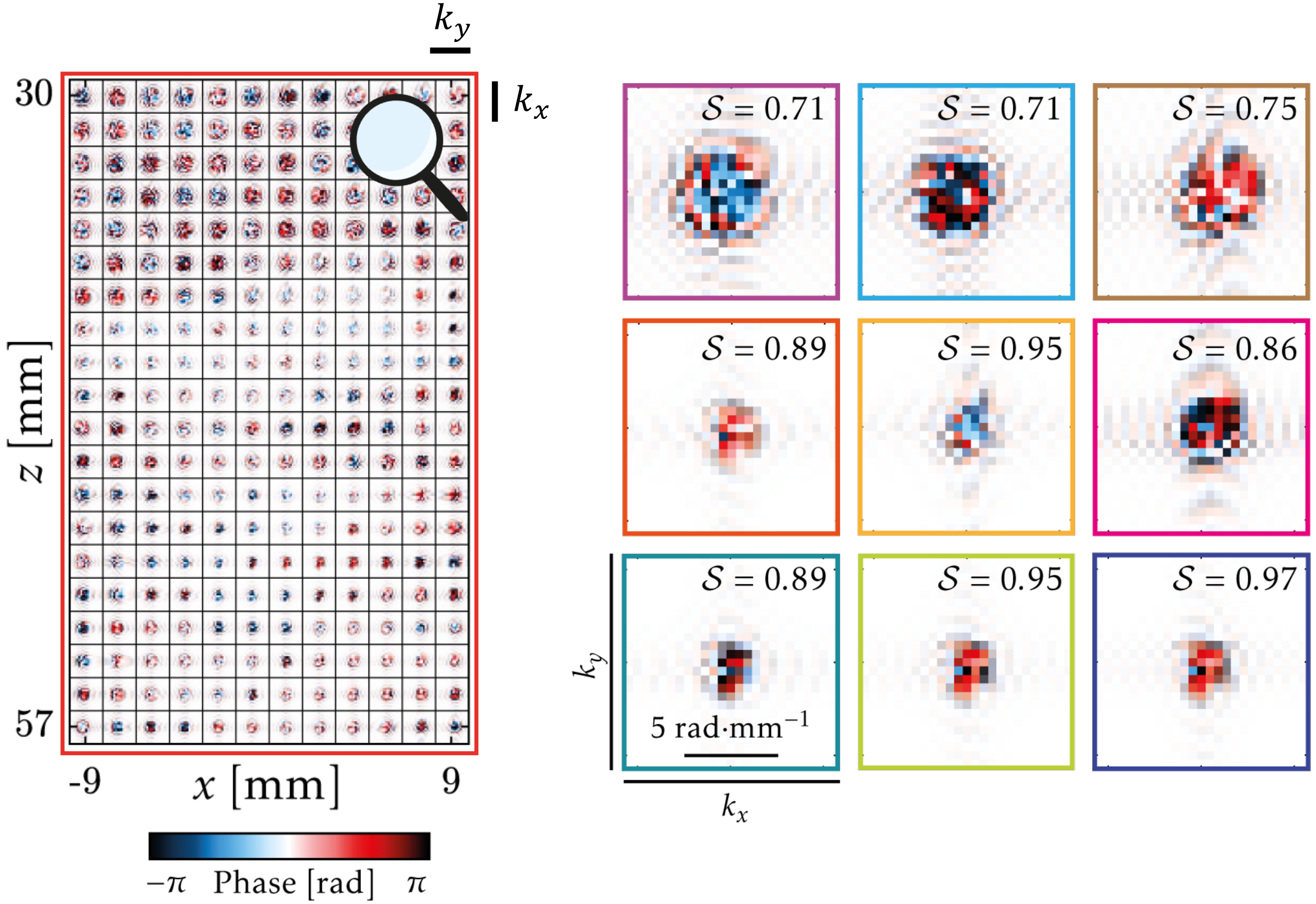

Correction of dynamic images

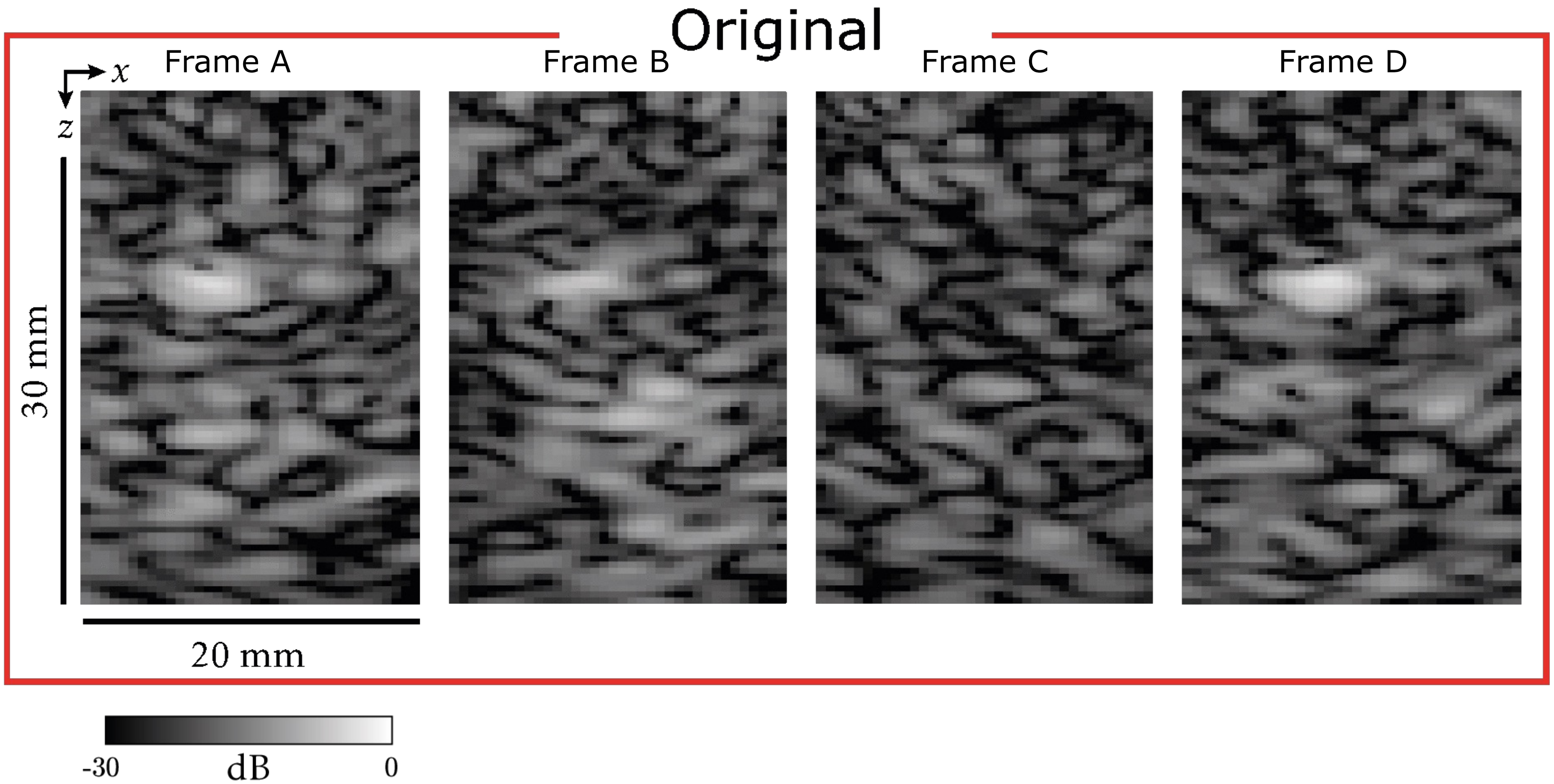

Drastic gain in contrast and resolution allows a better detection and localization of bubbles

Correction of dynamic images

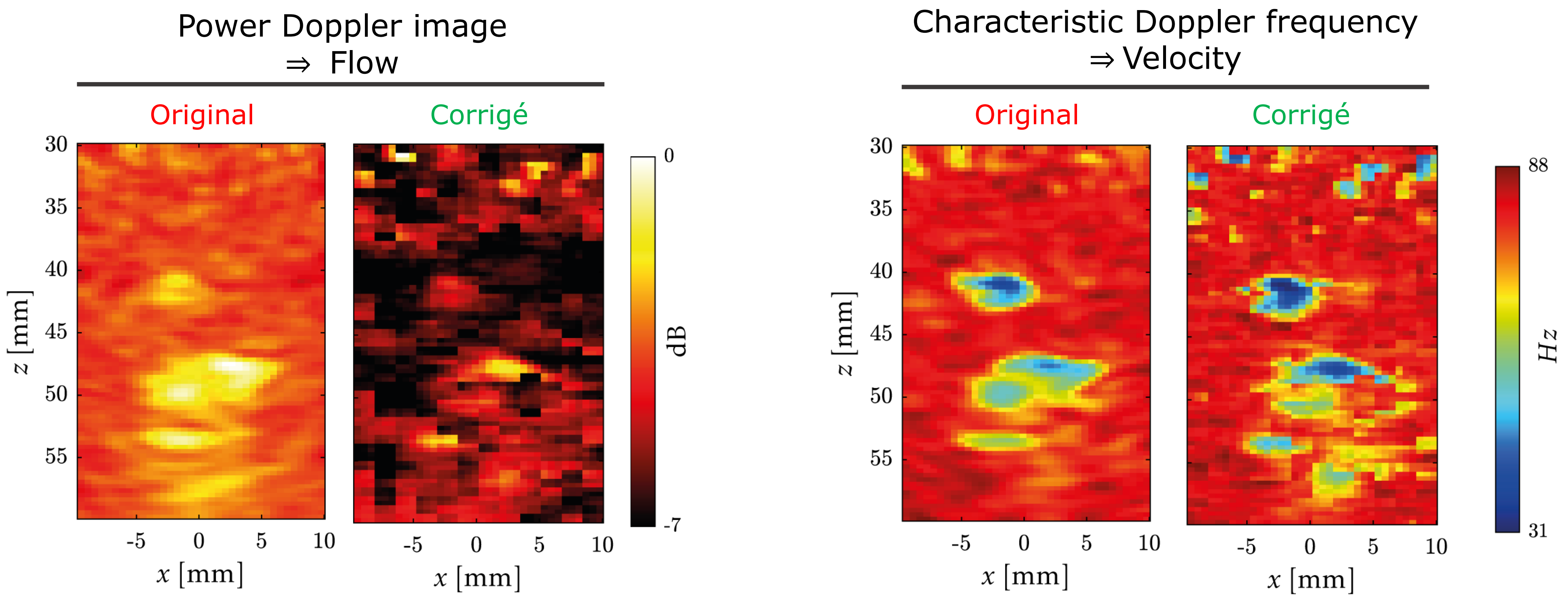

Drastic gain in contrast and resolution provides a better detection and localization of bubbles

Thank you !!!